

The Reactions of Acetylphenyl and Tetrafluoro Acetylphenylnitrene with Functional
Groups Present in Amino and Nucleic Acids

A Senior Honors Thesis

Presented in Partial Fulfillment of the Requirements for graduation
with distinction in Chemistry in the undergraduate colleges
of The Ohio State University

by

Meredith Rae Cline

The Ohio State University
June 2006

Project Advisor: Professor Matthew Platz, Department of Chemistry

ABSTRACT

Photoaffinity labeling (PAL) is a technique used to discover points of contact between protein and nucleic acid complexes. Learning which amino acid residue is proximal to which nucleic acid residue is crucial to understanding the structure and function of the complex. In the PAL experiment a photosensitive molecule, typically an azide (N_3) group, is appended to a nucleic acid or amino acid residue of the complex. In a successful experiment photolysis of the azide releases a singlet nitrene which can lead to a robust cross-link. Unfortunately, the PAL experiment is often plagued by low cross-linking efficiency. There is an urgent need to develop new azide probes which lead to highly efficient cross-linking.

During 2004-2006 the chemistry of para-azido acetophenone (4H) was studied in organic and aqueous solutions. Through laser flash photolysis (LFP) and time-resolved infra red spectroscopy (TRIR) it was found that the main reactive intermediate produced was triplet nitrene. It was later determined that the reason 4H forms mostly triplet nitrene is that when in aqueous solution, water catalyzes intersystem crossing (ISC) which is a fast transfer from the singlet nitrene to the triplet nitrene. The 4H compound reacts best with reducing agents such as sodium ascorbate, methionine, and glutathione. In organic solvents the singlet nitrene forms a ketenimine which reacts with phenol and N-methylimidazole. Since neither the organic or aqueous reactions form a reactive singlet nitrene it was concluded that the 4H compound is not a useful reagent for PAL experiments. It was hypothesized that the addition of four fluorine substituents to the

aromatic ring would enhance the bimolecular reactivity of para-acetylphenylnitrene and that this would increase the efficiency of cross-linking.

The new molecule 2,3,5,6-tetrafluoro para-azide acetophenone (4F) was also studied using LFP and TRIR techniques. It was found that in an aqueous environment 4F does not form a reactive singlet nitrene that can be intercepted, but in an organic environment it was found that the singlet nitrene has a long enough lifetime to react with pyridine to form an ylide which can be detected by LFP and TRIR methods. The 4F compound was also found to react with the unactivated CH bonds in cyclohexane to form an adduct which is evidence that it can form a successful crosslink. Based on the findings of this research it can be concluded that the 4H compound will not form a successful crosslink in either a hydrophobic or hydrophilic region of a protein or nucleic acid. The 4F compound would not be useful in a hydrophilic region, but it could be used successfully as a probe in a hydrophobic region where it has been found to form crosslinks with other molecules.

For my mother

ACKNOWLEDGEMENTS

I would like to thank Dr. Matt Platz for all of his support, encouragement, and advice. He opened my eyes to chemistry and all of the opportunities around me. Through his guidance I have become a better scientist and more importantly a better person, and for that I will always be grateful.

I would also like to thank Dr. Sarah Mandel for her enduring patience and motivation. She has been a wonderful teacher who has taught me almost every lab technique I know and whose hard work and resourcefulness I have always admired.

I would like to thank the entire Platz group, their support and advice has always been appreciated.

I would especially like to thank my family, through the good times and the hard times, they have always been there. Without their love and support none of this would be possible.

Finally, I would like to thank the teachers of Winterset Elementary School, Ridgeview Middle School, and Centennial High School. Thank you for instilling in me a love of science and of learning. You cheered me on, and challenged me, and when my mother died you held me up and would not let me fall. I hope that someday I will have the same impact on my students that you had on me.

VITA

July 15, 1984.....Born - Columbus, Ohio

2002-present.....Undergraduate Student,
The Ohio State University,
Columbus, Ohio

FIELDS OF STUDY

Major Field: Chemistry
Major Field: Biology

TABLE OF CONTENTS

ABSTRACT.....	2
DEDICATION.....	4
ACKNOWLEDGMENTS.....	5
VITA.....	6
LIST OF TABLES.....	9
LIST OF FIGURES.....	10
CHAPTER 1: INTRODUCTION.....	16
CHAPTER 2: 4-AZIDOACETOPHENONE (4H).....	23
2.1. Introduction.....	23
2.2. Methods.....	24
2.2.1. Preparation of 4H.....	24
2.2.2. Purification and Analysis of Azides for LFP and TRIR Work.....	26
2.2.3. Preparation of Quenchers for Kinetics Study.....	27
2.2.4. Treatment of Data for the Amino Acid Quenching Study.....	28
2.3 Results.....	29
2.3.1. OMA's Obtained by LFP of 4-azido acetophenone.....	29
2.3.2. 4H Reactive Intermediates Studied by Laser Flash Photolysis (LFP) in Water and Benzene.....	33
2.3.3. Kinetic Quenching Study of 4H in Water with Various Biological Molecules.....	35
2.3.4. Study of 4H Intermediates with Ketenimine Quenchers in Benzene.....	57
2.3.5. Studies to Confirm the Solvent Effect.....	60
2.3.6. TRIR Experiment with Ketenimine in Acetonitrile.....	62
2.4 Conclusions.....	65
CHAPTER 3: 2,3,5,6-TETRAFLUORO-4-AZIDOACETOPHENONE (4F).....	67
3.1. Introduction.....	67
3.2. Methods.....	69
3.2.1. Procedure for Synthesizing 2,3,5,6-tetrafluoro-4-azidoacetophenone (4F).....	69
3.2.2. Purification and Analysis of Azides for LFP and TRIR Work.....	70
3.2.3. Procedure for Preparation of Samples for Photolysis.....	71
3.2.4. Synthesis of Product Study Standards.....	71
3.3. Results.....	75
3.3.1. Laser Flash Photolysis Study of 4F.....	75

3.3.2. OMA's Produced by LFP of 4F in Varying Solvents with 1M pyridine: A Singlet Nitrene Trapping Study.....	78
3.3.3. Kinetics with Pyridine: Determining the Reactivity of Singlet Nitrene in Varying Solvents.....	85
3.3.4. Study of 4F Singlet Nitrene with Biological Quenchers in Organic Solvent.....	90
3.3.5. Study to Determine Presence or Absence of Ketenimine.....	95
3.3.6. Triplet Quencher Study.....	96
3.3.7. 5F Photochemistry – Control Experiments.....	98
3.3.8. DFT Calculations of the Vibrational Spectra of Reactive Intermediates.....	101
3.3.9. TRIR Studies.....	103
3.3.10. Product Study of 4F Reaction Products.....	112
3.4. Conclusions.....	115
CHAPTER 4: CREATION OF AN AZIDE LIBRARY.....	119
4.1 Introduction.....	119
4.2 Standard Procedures.....	119
4.3. Results.....	126
REFERENCES.....	131

LIST OF TABLES

Table 2.1: Summary of Rate Constants in Water

Table 2.2: Summary of Rate Constants in Benzene

Table 3.1: Summary of the Reactivity of Singlet Nitrene in Various Solvents

Table 3.2: Stable products formed in various solvents upon photolysis of 0.01M 4F

LIST OF FIGURES

- Figure 1.1: Example of photoaffinity labeling.
- Figure 1.2: Ketenimine formation and reaction with diethylamine
- Figure 1.3: Reagents of Study, 4H and 4F
- Figure 1.4: Hixson and Hixson's reagent
- Figure 2.1: Hixson and Hixson's reagent (1Br)
- Figure 2.2: The reagent 4H
- Figure 2.3: The transient spectrum produced upon LFP of 4-azidoacetophenone in water. The spectrum was recorded with a 100 ns delay at 266 nm excitation wavelength taken on 8/11/04.
- Figure 2.4: The transient spectrum produced upon LFP of 4-azidoacetophenone in water. The spectrum was recorded with no delay at 308 nm excitation wavelength taken on 8/18/04.
- Figure 2.5: The transient spectrum produced upon LFP of 4-azidoacetophenone in water. The spectrum was recorded with a 20 ns delay at 355 nm excitation wavelength taken on 8/31/04.
- Figure 2.6: The transient spectrum produced upon LFP of 4-azidoacetophenone in water. The spectrum was recorded with a 100 ns delay at 266 nm excitation wavelength taken on 8/11/04.
- Figure 2.7: The transient spectrum produced upon LFP of 4-azidoacetophenone in water. The spectrum was recorded with no delay at 308 nm excitation wavelength taken on 8/18/04.
- Figure 2.8: The transient spectrum produced upon LFP of 4-azidoacetophenone in water. The spectrum was recorded with various delays at 308 nm excitation wavelength.
- Figure 2.9: The transient spectrum produced upon LFP of 4-azidoacetophenone in benzene. The spectrum was recorded with various delays at 308 nm excitation wavelength.
- Figure 2.10: The transient spectrum produced upon LFP of 4-azidoacetophenone in benzene (red) and water (blue). The spectrum was recorded with 100 ns delays at 308 nm excitation wavelength.
- Figure 2.11: The transient spectrum produced upon LFP of 4-azidoacetophenone in benzene (red) and water (blue). The spectrum was recorded with 10 us delays at 308 nm excitation wavelength.
- Figure 2.12: The transient decay spectrum produced upon LFP of 4-azidoacetophenone in water and. The spectrum was recorded with no delay at 355 nm excitation wavelength and 420 nm probe.
- Figure 2.13: The transient decay spectrum produced upon LFP of 4-azidoacetophenone in water and. The spectrum was recorded with no delay at 308 nm excitation wavelength and 420 nm probe.
- Figure 2.14: The decay of 420 nm absorption in the presence of 20 uL of adenosine (red) and 500 uL of adenosine (blue) solution with 4-azido acetophenone in H₂O intermediate produced from 4-azido acetophenone experiments in H₂O.

Figure 2.15: The decay of 420 nm absorption in the presence of 15 μ L of uracil (blue) and 30 μ L of uracil (red) solution with 4-azido acetophenone in H_2O , note the poor signal to noise ratio.

Figure 2.16: A plot of k_{obs} versus [uracil] concentration obtained by LFP of 4H in water.

Figure 2.17: The decay of 420 nm absorption in the presence of 20 μ L of tyrosine (blue) and 35 μ L of tyrosine (red) solution with 4-azido acetophenone in H_2O , note the poor signal to noise ratio.

Figure 2.18: The decay of 420 nm absorption in the presence of 5 μ L of tyrosine solution with 4-azido acetophenone in H_2O , note the wavy baseline and the poor signal to noise ratio.

Figure 2.19: The decay of 420 nm absorption in the presence of 35 μ L of tyrosine solution with 4-azido acetophenone in H_2O .

Figure 2.20: A plot of k_{obs} versus [tyrosine] concentration obtained by LFP of 4H in water.

Figure 2.21: The decay of 420 nm absorption in the presence of 50 μ L of alanine solution with 4-azido acetophenone in H_2O , note the poor signal to noise ratio.

Figure 2.22: A plot of k_{obs} versus [alanine] concentration obtained by LFP of 4H in water.

Figure 2.23: The decay of 420 nm absorption in the presence of 5 μ L of tryptophan (red) and 40 μ L of tryptophan (blue) solution upon LFP of 4H in H_2O .

Figure 2.24: A plot of k_{obs} versus [tryptophan] concentration obtained by LFP of 4H in water.

Figure 2.25: The decay of 420 nm absorption in the presence of 5 μ L of cystine (blue) and 25 μ L of cystine (red) solution upon LFP of 4H in H_2O .

Figure 2.26: A plot of k_{obs} versus [cystine] concentration obtained by LFP of 4H in water.

Figure 2.27: The decay of 420 nm absorption in the presence of 5 μ L of methionine (blue) and 50 μ L of methionine (red) solution upon LFP of 4H in H_2O .

Figure 2.28: A plot of k_{obs} versus [methionine] concentration obtained by LFP of 4H in water.

Figure 2.29: The decay of 420 nm absorption in the presence of 30 μ L of NH_4Cl (blue) and 100 μ L of NH_4Cl (red) solution upon LFP of 4H in H_2O .

Figure 2.30: A plot of k_{obs} versus [NH_4Cl] concentration obtained by LFP of 4H in water.

Figure 2.31: The decay of 420 nm absorption in the presence of 10 μ L of histidine (blue) and 30 μ L of histidine (red) solution upon LFP of 4H in H_2O .

Figure 2.32: A plot of k_{obs} versus [histidine] concentration obtained by LFP of 4H in water.

Figure 2.33: The decay of 420 nm absorption in the presence of 10 μ L of N-methyl imidazole (blue) and 100 μ L of N-methyl imidazole (red) solution upon LFP of 4H in H_2O .

Figure 2.34: A plot of k_{obs} versus [N-methyl imidazole] concentration obtained by LFP of 4H in water.

Figure 2.35: A plot of k_{obs} versus [glutathione] concentration obtained by LFP of 4H in water.

Figure 2.36: A plot of k_{obs} versus [Na ascorbate] concentration obtained by LFP of 4H in water.

Figure 2.37: Reaction of ketenimine with diethyl amine.

Figure 2.38: Demonstration of triplet nitrene reacting with a reducing agent.

Figure 2.39: A plot of k_{obs} versus [phenol] concentration obtained by LFP of 4H in benzene.

Figure 2.40: A plot of k_{obs} versus [dibutyl sulfide] concentration obtained by LFP of 4H in benzene.

Figure 2.41: A plot of k_{obs} versus [indole] concentration obtained by LFP of 4H in benzene.

Figure 2.42: A plot of k_{obs} versus [N-methyl imidazole] concentration obtained by LFP of 4H in benzene.

Figure 2.43: A plot of k_{obs} versus [concentration] of N-methyl imidazole, dibutyl sulfide, and phenol obtained by LFP of 4H in benzene.

Figure 2.44: Transient absorption spectra produced upon LFP of 4H in water (solid line) and benzene (dotted line), recorded 10 ns after the pulse (308 nm).

Figure 2.45: Change in the rate of decay of ketenimine in benzene with different concentrations of phenol (solid line 0.47 M phenol, dotted line 0 M phenol, 308 nm excitation, 415 nm detection). The slow growth observed in the absence of phenol is due to the formation of azo dimer **7a** by reaction of triplet nitrene **3a** with azide 4H.

Figure 2.46: Transient IR spectra of 4H in CH₃CN (266 nm excitation, 3.1 ms after the pulse, 3 mM azide concentration)

Figure 2.47: First order quenching of ketenimine with water in CH₃CN (266 nm excitation, 1890 cm⁻¹ detection, 3 mM concentration of 4H).

Figure 2.48: Stern Volmer treatment of the quenching of 4H ketenimine with water in CH₃CN (266 nm excitation, 1890 cm⁻¹ detection, 3 mM, 4H concentration).

Figure 3.1: Photochemistry of 2,6-difluorophenyl azide.

Figure 3.2: Formation of adduct using singlet pentafluorophenyl nitrene.

Figure 3.3: Proposed adduct formation with 4F.

Figure 3.4: The reagent 4F.

Figure 3.5: The amine produced upon photolysis of 4F.

Figure 3.6: The azo dimer photo product produced upon photolysis of 4F.

Figure 3.7: The nitro compound produced upon photolysis of 4F.

Figure 3.8: The adduct produced upon photolysis of 4F in cyclohexane.

Figure 3.9: The transient spectrum produced by LFP of 4F in dichloroethane.

Figure 3.10: The transient spectrum produced by LFP of 4F in cyclohexane.

Figure 3.11: The transient spectrum produced by LFP of 4F in methanol.

Figure 3.12: The transient spectrum produced by LFP of 4F in benzene.

Figure 3.13: The transient spectrum produced by LFP of 4F in cyclohexane. The absorption seen in the figure is the result of growth of the 4F azo dimer. The spectra were recorded 20, 25, and 225 ns after the pulse with 266 nm excitation.

Figure 3.14: Transient UV spectra of 4F in water at 10 ns delay (solid line), 1 ms (dotted line), and 10 ms (dashed line), 308 nm excitation. With increasing delay the azo dimer grows in.

Figure 3.15: Production of azo dimer.

Figure 3.16: Production of the pyridine ylide.

Figure 3.17: Transient spectrum produced by LFP of 4F in acetonitrile containing 1M pyridine.

Figure 3.18: Transient spectrum produced by LFP of 4F in cyclohexane containing 1M pyridine.

Figure 3.19: Transient spectrum produced by LFP of 4F in dichloromethane containing 1M pyridine.

Figure 3.20: Transient spectrum produced by LFP of 4F in methanol containing 1M pyridine.

Figure 3.21: Transient spectrum produced by LFP of 4F in benzene containing 1M pyridine (dark line) and 0M pyridine (dotted line).

Figure 3.22: Singlet Nitrene reacts with Pyridine to form the Pyridine Ylide.

Figure 3.23: Transient spectrum produced by LFP of 4F in acetonitrile containing varying concentration of pyridine.

Figure 3.24: A plot of k_{obs} versus [Pyridine] concentration obtained by LFP of 4F in benzene.

Figure 3.25: A plot of k_{obs} versus [Pyridine] concentration obtained by LFP of 4F in methylene chloride.

Figure 3.26: A plot of k_{obs} versus [Pyridine] concentration obtained by LFP of 4F in acetonitrile.

Figure 3.27: A plot of k_{obs} versus [Pyridine] concentration obtained by LFP of 4F in cyclohexane.

Figure 3.28: The adduct formed upon photolysis of 4F in cyclohexane.

Figure 3.29: Transient spectrums produced by LFP of 4F in cyclohexane containing adduct (blue) and without adduct (red).

Figure 3.30: Mechanistic representation of how 4F singlet nitrene can be measured in the presence of biological quenchers.

Figure 3.31: Stern Volmer analysis of the quenching of the yield of ylide by N-methylimidazole.

Figure 3.32: Stern Volmer analysis of the quenching of the yield of ylide by methanol

Figure 3.33: Stern Volmer analysis of the quenching of the yield of ylide by dibutyl sulfide.

Figure 3.34: Stern Volmer analysis of the quenching of the yield of ylide by indole.

Figure 3.35: Stern Volmer analysis of the quenching of the yield of ylide by water.

Figure 3.36: Stern Volmer analysis of the quenching of the yield of ylide by all biological quenchers.

Figure 3.37: Transient spectrum produced by LFP of 4F in cyclohexane containing diethylamine (DEA).

Figure 3.38: Transient spectrum produced by LFP of 4F in methylene chloride containing imidazole.

Figure 3.39: Production of Azo Dimer

Figure 3.40: A plot of k_{obs} versus [Na Ascorbate] concentration obtained by LFP of 4F in water.

Figure 3.41: A plot of k_{obs} versus [Glutathione, reduced] concentration obtained by LFP of 4F in water.

Figure 3.42: Transient spectrum produced by LFP of 5F in acetonitrile.

Figure 3.43: Transient spectrum produced by LFP of 5F in acetonitrile with 0.75 M pyridine.

- Figure 3.44: Transient spectrum produced by LFP of 4F in cyclohexane with 1 M pyridine.
- Figure 3.45: Transient spectrum produced by LFP of 5F in cyclohexane with 1 M pyridine.
- Figure 3.46: Complete theoretical IR of reactive intermediates produced upon irradiation of 4F.
- Figure 3.47: Theoretical calculations for the vibrational bands in the region of interest of reactive intermediates produced upon irradiation of 4F.
- Figure 3.48: TRIR spectrum of 4F reactive intermediates produced upon photolysis of 4F from 1600 cm^{-1} to 1350 cm^{-1} .
- Figure 3.49: Complete TRIR spectrum produced by flash photolysis of 4F. Maximum range of 1950 cm^{-1} to 1250 cm^{-1} .
- Figure 3.50: The transient decay kinetics produced upon flash photolysis of 4F. The kinetics were recorded at 1520 cm^{-1} . The decay kinetics were assigned to the singlet nitrene with a rate constant of $1.27\text{e}6\text{ s}^{-1}$ and a lifetime of 800 us. There is much error in this number because of the poor signal to noise ratio.
- Figure 3.51: The transient decay kinetics produced upon flash photolysis of 4F. The kinetics were recorded at 1434 cm^{-1} . The decay kinetics were assigned to the triplet nitrene with a rate constant of $3.53\text{e}5\text{ s}^{-1}$.
- Figure 3.52: The transient decay kinetics produced upon flash photolysis of 4F. The kinetics were recorded at 1348 cm^{-1} . The decay kinetics were assigned to the triplet nitrene with a rate constant of $3.06\text{e}5\text{ s}^{-1}$.
- Figure 3.53: The growth of transient absorption produced upon flash photolysis of 4F. The kinetics were recorded at 1308 cm^{-1} . The growth kinetics were assigned to azo dimer formation. The concentration of azo dimer grows in with time and does not decay.
- Figure 3.54: The transient decay kinetics produced upon flash photolysis of 4F measured at 1434 cm^{-1} in deuterated acetonitrile. The decay kinetics has been assigned to the triplet nitrene with a rate constant of $1.50\text{e}5\text{ s}^{-1}$ in air and $1.32\text{e}6\text{ s}^{-1}$ under argon purge.
- Figure 3.55: The transient decay produced upon flash photolysis of 4F measured at 1340 cm^{-1} in deuterated acetonitrile. The decay spectrum has been assigned to the triplet nitrene with a rate constant of $1.35\text{e}5\text{ s}^{-1}$ in air and $1.46\text{e}6\text{ s}^{-1}$ under argon purge.
- Figure 3.56: The transient decay produced upon flash photolysis of 4F measured at 1520 cm^{-1} in deuterated acetonitrile. The decay kinetics has been assigned to the singlet nitrene with a rate constant of $2.30\text{e}6\text{ s}^{-1}$ in air and $2.60\text{e}6\text{ s}^{-1}$ under argon purge.
- Figure 3.57: TRIR spectrum of 4F reactive intermediates produced upon photolysis of 4F at low temperature in deuterated acetonitrile.
- Figure 3.58: The transient decay kinetics produced upon flash photolysis of 4F at 1434 cm^{-1} in deuterated acetonitrile. The decay kinetics were assigned to the triplet nitrene with a rate constant of $3.95\text{e}5\text{ s}^{-1}$ in air.
- Figure 3.59: The transient decay kinetics produced upon flash photolysis of 4F measured at 1520 cm^{-1} in deuterated acetonitrile. The decay kinetics were assigned to the singlet nitrene with a rate constant of $1.3\text{e}6\text{ s}^{-1}$ in air.

Figure 3.60: The transient absorption kinetics produced upon flash photolysis of 4F. The kinetics were recorded at 1308 cm^{-1} . The growth kinetics are assigned as azo dimer formation.

Figure 3.61: TRIR spectrum of 4F reactive intermediates produced upon photolysis of 4F at room temperature ($\sim 23\text{ }^{\circ}\text{C}$) in deuterated cyclohexane.

Figure 3.62: TRIR spectrum of 4F reactive intermediates produced upon photolysis of 4F at low temperature ($\sim 0\text{ }^{\circ}\text{C}$) in deuterated cyclohexane.

Figure 3.63: Example of the formation of an azo compound.

Figure 3.64: Triplet nitrene reaction.

Figure 3.65: Closed shell nature of a singlet carbene.

Figure 3.66: Zwitterionic singlet carbene relaxing to a biradical triplet state.

Figure 3.67: Singlet aryl nitrene open shell electronic structure.

Figure 3.68: Quinoidal structure of singlet phenylnitrene.

Figure 3.69: Hydrogen bonding with quinoidal structure.

CHAPTER 1: INTRODUCTION

Photoaffinity labeling (PAL) is a technique used by scientists to discover and study the binding pockets of enzymes. Photo cross-linking is a related technique to discover and study points of contact between protein-protein complexes or protein-nucleic acid complexes¹. Study of the results of these experiments can lead, for example, to a better understanding of which amino acid residues are next to which specific nucleic acid complexes. This information makes it possible to further understand protein binding sites to discover which amino acids are present and active in the catalytic action of the protein. PAL and photo cross-linking experiments are useful for several reasons: (1) they provide structural information for large macromolecular cellular complexes,² (2) in situations where high-resolution structural information is not available,³ and (3) in cases where the dynamics of a system (and not just a static structure) are important.⁴ Typically, a photosensitive molecule, such as an azide (N_3) is appended to an amino acid or nucleic acid residue of the complex. In a successful experiment, the reactive intermediate produced from the photolyzed azide goes on to form a robust covalent cross-link with the biological molecule as shown in Figure 1.

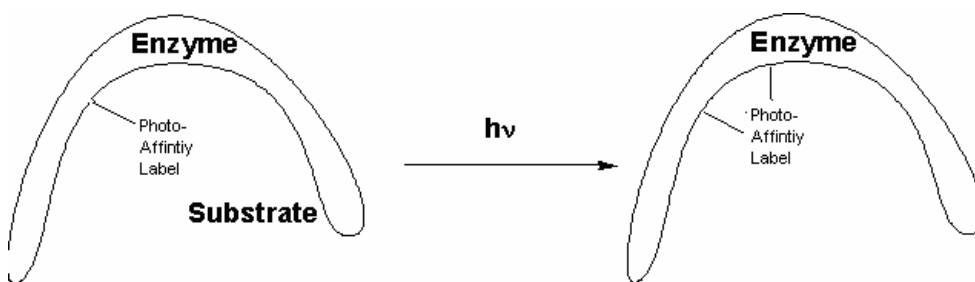


Figure 1.1 Example of photoaffinity labeling.

Many diseases are the result of abnormal activity of enzymes. PAL experiments are important because they allow scientists to create drugs based on what is known about the binding sites of enzymes. This can lead to the correction of abnormal enzyme activity through more efficient drugs that target enzyme binding sites.

Aryl azide based cross linking experiments have been widely used to obtain information on the higher order structure of RNA⁵ and RNA-protein complexes⁶, DNA-protein⁷, protein-protein⁸ and protein-ligand⁹ interactions. Aryl azides are especially useful because they are both inexpensive and easy to work with, and they are stable at physiological pH which makes them ideal for studying biological systems. The addition of a carbonyl group to the para position of the aryl azide leads to a molecule with a longer wavelength absorbance of the reagent that does not overlap with the absorbance of nucleic acids or proteins¹⁰. This allows for selective studies of the photochemistry of the aryl azide and the reactive intermediate it forms in the presence of biomolecules. Aryl azides, though effective, do have a few limitations. The biggest of which is the fast isomerization of the singlet nitrene to a ketenimine. This is problematic because although ketenimines may react very slowly and selectively with nucleophiles such as diethylamine. For this reason they may report residues that are not present in the binding pocket.

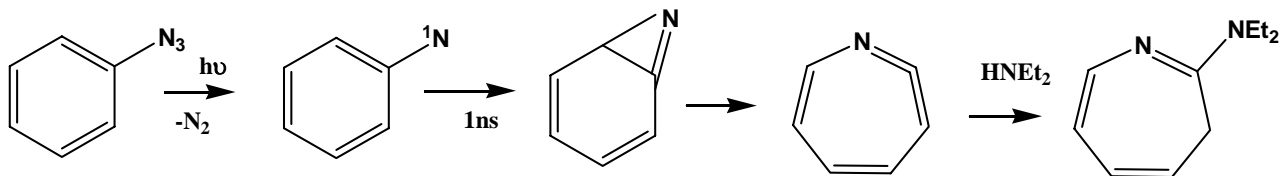


Figure 1.2 Ketenimine formation and reaction with diethylamine

Many photosensitive molecules have been studied for use as PAL reagents¹, however, most of these studies have only been carried out in organic solvents. This leaves a large and relatively unexplored area requiring study considering that PAL experiments are performed in water. It is important to study the reactivity of azide photo labels in water because their reactivity may be very different than their typical reactivity in organic solvent and because many proteins have both hydrophobic and hydrophilic regions.

In order for a photo label to be efficient it must have a short lifetime (0.1-100 ns) and have broad reactivity so that it will react unselectively with numerous residues in the protein-protein or protein-nucleic acid complex. It is important to have a short lifetime because if the photo-generated intermediate lives too long ($\tau > 100$ ns), it may react with residues that are not near the intermediate at its moment of birth, thus not providing any information about the binding site of the biological molecule. Surprisingly, many experiments reported in the literature^{1,11,12} have been interpreted on the assumption that the lifetimes of reactive intermediates are short. However, research done in the Platz laboratory has shown that this is not always the case. There is a specific optimum lifetime window for an effective photo label, if the reactive intermediate has a lifetime of less than

0.1 ns it is highly likely that it will rearrange to a less reactive molecule and if it is longer than 100 ns it may react with residues outside of the binding site. This leaves the time window of 0.1 ns to 100 ns for an effective reactive intermediate to form a cross-link in a PAL experiment.

The following experiments and studies have sought to explore the reactivities of two specific azides, 4-azidoacetophenone (**1a**, also referred to as 4H due to the four hydrogens on the 2,3,5, and 6 positions of the benzene ring) and 2,3,5,6-tetrafluoro-4-azidoacetophenone (**1b**, also referred to as 4F due to the fluorines on the 2,3,5, and 6 positions on the benzene ring), and to determine their effectiveness in both polar and non polar environments.

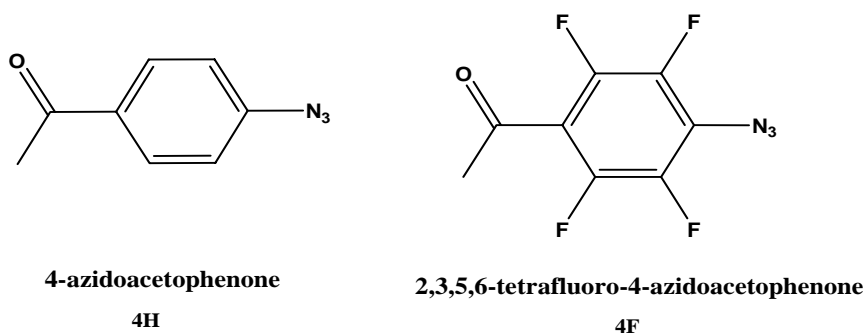


Figure 1.3 Reagents of Study, 4H and 4F

These studies are motivated by the fact that many biophysical chemists have used Hixson and Hixson's reagents⁵ in PAL and cross-linking studies yet nothing is known about the photochemistry of this class of reagent in water.

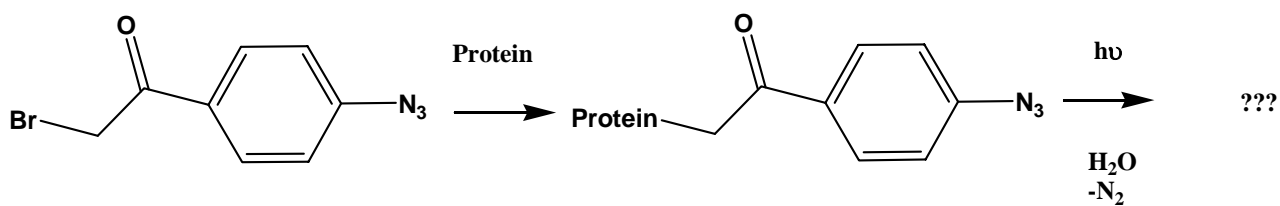
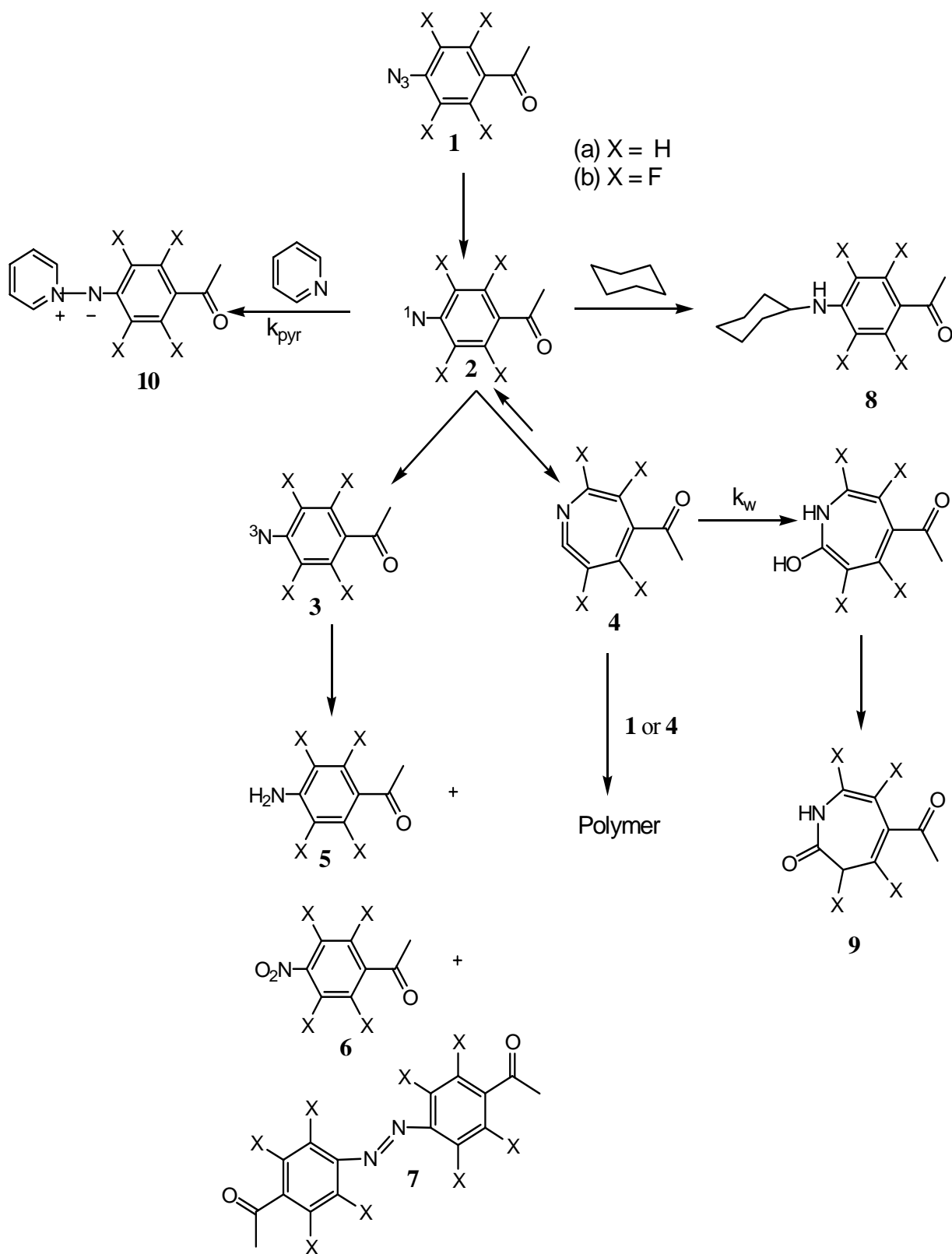


Figure 1.4 Hixson and Hixson's reagent

Product studies of both azides were performed in order to quantify and determine the intermediates formed and whether or not they would form a successful cross link in a PAL experiment. The following mechanistic scheme was developed to show the various products and mechanisms typically shown by aryl azides and which also applies to 4H and 4F.

Scheme 1



When an azide is photolyzed, it immediately fragments to form singlet nitrene (**2**). The singlet can then form four different products: cross-link (adduct) (**8**), a trapped singlet nitrene in the form of a pyridine ylide (**10**), triplet nitrene (**3**), and ketenimine (**4**). The cross-linked product is the result of singlet nitrene reacting with a biological model, in the above case, cyclohexane as a model of an unactivated residue. This is the most useful product in a PAL experiment. The trapped singlet nitrene is useful in understanding the reactivity of the singlet nitrene (**2**). A singlet nitrene is a very short lived and often has a weak ultra violet (UV) spectrum, thus to increase its detection, it is reacted with pyridine to form a highly absorbent ylide. The triplet nitrene (**3**) is longer lived and not useful as a PAL reagent. It reacts with reducing agents and goes on to form amino and nitro compounds and also azo-dimer. Finally, the ketenimine (**4**) product is the result of a rearrangement of the singlet nitrene as show in Scheme 1. It reacts with nucleophiles and its slow and unselective reactivity often results in polymer formation which is not useful in the PAL experiments.

CHAPTER 2: 4-AZIDOACETOPHENONE (4H)

2.1. Introduction

Azido acetophenones were first synthesized and proposed as a PAL reagents⁵ by Hixson and Hixson.

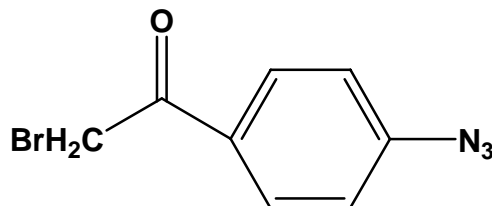


Figure 2.1 Hixson and Hixson's reagent (**1Br**)

They found these azides to possess several desirable qualities such as being inexpensive and easy to synthesize. Azido acetophenones also absorb light at wavelengths longer than nucleic acids and proteins, making it possible to selectively excite the probe azide in the presence of biomolecules. After the findings of Hixson and Hixson, over 80 papers have been published by biophysical chemists on the usefulness of azido acetophenones as PAL reagents¹⁰.

This project involves study of a model of the Hixson and Hixson molecule, replacing the Br with a hydrogen atom⁵. The few papers published regarding azido acetophenones are mostly based on studies performed in organic solvents. The molecule 4H (also **1a** from scheme 1.1) was studied by Li and Schuster, but only in organic solvents¹³. It was found upon photolysis of 4H in cyclohexane that ketenimine **4a** (see scheme 1.1) could be trapped by diethyl amine. Upon photolysis of 4H (at high dilution)

in cyclohexane the presence of triplet nitrene intermediate **3** could be detected as azo dimer **7a** and amine product **5a**.

Based on these results and the conventional wisdom that **1Br** is a good PAL reagent, studies of 4H in water and in select organic solvents were performed.

2.2. Methods

2.2.1. Preparation of 4H

Stock Solutions Prepared

At the beginning of the quarter three stock solutions were prepared for use throughout the quarter. Stock Solution A was composed of 100 mL of concentrated HCl diluted with 900 mL of distilled water. Stock Solution B was composed of 56 g of NaNO₂ diluted in 800 mL of distilled water. Stock Solution C was composed of 72 g and diluted into 800 mL of distilled water.

A stock solution of HEPES buffer was also prepared by mixing 50 mM HEPES salt (MW 238) with 50 mM concentrations of KCl and MgCl₂. To prepare 1 liter of HEPES buffer, 11.9 g of HEPES salt was added to 10.165 g MgCl₂, 3.73 g KCl, and 1 liter of water.

(A) Procedure for Preparation of 4-Azidoacetophenone (4H)¹⁴

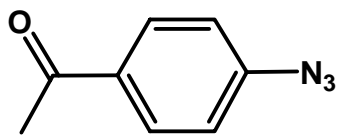


Figure 2.2 The reagent 4H

A solution of 0.02 mol of 4-aminoacetophenone was dissolved in 10 mL of THF (Tetrahydrofuran) and placed in a three necked round bottom flask containing a magnetic stir bar. To the flask 90 mL of Stock Solution A (HCl/H₂O) was added. The flask was then put in an ice bath on top of a magnetic stirrer and clamped to a ring stand. Ethyl alcohol was added to the ice bath to help keep the temperature of the reaction below 5-10 °C. The reaction mixture was then stirred for 15 minutes. Next, 40 mL of Stock Solution B (NaNO₂/H₂O) was added to the reaction mixture dropwise at 0 °C. The reaction mixture was kept below 5 °C and stirred for 15 minutes. Excess nitrous acid was removed by the addition of a spatula tip of urea. To the cooled reaction mixture 40 mL of Stock Solution C (NaN₃/H₂O) was added dropwise to the reaction mixture at a temperature between 0 °C and 5 °C. In most cases the solution bubbled as Stock Solution C was added indicating the formation of nitrogen gas. After the addition was complete the reaction mixture was then stirred for 1.5 hours at room temperature. The reaction mixture was then stored in the laboratory refrigerator.

(B) Purification of Crystalline 4H

Crystallization

The reaction mixture was taken from the refrigerator and the crystals were dried using a vacuum filtration process. A funnel was set up in an Erlenmeyer filter flask and the vacuum hose was attached to the flask. An appropriately sized piece of filter paper was placed in the funnel to avoid losing crystals. The solution containing the crystals was poured quickly into the funnel and any crystals that remained in the previous flask were scraped out and placed into the funnel. The crystals were left to dry in the funnel for an

hour. After the crystals were dried they were added to heated hexanes in the hood. After the crystals were added they were placed on a hot plate, warmed and stirred so that the crystals would go into solution. After the crystals had dissolved the remaining solution was placed in the fume hood to evaporate off excess solvent. After some solvent had evaporated away, the remaining mixture was placed in the refrigerator to crystallize in an ice bath. The formed crystals were then suction filtrated again and left to dry. Once these crystals were dried they were placed in a vial and stored in the refrigerator.

2.2.2. Purification and Analysis of Azides for LFP and TRIR Work

4H was studied by LFP and TRIR techniques; however, before LFP work could be performed it was necessary to ensure the purity of the azide. A plug column was prepared to filter out any unwanted impurities. The column used was packed with silica gel (approx. 75 mL) and approx. 150 mL of hexanes. The solid, 4-azido acetophenone, was dissolved in hexanes and then added to the top of the column. After the addition of the azide, approx. 1 inch of sea sand was added to the top of the column. The column was eluted with hexanes and fractions of approx. 15 mL were collected in test tubes. Air pressure was used to increase the flow through the column. Then Thin Layer Chromatography (TLC) was used to analyze each fraction. The azide was the first compound to elute off of the column. Test tubes of the pale yellow azide containing solutions were alternately tested for the presence of the azide using TLC chromatography plates and hexanes. After all of the tubes found to contain the azide were found they were combined and the solution was concentrated by rotary evaporation. The resulting product was usually a pale yellow color. The azide was then stored in a clean vial.

Usually, the solution to be used for LFP work was prepared the day before the laser work. The main goal was to have the absorbance of the solution to be about 1 at whichever laser wavelength would be used to irradiate the solution. A test solution would be made up in a 5 mL cuvette and a small amount of azide would be added. The solvent would then be poured into the cuvette and it would be analyzed by UV-Vis spectroscopy. The solution was modified depending on its absorbance, if its absorbance was more than 1 it was diluted accordingly, if it was less than 1, then more azide was added. This procedure was then repeated if a larger sample volume (example 25 mL) was desired.

Samples used for the TRIR generally had a concentration of 3 mM and were prepared the day of the experiment.

2.2.3. Preparation of Quenchers for Kinetics Study

When studying kinetics with 4H in water, quenching solutions had to be prepared. The quenchers were added to the appropriate amount of water, usually 10 mL, in a cuvette. For glutathione, L-tyrosine methyl ester hydrochloride, L-alanine methyl ester hydrochloride, uracil, L-tryptophan methyl ester hydrochloride, L-ascorbate sodium salt, L-cystine dimethyl ester dihydrochloride and L-methionine methyl ester hydrochloride, 0.1M concentrations were used. For adenosine, 0.038 M was used because the adenosine did not dissolve freely in water. It was also important to check the UV of all of the quenchers to make sure that they did not absorb at the laser wavelength. Only tryptophan was studied at 355 nm because it absorbed too much at 308 nm for LFP studies at this wavelength.

When mixing the quencher with the azide solution, a UV spectrum was taken to ensure an absorbance in the range of 0.8 to 1.2, if this was not observed then depending on the absorbance, more of the azide solution was added or water was added for dilution. Once the absorbance was in the desired range then those same measurements would be used for the water and azide solution throughout the experiment. The only variable was the quencher.

2.2.4. Treatment of Data for the Amino Acid Quenching Study

The quenchers ascorbate, tryptophan, cystine, methionine, histidine ethyl ester ammonium salts, ammonium chloride, and n-methyl imidazole were studied at 355 nm; all other quenchers were studied at 308 nm excitation wavelength. A 0.1M solution of the quencher was prepared (except for adenosine which was 0.038M) and then it was analyzed by UV spectroscopy to make sure that it had a low absorption at the desired excitation wavelength. The quenchers that were not studied at 308 nm, usually (but not always) absorbed too highly at 308 nm and would have interfered with the absorption of the intermediate and so they were studied at 355 nm where their absorption was low. At 308 nm a probe wavelength of 420 nm was used and at 355 nm a probe wavelength of 420 nm was used. The amount of azide was always constant while the concentration of quencher was the variable.

To give examples that show decreasing/constant lifetimes the raw data was combined on a single graph. One must keep in mind that only graphs on the same timescales can be combined and so for this reason some of the raw kinetic data will not look very different. For example the graph of tyrosine ethyl ester hydrochloride uses 20

uL and 35 uL volumes of quencher, and the 5 uL and the 35 uL could not be shown together because the 5 uL sample was studied on a 500 ns scale while the 35 uL sample was studied on a 100 ns scale. In the case of tyrosine ethyl ester hydrochloride there are two accompanying graphs that show the 5 uL sample and the 35 uL sample individually to display how the rate differs.

2.3 Results

2.3.1. OMA's Obtained by LFP of 4-azido acetophenone

In an LFP experiment one must first determine the absorption spectrum of reactive intermediates produced upon excitation of the precursor. This is accomplished using an Optical Multi-channel Analyzer (OMA). In this experiment one records a difference spectrum. The absorption of precursor in solvent is recorded. Then the absorption of the solution is recorded slightly after the laser pulse. The delay between the firing of the laser and the recording of the spectrum is variable (0, 1, 10, 100 ns or 1, 10, 100 us). Then the spectrum recorded without a laser pulse is subtracted from the spectrum recorded after the laser pulse. A “difference spectrum” is thereby produced, when the difference spectrum is negative it is due to “bleaching” of azide precursor into scattered laser light or fluorescence. Where the difference spectrum is positive it is due to absorption of a light generated species. “Difference” or “transient” spectra produced by LFP of 4H in water are shown in figures 2.3-2.7.

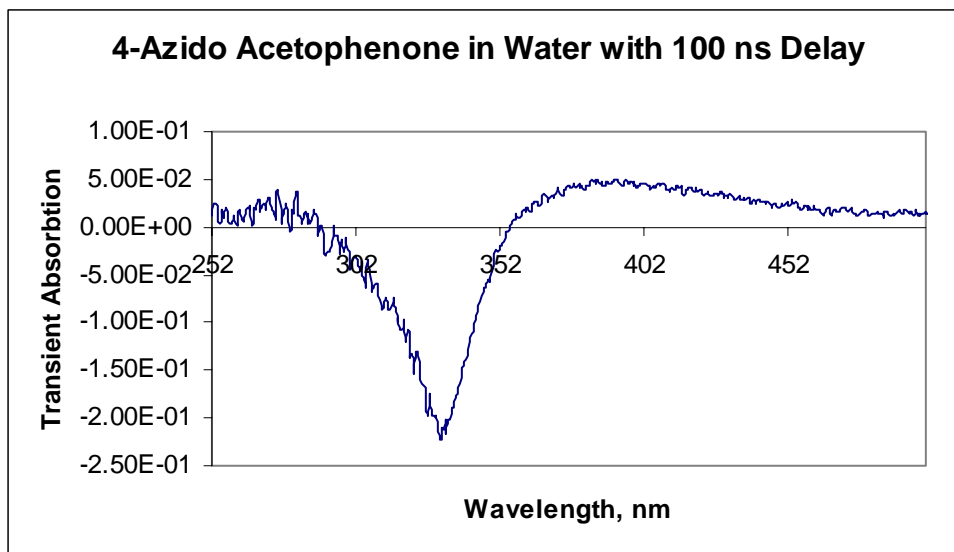


Figure 2.3 The transient spectrum produced upon LFP of 4-azidoacetophenone in water. The spectrum was recorded with a 100 ns delay at 266 nm excitation wavelength taken on 8/11/04.

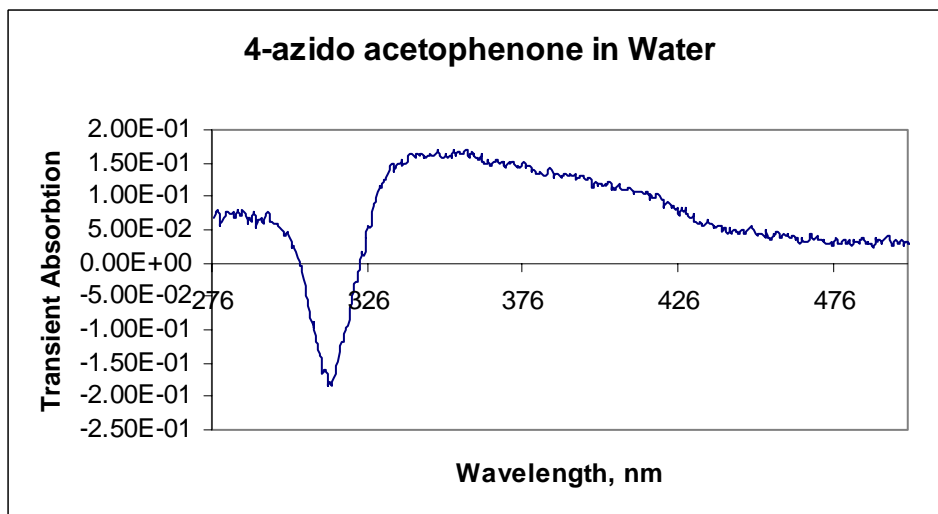


Figure 2.4 The transient spectrum produced upon LFP of 4-azidoacetophenone in water. The spectrum was recorded with no delay at 308 nm excitation wavelength taken on 8/18/04.

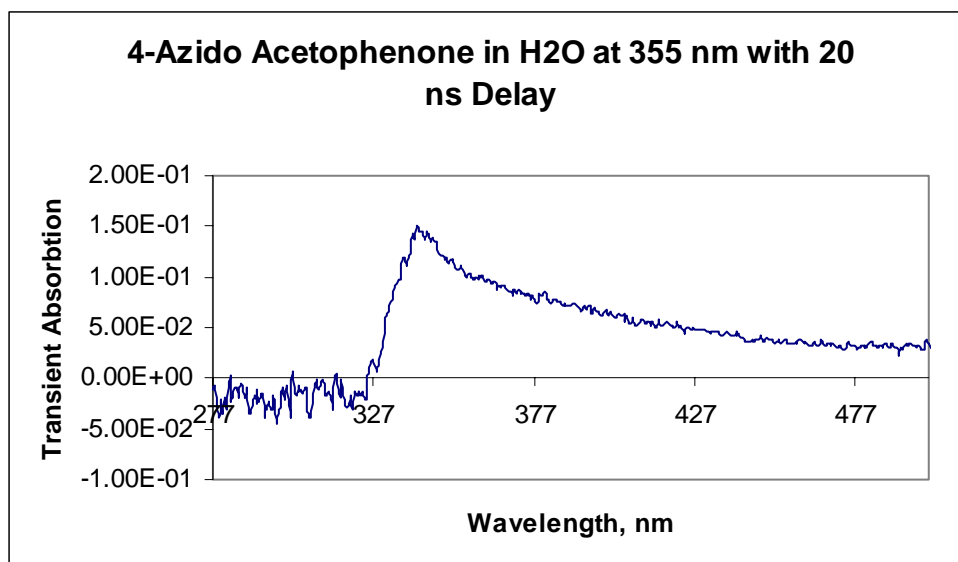


Figure 2.5 The transient spectrum produced upon LFP of 4-azidoacetophenone in water. The spectrum was recorded with a 20 ns delay at 355 nm excitation wavelength taken on 8/31/04.

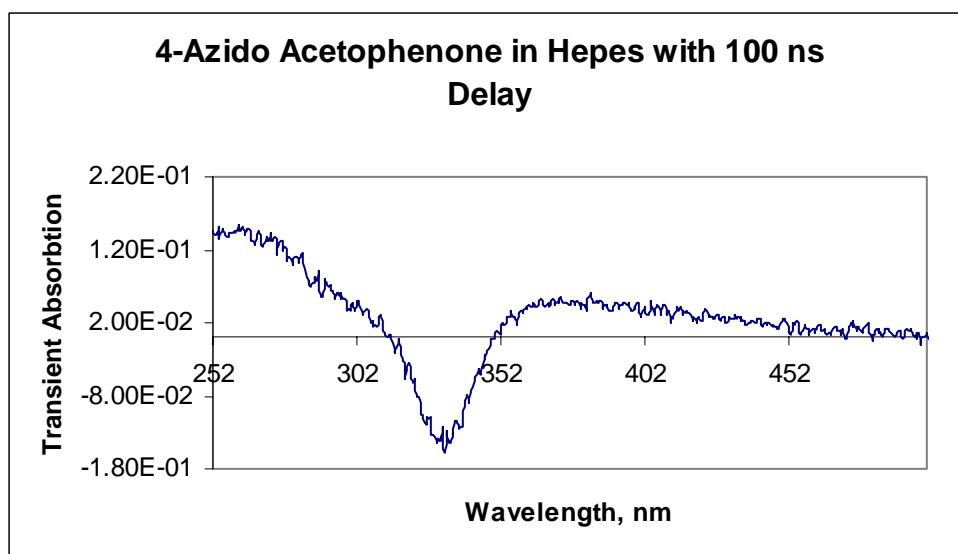


Figure 2.6 The transient spectrum produced upon LFP of 4-azidoacetophenone in water. The spectrum was recorded with a 100 ns delay at 266 nm excitation wavelength taken on 8/11/04.

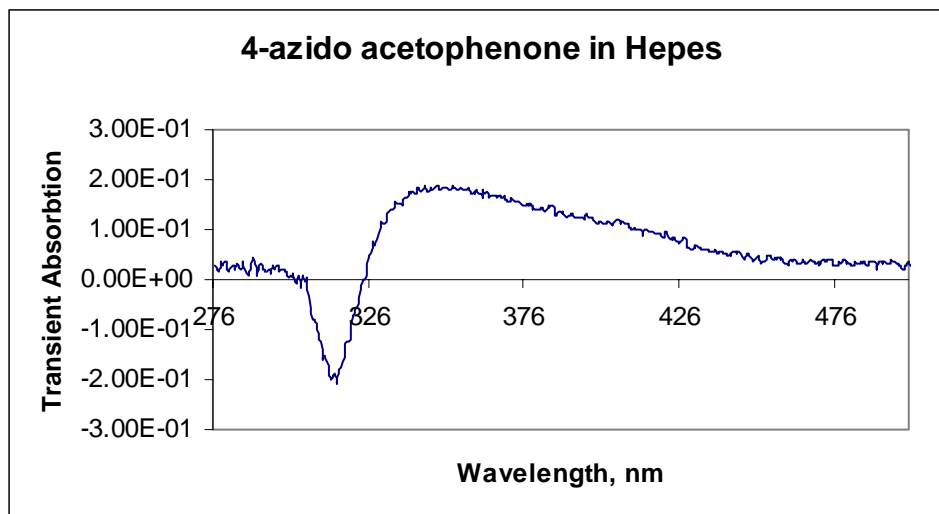


Figure 2.7 The transient spectrum produced upon LFP of 4-azidoacetophenone in water. The spectrum was recorded with no delay at 308 nm excitation wavelength taken on 8/18/04.

Discussion of OMA's obtained by LFP of 4H

The purpose of collecting the OMA's was to learn where the intermediates produced upon photolysis of 4H absorb and to observe the general characteristics of their kinetics. It was found that the maximum absorbance of the intermediates was at approximately 330 nm to 380 nm depending on solvent and wavelength.

2.3.2. 4H Reactive Intermediates Studied by Laser Flash Photolysis (LFP) in Water and Benzene

OMA

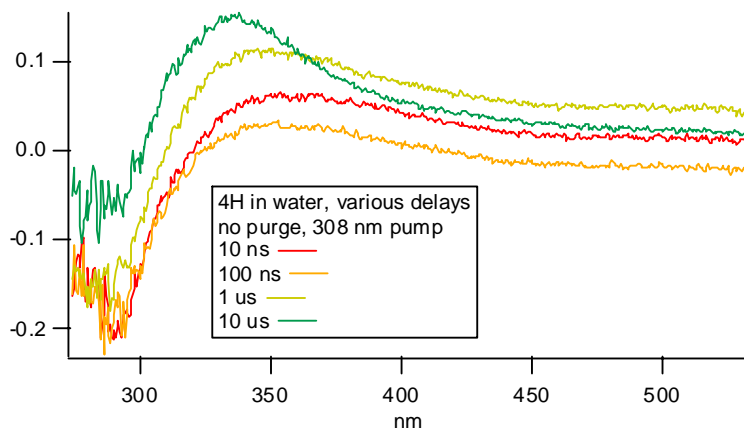


Figure 2.8 The transient spectrum produced upon LFP of 4-azidoacetophenone in water.

The spectrum was recorded with various delays at 308 nm excitation wavelength.

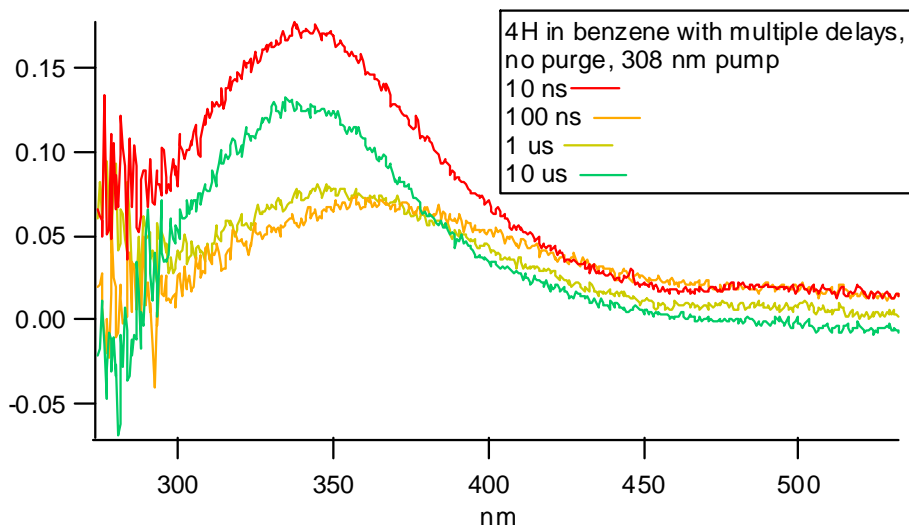


Figure 2.9 The transient spectrum produced upon LFP of 4-azidoacetophenone in benzene. The spectrum was recorded with various delays at 308 nm excitation wavelength.

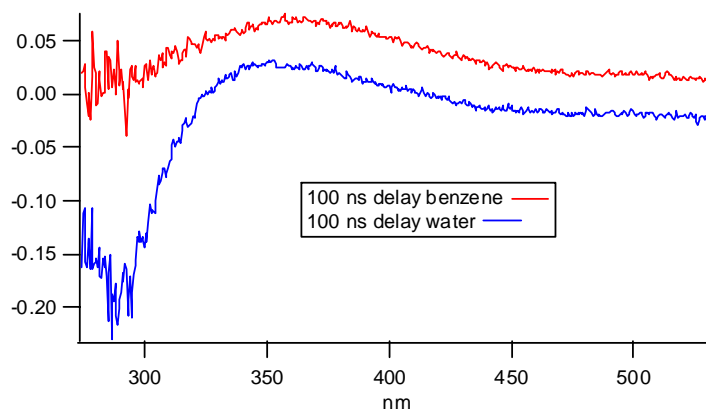


Figure 2.10 The transient spectrum produced upon LFP of 4-azidoacetophenone in benzene (red) and water (blue). The spectrum was recorded with 100 ns delays at 308 nm excitation wavelength.

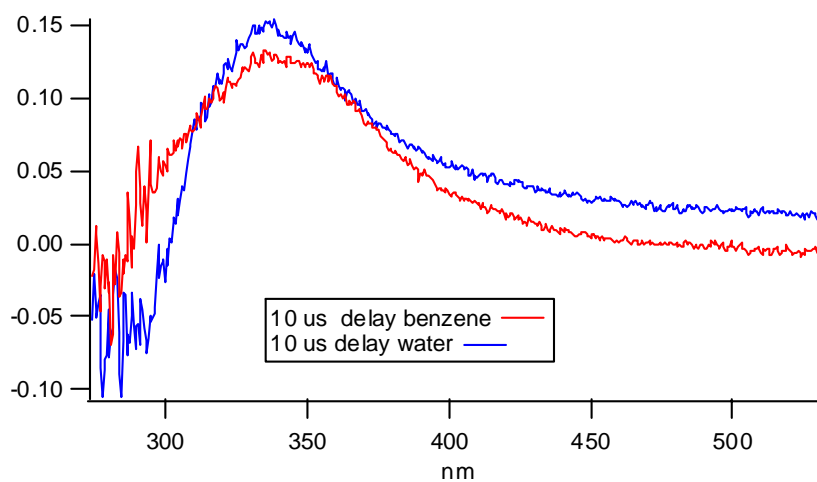


Figure 2.11 The transient spectrum produced upon LFP of 4-azidoacetophenone in benzene (red) and water (blue). The spectrum was recorded with 10 us delays at 308 nm excitation wavelength.

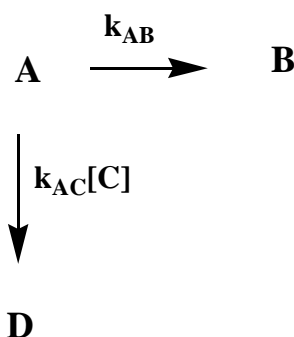
Discussion of the OMA's Recorded in Water and Benzene

This experiment was important in understanding the solvent effect observed on the reactive intermediates produced upon photolysis of 4H. When viewing the figure pertaining to this experiment, Figure 2.10, it is obvious that two slightly different transient UV spectra are observed. This will support the conclusion that different intermediates are initially formed in different solvents depending on the polarity of the solvent. Figure 2.11, recorded 100 us after the flash will be assigned to azo dimer **7a**, formed by triplet nitrene dimerization.

2.3.3. Kinetic Quenching Study of 4H in Water with Various Biological Molecules

The general kinetic scheme observed is shown below in scheme 2.1:

Scheme 2.1



Reactive intermediate A is produced in a 5-17 ns laser pulse. It decays by first order and pseudo first order processes. The sum of all first order and pseudo first order rate constants is represented as k_{ab} where B is all the products formed.

In the presence of C, some of intermediate A reacts with C to form D. The concentration of C greatly exceeds that of transient species A and thus is also a pseudo first order process.

Under these conditions, equation 2.1 is valid.

$$\frac{-dA}{dt} = k_{AB}[A] + k_{AC}[A][C] = (k_{AB} + k_{AC}[C]) * [A] \quad 2.1$$

The decay of A will be exponential,

$$A_t = A_0 e^{-(k_{AB} + k_{AC}[C]) * t} \quad 2.2$$

where A_t is the concentration of A at time t and A_0 is the concentration of A immediately after the laser flash.

The decay of A is fit to the best exponential to obtain a time constant, k_{obs} , where

$$k_{obs} = k_{AB} + k_{AC}[C] \quad 2.3$$

The experiment is then repeated at several concentrations of C. A plot of k_{obs} versus $[C]$ is linear with slope = k_{ac} , a second order rate constant. The intercept of the plot is k_{ab} . By definition the lifetime of A in the absence of C, is τ , where $\tau = 1/k_{\text{ab}}$.

In each of the kinetic experiments a biological quencher was present in an attempt to trap reactive intermediates produced by LFP of 4-azido acetophenone in water and then the rate of decay of the intermediate was recorded. The biological quenchers tested were: glutathione, adenosine, uracil, L-tyrosine methyl ester hydrochloride, L-alanine methyl ester hydrochloride, L-tryptophan methyl ester hydrochloride, L-ascorbate sodium salt, L-cystine dimethyl ester dihydrochloride, L-methionine methyl ester hydrochloride, ammonium chloride, L-histidine methyl ester dihydrochloride, and N-methyl imidazole.

Lifetimes of 4H Derived Intermediates in the Presence of Ketenimine Quenchers

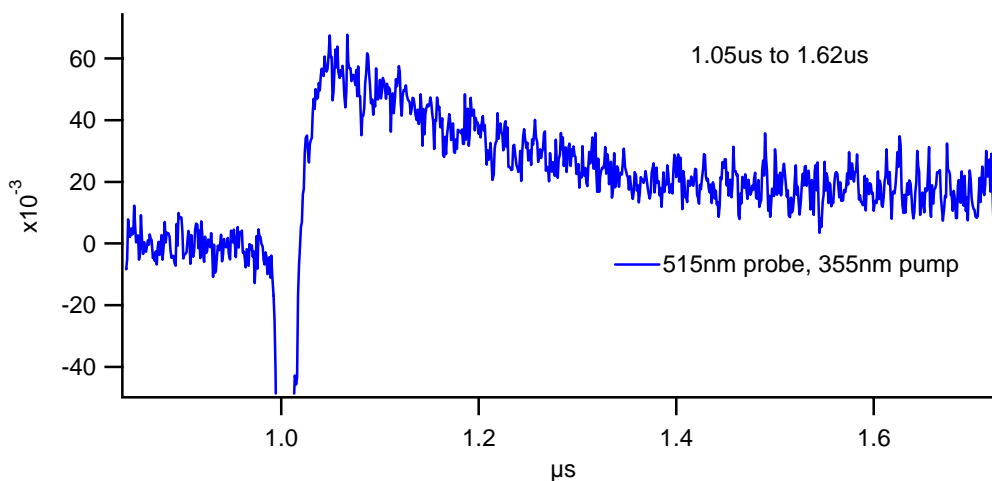


Figure 2.12 The transient decay spectrum produced upon LFP of 4-azidoacetophenone in water. The spectrum was recorded with no delay at 355 nm excitation wavelength and 515 nm probe.

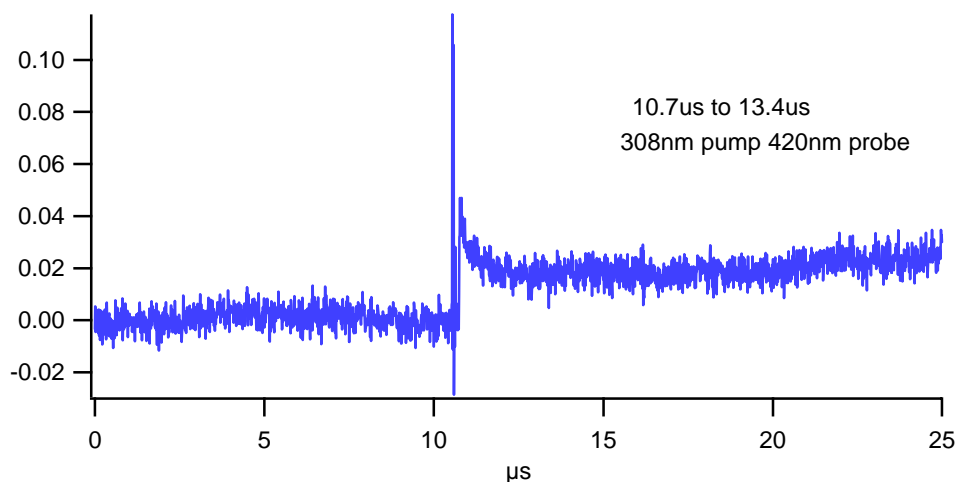


Figure 2.13 The transient decay spectrum produced upon LFP of 4-azidoacetophenone in water. The spectrum was recorded with no delay at 308 nm excitation wavelength and 420 nm probe.

4-azido acetophenone in H₂O with Adenosine

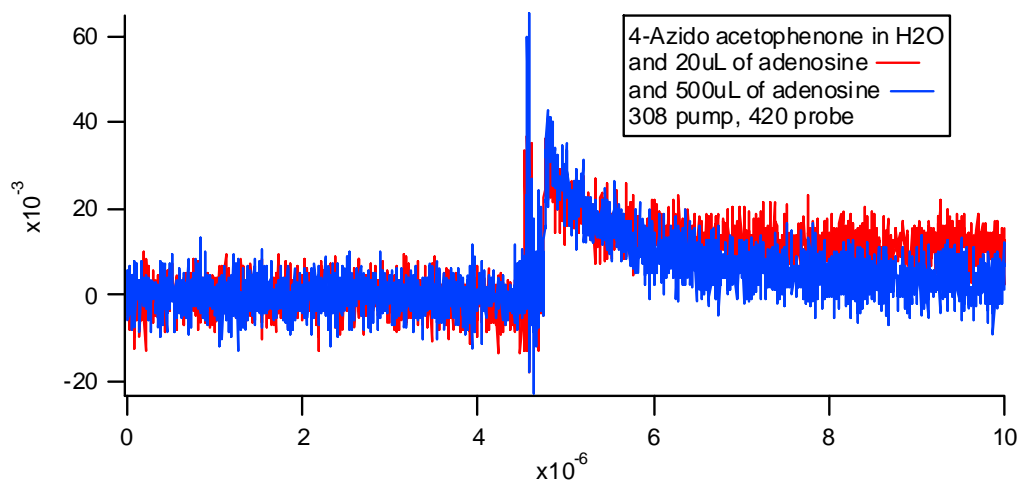


Figure 2.14 The decay of 420 nm absorption in the presence of 20 μL of adenosine (red) and 500 μL of adenosine (blue) solution with 4-azido acetophenone in H₂O intermediate produced from 4-azido acetophenone experiments in H₂O.

The observed pseudo first order rate constant of decay (k_{obs}) of the 420 nm species does not change with adenosine concentration. Thus, the 420 nm species is not reacting with adenosine at a measurable rate under the experimental conditions.

4-azido acetophenone in H₂O with Uracil

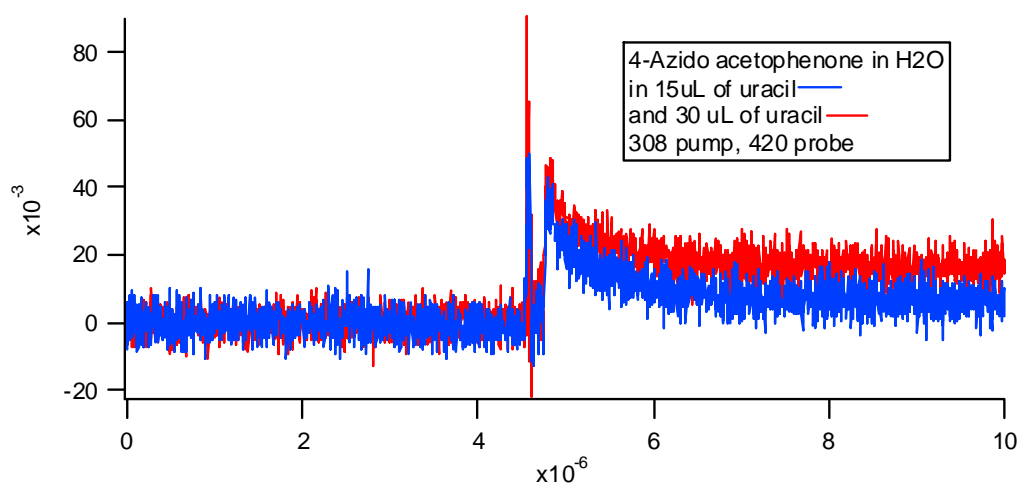


Figure 2.15 The decay of 420 nm absorption in the presence of 15 uL of uracil (blue) and 30 uL of uracil (red) solution with 4-azido acetophenone in H₂O, note the poor signal to noise ratio.

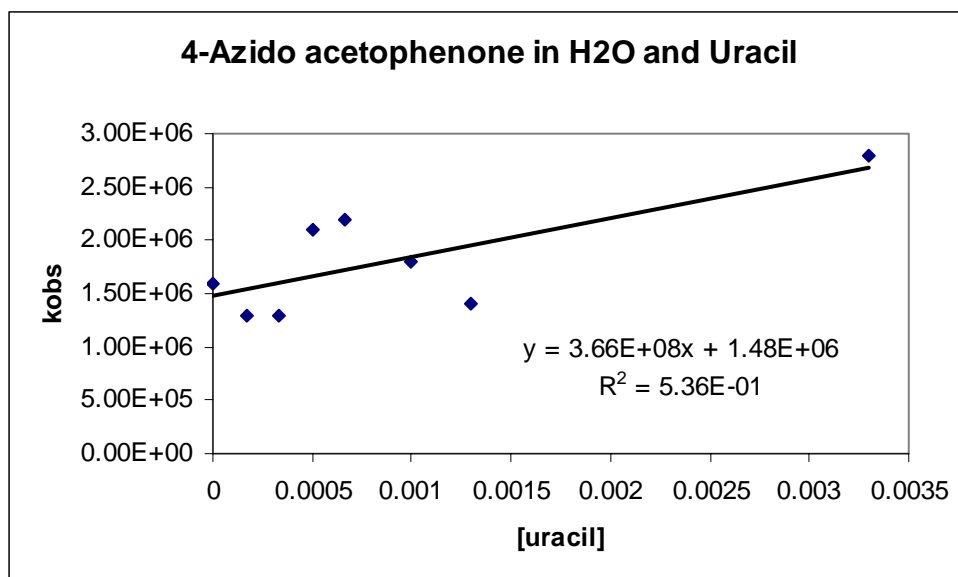


Figure 2.16 A plot of k_{obs} versus $[uracil]$ concentration obtained by LFP of 4H in water.

A plot of k_{obs} vs. $[uracil]$ is highly scattered. This plot indicates that the carrier of the 420 nm absorption does not react with uracil.

4-azido acetophenone in H₂O and L-Tyrosine methyl ester hydrochloride

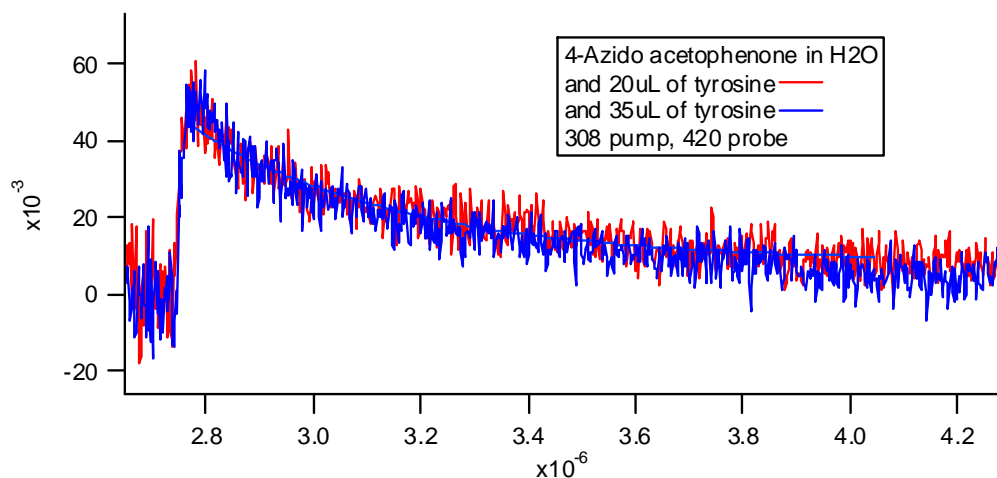


Figure 2.17 The decay of 420 nm absorption in the presence of 20 uL of tyrosine (blue) and 35 uL of tyrosine (red) solution with 4-azido acetophenone in H₂O, note the poor signal to noise ratio.

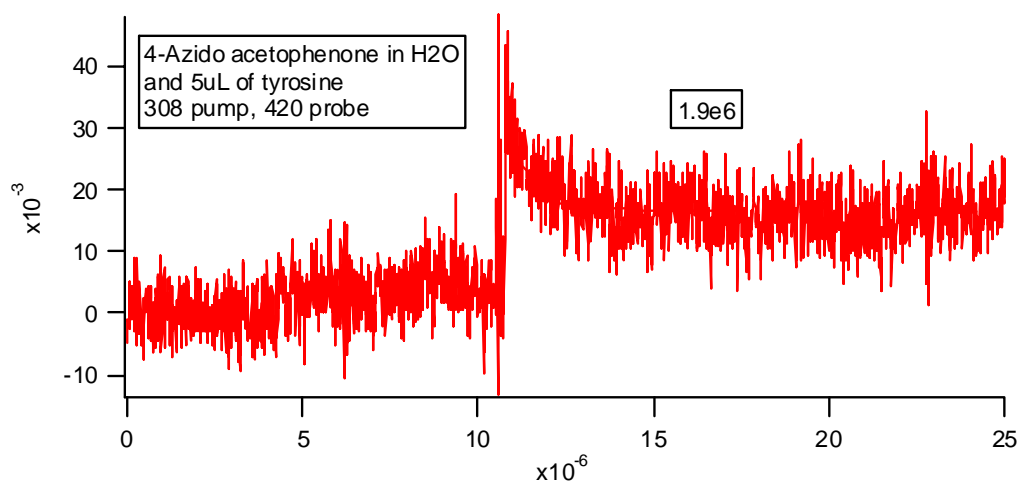


Figure 2.18 The decay of 420 nm absorption in the presence of 5 uL of tyrosine solution with 4-azido acetophenone in H₂O, note the wavy baseline and the poor signal to noise ratio.

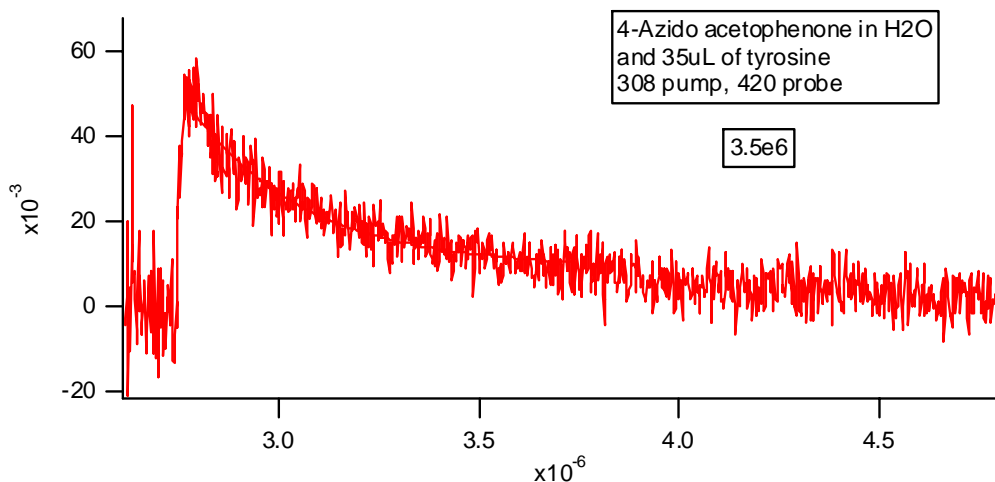


Figure 2.19 The decay of 420 nm absorption in the presence of 35 uL of tyrosine solution with 4-azido acetophenone in H₂O.

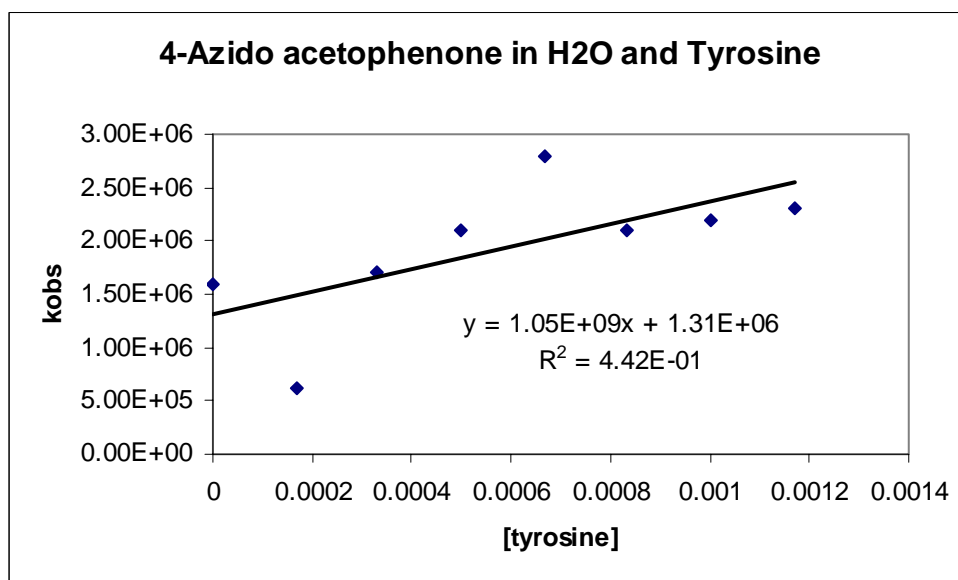


Figure 2.20 A plot of k_{obs} versus [tyrosine] concentration obtained by LFP of 4H in water.

The data is scattered and there is no evidence of reaction between the 420 nm absorbing species and tyrosine.

4-azido acetophenone in H₂O and L-Alanine methyl ester hydrochloride

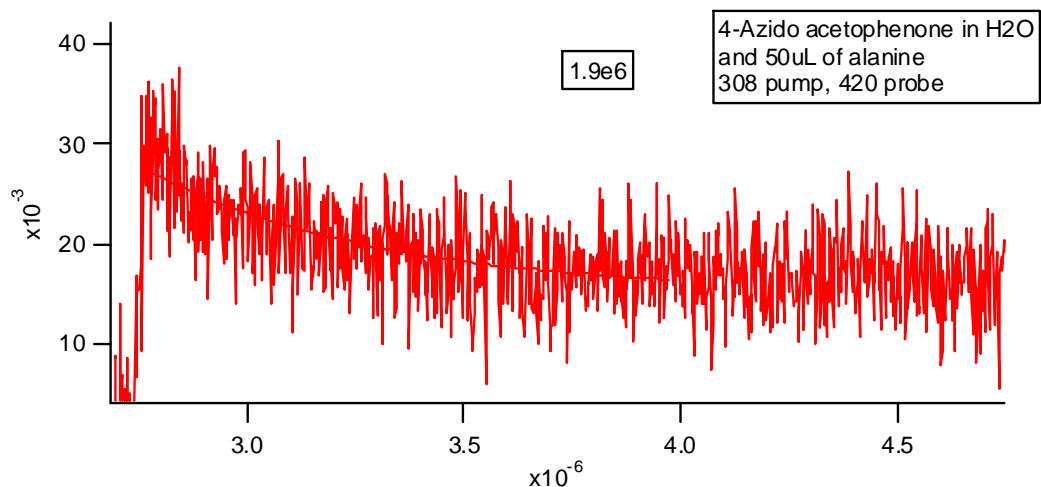


Figure 2.21 The decay of 420 nm absorption in the presence of 50 uL of alanine solution with 4-azido acetophenone in H₂O, note the poor signal to noise ratio.

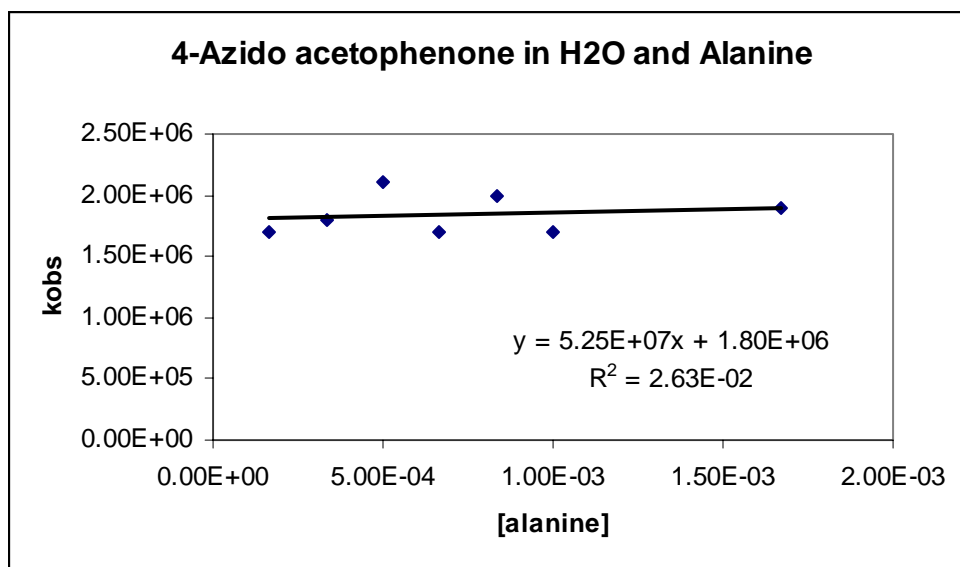


Figure 2.22 A plot of k_{obs} versus [alanine] concentration obtained by LFP of 4H in water.

The value of k_{obs} does not vary as a function of alanine concentration. The carrier of the 420 nm absorption does not react with alanine.

4-azido acetophenone in H₂O and L-Tryptophan methyl ester hydrochloride

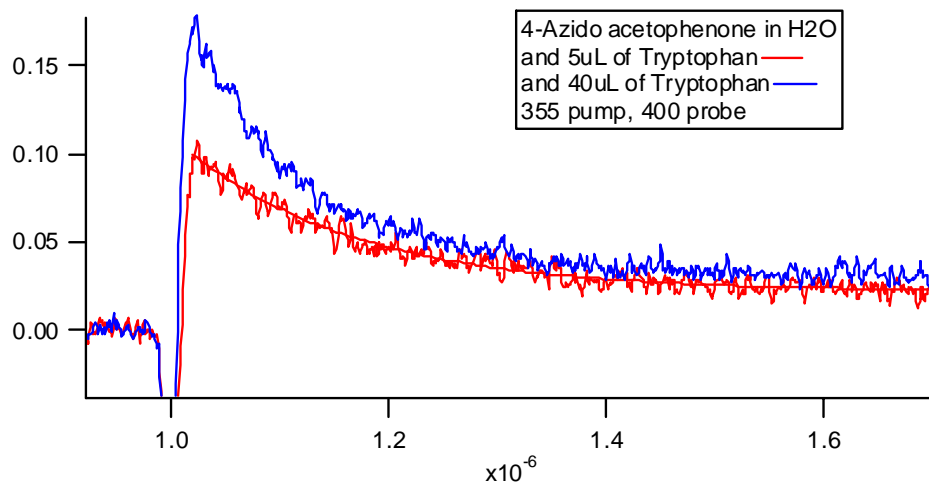


Figure 2.23 The decay of 420 nm absorption in the presence of 5 uL of tryptophan (red) and 40 uL of tryptophan (blue) solution upon LFP of 4H in H₂O.

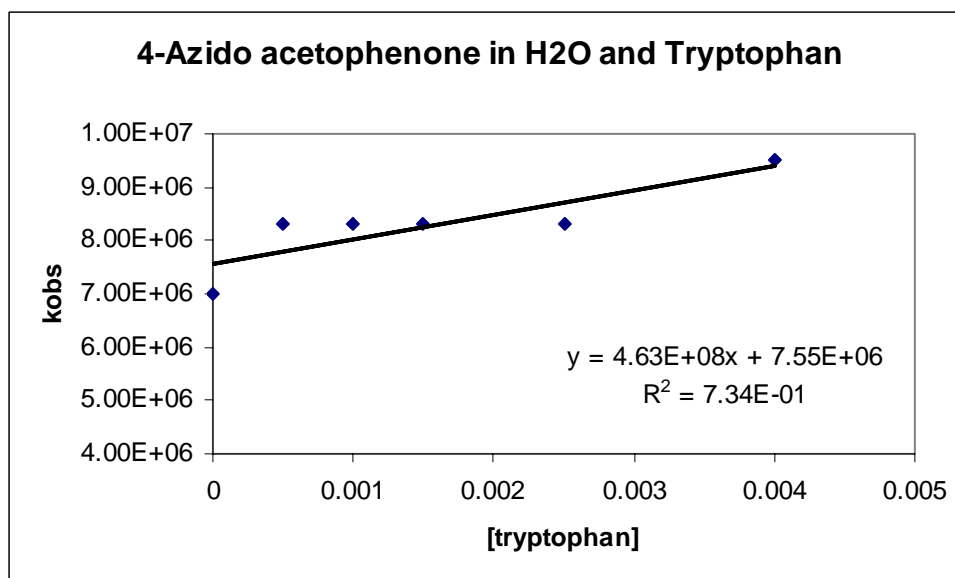


Figure 2.24 A plot of k_{obs} versus [tryptophan] concentration obtained by LFP of 4H in water.

The data indicates that the carrier of the 420 nm absorption does not react with tryptophan.

4-azido acetophenone in H₂O and L-Cystine dimethyl ester dihydrochloride

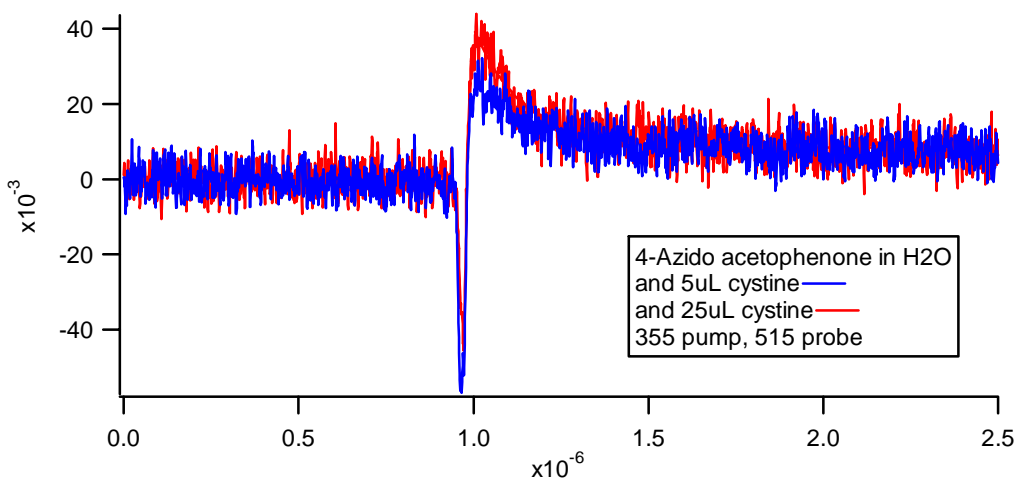


Figure 2.25 The decay of 420 nm absorption in the presence of 5 uL of cystine (blue) and 25 uL of cystine (red) solution upon LFP of 4H in H₂O.

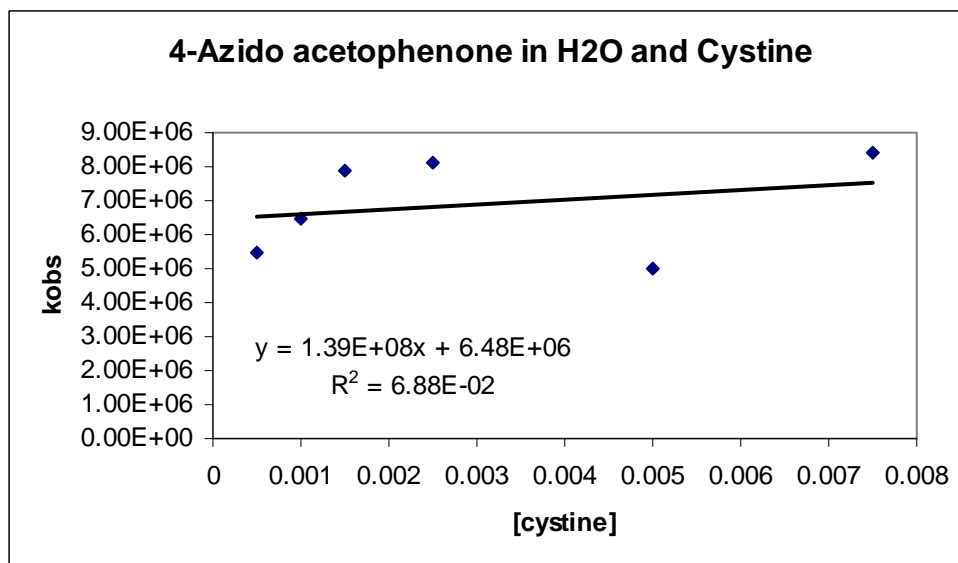


Figure 2.26 A plot of k_{obs} versus [cystine] concentration obtained by LFP of 4H in water.

The plot indicates that the carrier of the 420 nm absorption does not react with cystine.

4-azido acetophenone in H₂O and L-Methionine methyl ester hydrochloride

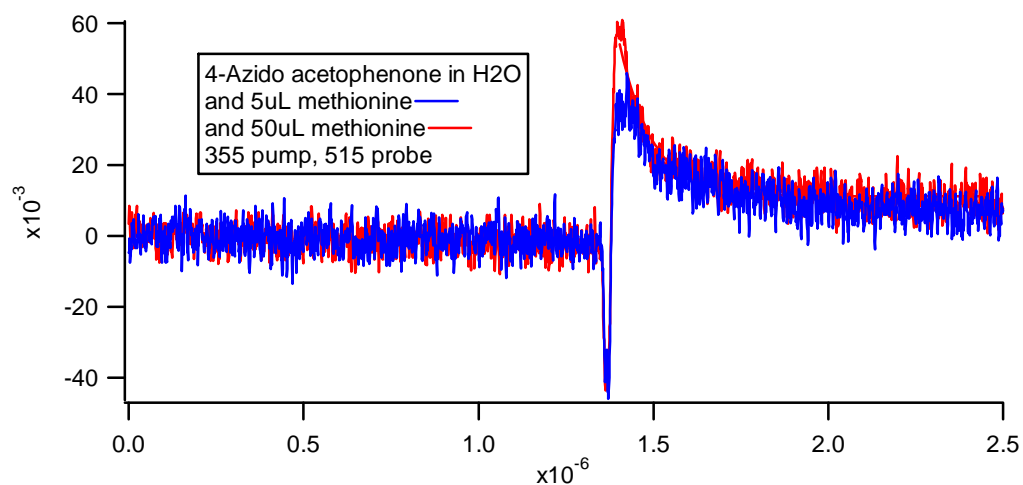


Figure 2.27 The decay of 420 nm absorption in the presence of 5 uL of methionine (blue) and 50 uL of methionine (red) solution upon LFP of 4H in H₂O.

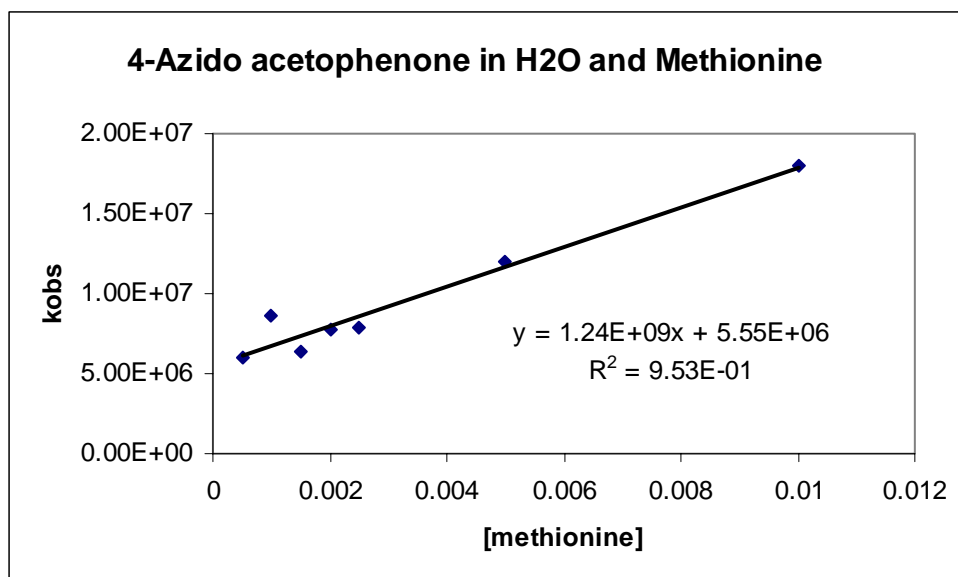


Figure 2.28 A plot of k_{obs} versus [methionine] concentration obtained by LFP of 4H in water.

There is clear evidence of reaction with the carrier of transient absorption in the case of methionine.

4-azido acetophenone in H₂O and Ammonium Chloride

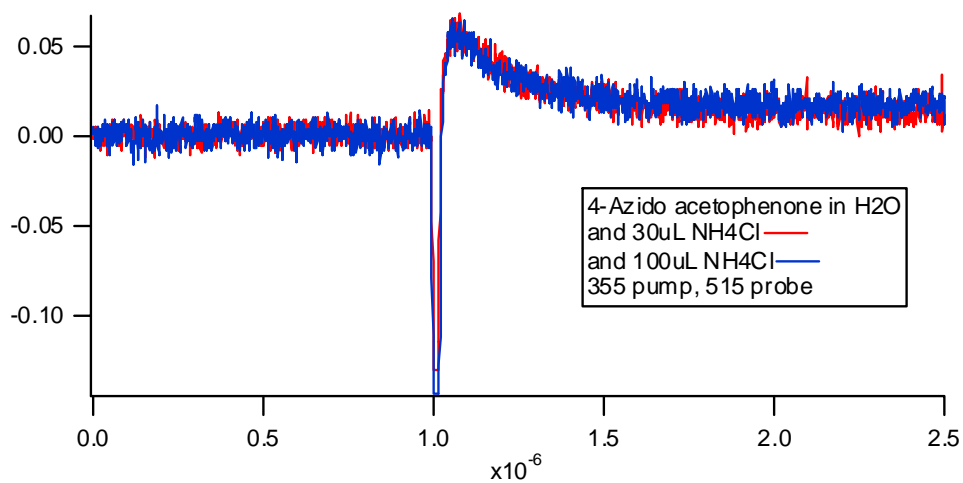


Figure 2.29 The decay of 420 nm absorption in the presence of 30 uL of NH₄Cl (blue) and 100 uL of NH₄Cl (red) solution upon LFP of 4H in H₂O.

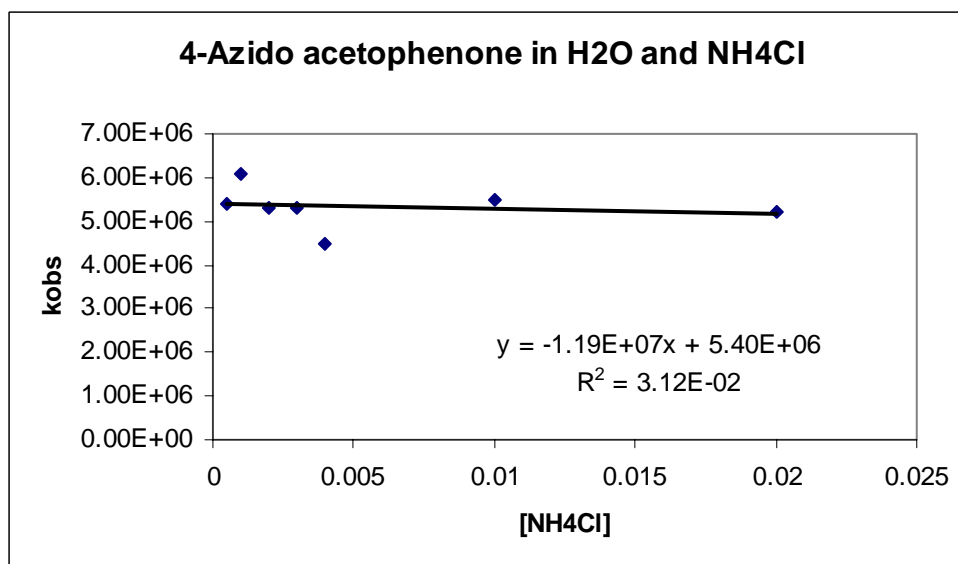


Figure 2.30 A plot of k_{obs} versus [NH₄Cl] concentration obtained by LFP of 4H in water.

The decay rate does not depend on the concentration of ammonium chloride. Hence, there is no evidence of reaction of the carrier of the 420 nm absorption with ammonium chloride.

4-azido acetophenone in H₂O and L-Histidine methyl ester dihydrochloride

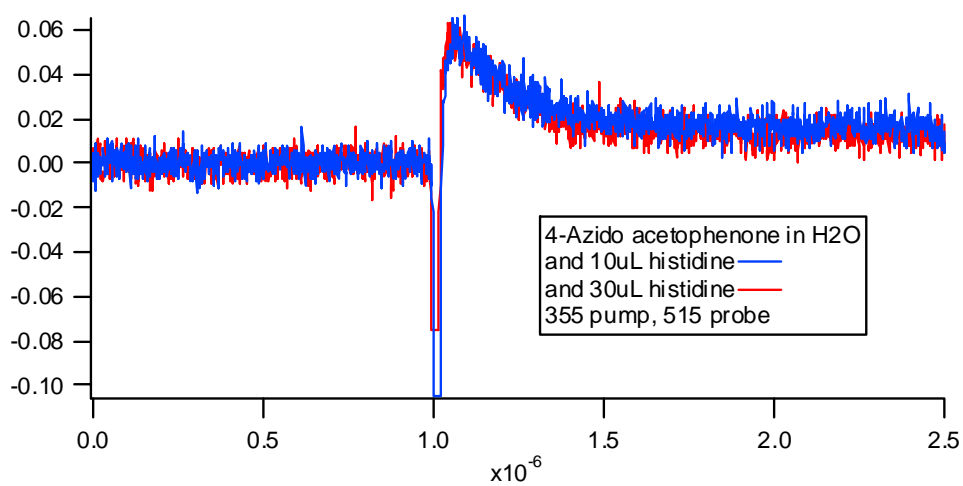


Figure 2.31 The decay of 420 nm absorption in the presence of 10 uL of histidine (blue) and 30 uL of histidine (red) solution upon LFP of 4H in H₂O.

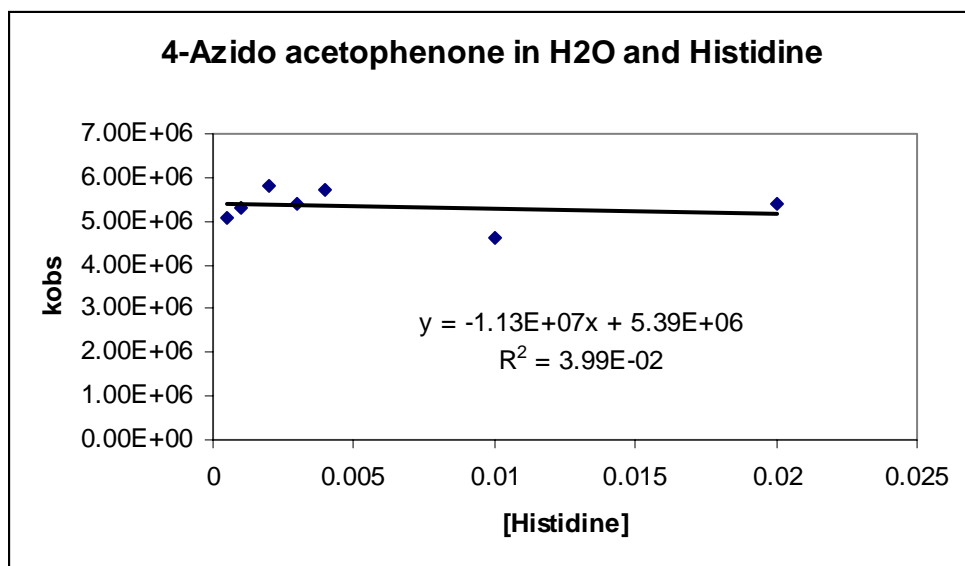


Figure 2.32 A plot of k_{obs} versus [histidine] concentration obtained by LFP of 4H in water.

The data indicates that the carrier of the 420 nm absorption does not react with histidine.

4-azido acetophenone in H₂O and N-methyl imidazole

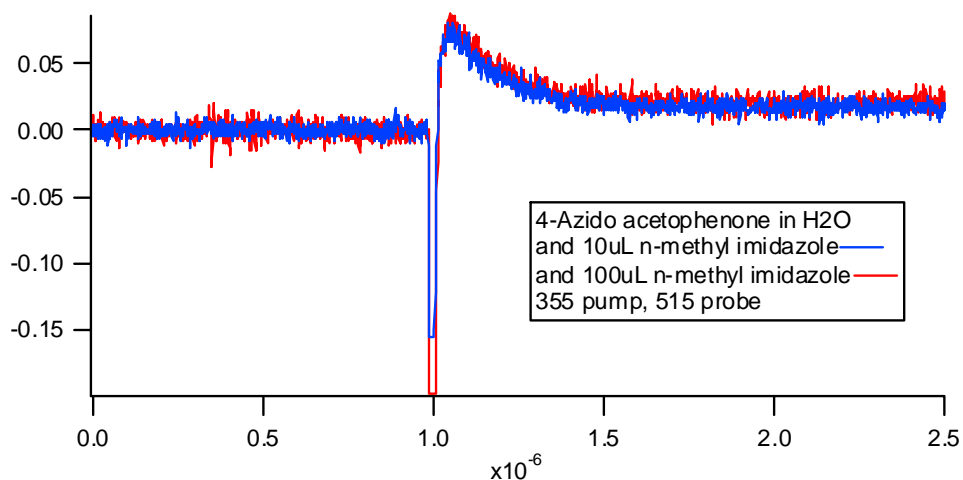


Figure 2.33 The decay of 420 nm absorption in the presence of 10 uL of N-methyl imidazole (blue) and 100 uL of N-methyl imidazole (red) solution upon LFP of 4H in H₂O.

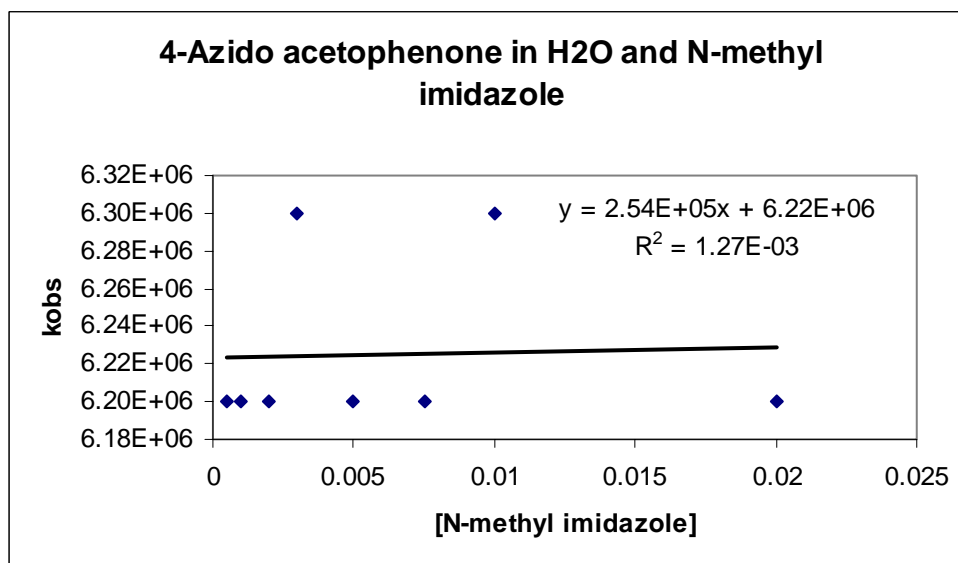


Figure 2.34 A plot of k_{obs} versus [N-methyl imidazole] concentration obtained by LFP of 4H in water.

The data indicates that the carrier of the 420 nm absorption does not react with N-methyl imidazole.

Lifetimes of 4H Derived Intermediates in the Presence of Reducing Agents: Glutathione (GSH) and Sodium Ascorbate

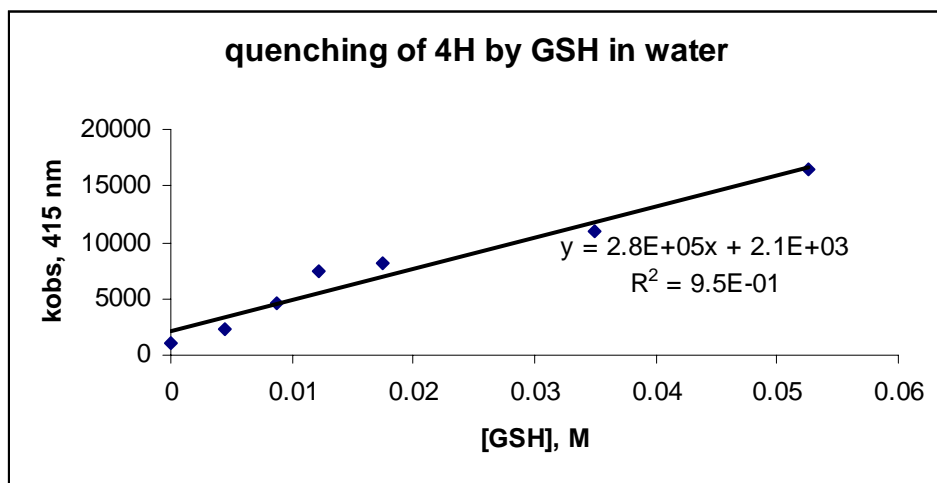


Figure 2.35 A plot of k_{obs} versus [glutathione] concentration obtained by LFP of 4H in water.

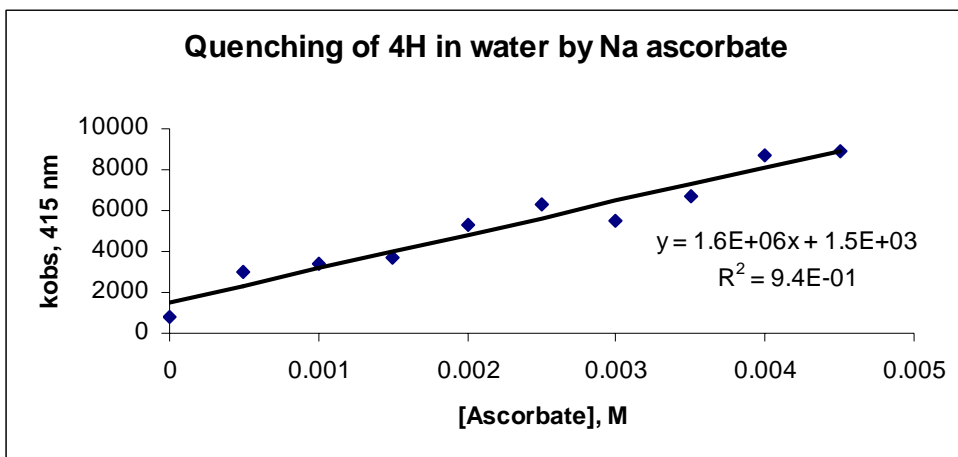


Figure 2.36 A plot of k_{obs} versus [Sodium ascorbate] concentration obtained by LFP of 4H in water.

Both of the above triplet quenchers show clear evidence that the carrier 420 nm absorption react with glutathione and sodium ascorbate.

Summary of Kinetic Data in Water

Table 2.1 contains a summary of all of the rate constants determined by LFP of 4-azidoacetophenone (4H) in water as a function of quencher. All measurements were made at 420 nm at ambient temperature in air.

Table 2.1 Summary of Rate Constants in Water

Quencher	Reactivity in Water (M⁻¹s⁻¹)
Adenosine	None
Alanine	None
Ammonium Cl	None
Ascorbate	1.6E+06
Cystine	None
Glutathione	2.8E+05
Histidine	None
Methionine	1.24E+09
N-methyl Imidazole	None
Tryptophan	None
Tyrosine	None
Uracil	None

Discussion of Quenching Studies in Water

Ketenimines are electrophiles and as such react with nucleophiles. This is illustrated by the reaction of parent 1,2-didehydroazepine (cyclic ketenimine, 1,2,4,6-azacyloheptatetranene) with diethyl amine¹⁵.

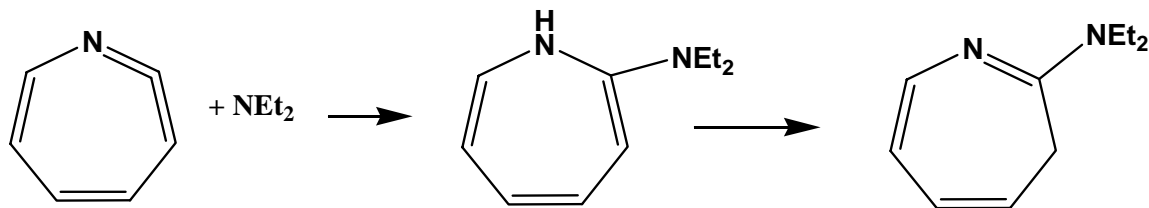


Figure 2.37 Reaction of ketenimine with diethyl amine.

Mary Rizk¹⁶ discovered that photolysis of phenyl azide, 3-methoxy phenyl azide and 3-nitrophenyl azide in water produces the corresponding ketenimines. These ketenimines react with biologically relevant nucleophiles such as indole (tryptophan), phenol (tyrosine) and imidazole (histidine). The nitro group accelerates the reactivity and the electron donating methoxy group decelerates the reactivity. Thus, we expected that the electron withdrawing acetyl group would lead to the formation of a highly reactive ketenimine. However, as shown in Table 2.1 the reactive intermediate produced in water does not react with nucleophiles. In fact, it only reacts with reducing agents such as ascorbate, glutathione, and methionine.

Li and Schuster¹³ have demonstrated that triplet nitrenes react with reducing agents. This reaction produces aniline, not adducts as desired in PAL and cross-linking experiments.

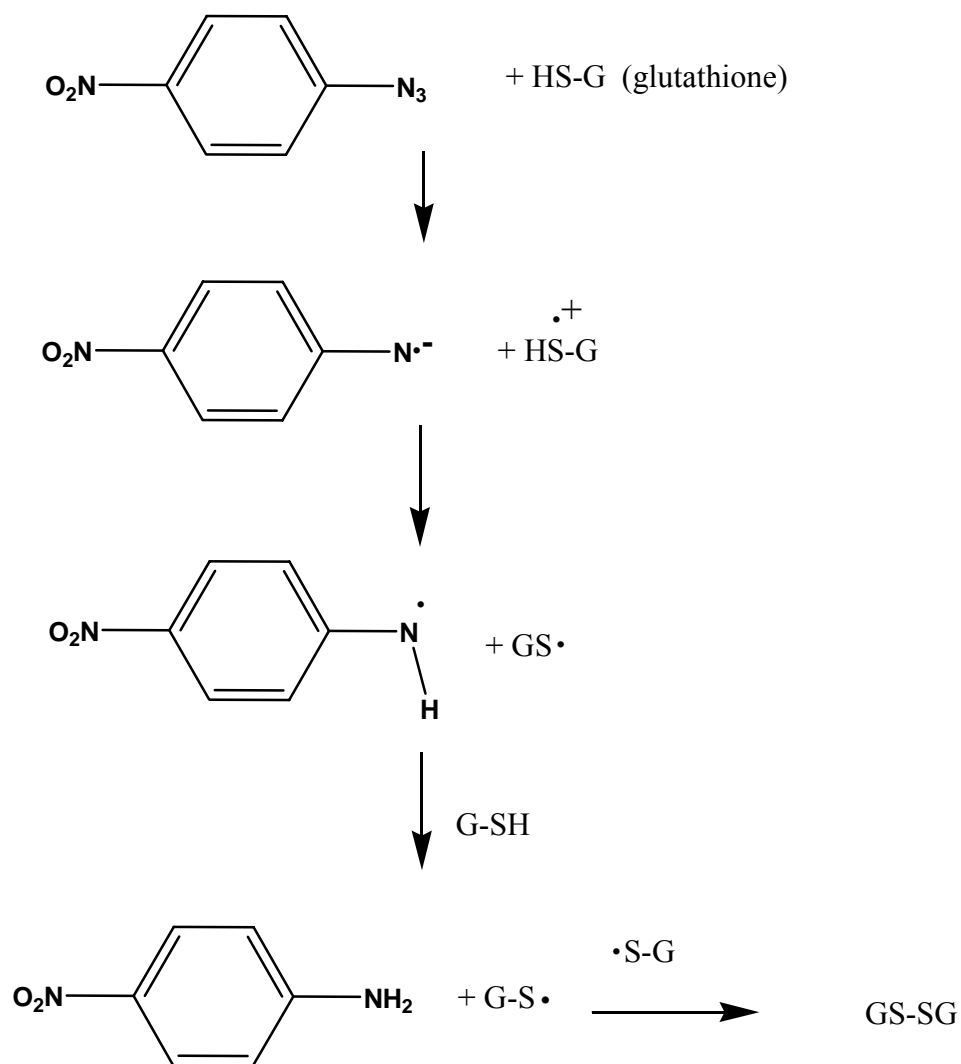


Figure 2.38 Demonstration of triplet nitrene reacting with a reducing agent.

Therefore, our data indicates that the reactive intermediate produced upon photolysis of 4H in water is triplet 4-acetylphenylnitrene **3a** (Scheme 1.1).

2.3.4. Study of 4H Intermediates with Ketenimine Quenchers in Benzene

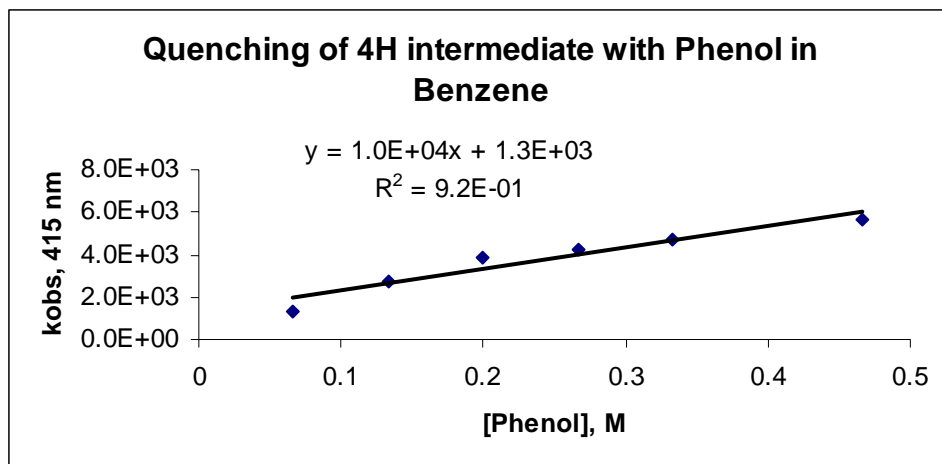


Figure 2.39 A plot of k_{obs} versus [phenol] concentration obtained by LFP of 4H in benzene.

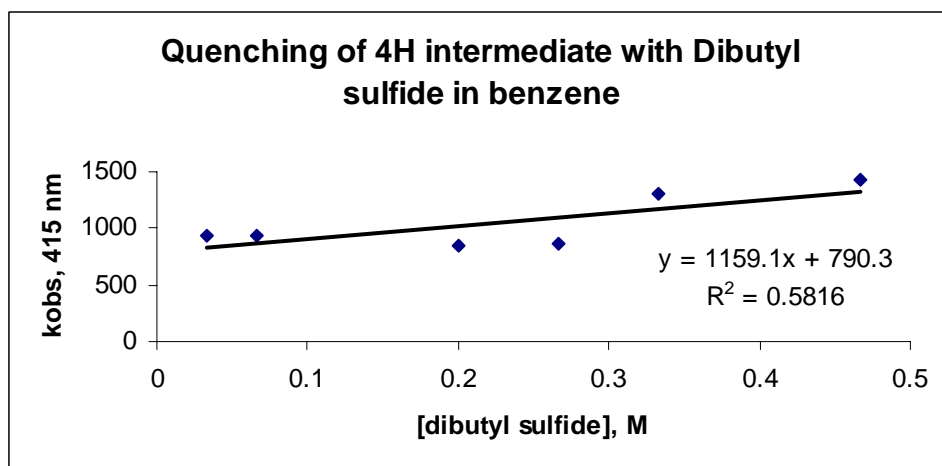


Figure 2.40 A plot of k_{obs} versus [dibutyl sulfide] concentration obtained by LFP of 4H in benzene.

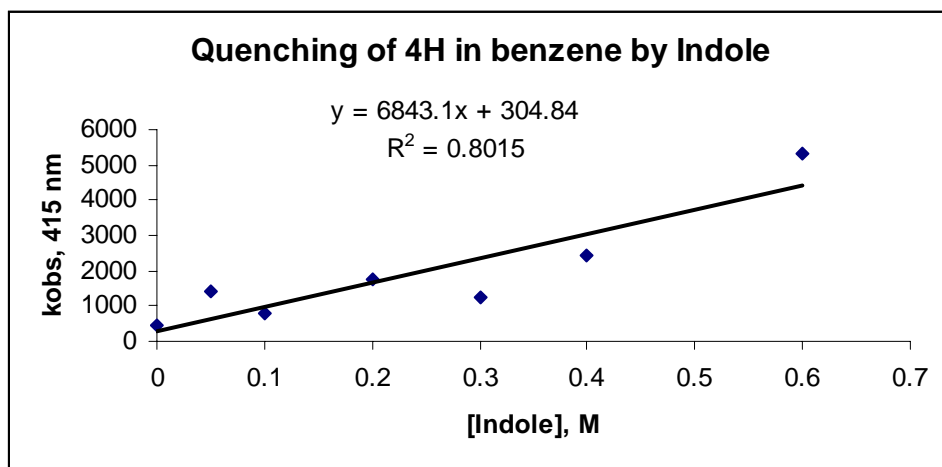


Figure 2.41 A plot of k_{obs} versus [indole] concentration obtained by LFP of 4H in benzene.

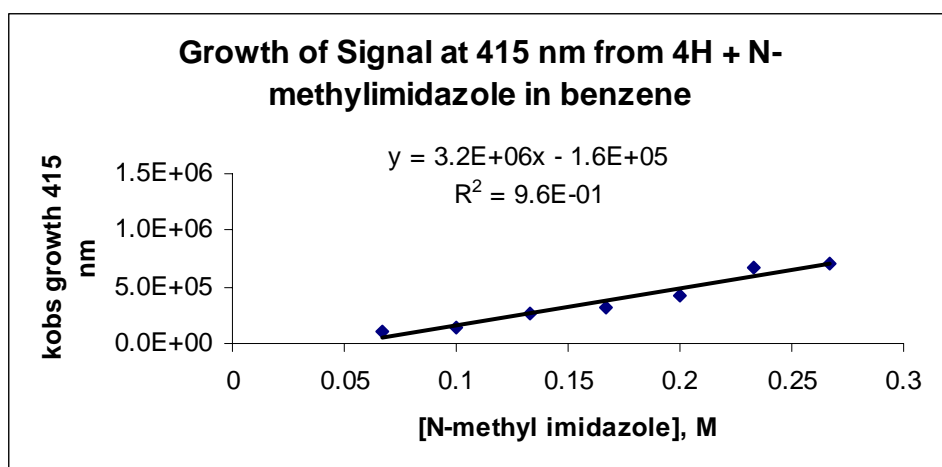


Figure 2.42 A plot of k_{obs} versus [N-methyl imidazole] concentration obtained by LFP of 4H in benzene.

Summary of reactivity of 4H intermediates with biological quenchers in organic solvent.

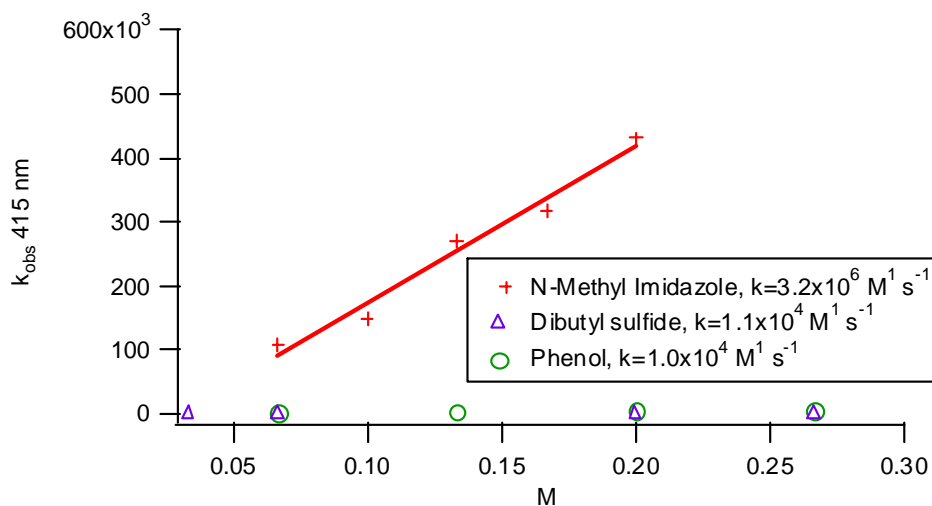


Figure 2.43 A plot of k_{obs} versus [concentration] of N-methyl imidazole, dibutyl sulfide, and phenol obtained by LFP of 4H in benzene.

Summary of the Reactivity of 4H Intermediate in Benzene

Table 2.2 Summary of Rate Constants in Benzene

Quencher	Reactivity in Benzene ($M^{-1}s^{-1}$)
N-methylimidazole	3.2E+6
Dibutylsulfide	1.1E+3
Phenol	1.0E+4
Indole	6.8E+3

Discussion of Quenching Study in Benzene

LFP of 4H in benzene produces a transient species which does react with nucleophiles (Table 2.2) unlike the transient species observed in water. Furthermore, the transient signals observed in benzene were stronger than those obtained in water. Thus,

the signal to noise ratio is better in the organic solvent and better quality data was obtained. This also indicates that different intermediates are formed in benzene and in water. Thus, we conclude that photolysis of 4H in benzene produces ketenimine as the reactive intermediate. We conclude that there is a huge solvent effect on the photochemistry of 4-azidoacetophenone and singlet para-acetylphenylnitrene.

2.3.5. Studies to Confirm the Solvent Effect

LFP Experiments

The following LFP experiments were performed in order to confirm the solvent effect present between hydrophobic and hydrophilic solvents.

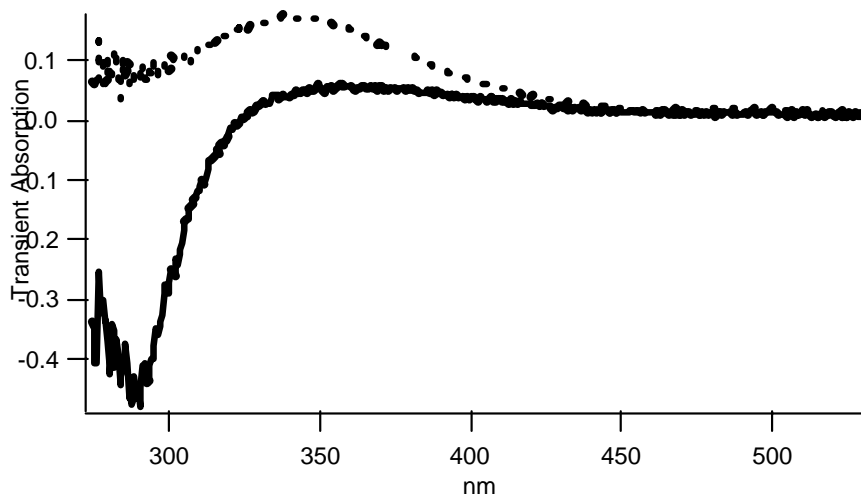


Figure 2.44 Transient absorption spectra produced upon LFP of 4H in water (solid line) and benzene (dotted line), recorded 10 ns after the pulse (308 nm). Note the greater signal to noise intensity in benzene and the wavelength shift of the absorption maximum.

The carrier of transient absorption has a lifetime of several hundred μs at ambient temperature in both solvents.

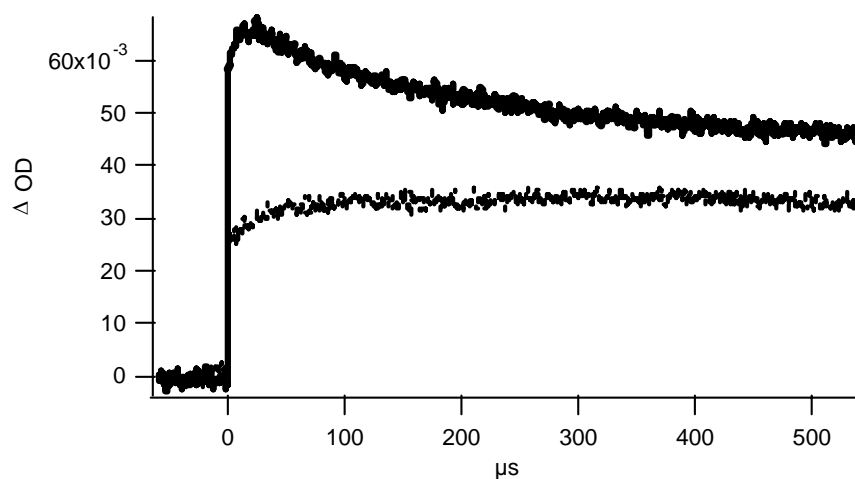


Figure 2.45 Change in the rate of decay of ketenimine in benzene with different concentrations of phenol (solid line 0.47 M phenol, dotted line 0 M phenol, 308 nm excitation, 415 nm detection). The slow growth observed in the absence of phenol is due to the formation of azo dimer **7a** by reaction of triplet nitrene **3a** with azide 4H.

The pseudo first order rate constant of growth (k_{obs}) of the azo dimer absorption increases in the presence of nucleophiles such as phenol.

Discussion of Studies to Confirm Solvent Effect

From the OMA collected it can be seen that there are two different intermediates formed shortly after the laser pulse depending on the solvent used. In non-polar solvents,

the ketenimine is observed and in polar solvents the triplet is formed. Both solvents lead to the same product after time (10us as shown in the example located in the results section) and that has been determined to be azo-benzene, a dimerization product.

2.3.6. TRIR Spectroscopy Experiment with Ketenimine in Acetonitrile

A TRIR experiment is similar to an LFP experiment. In both experiments a pulse of laser radiation is absorbed by the aryl azide which decomposes to form reactive intermediates. In the LFP experiment the reactive intermediates are detected by their absorption in the UV-Vis region of the spectrum. In the TRIR experiment the reactive intermediate is detected in the IR region of the spectrum.

IR detectors are less sensitive than UV-Vis detectors thus acquiring TRIR spectra requires extensive signal averaging. The TRIR detectors used in this work have a time resolution of 200 ns, thus the maximum reliable pseudo first order rate constant that can be obtained is $5.0 \times 10^6 \text{ s}^{-1}$. The UV-Vis detectors used in this work have a time resolution of approximately 1-2 ns. The advantage of TRIR spectroscopy and DFT calculations (used in chapter 3) is that together they can obtain structural information about the reactive intermediate.

In this experiment, DFT calculations were not needed because most ketenimines absorb at approximately 1900 cm^{-1} .

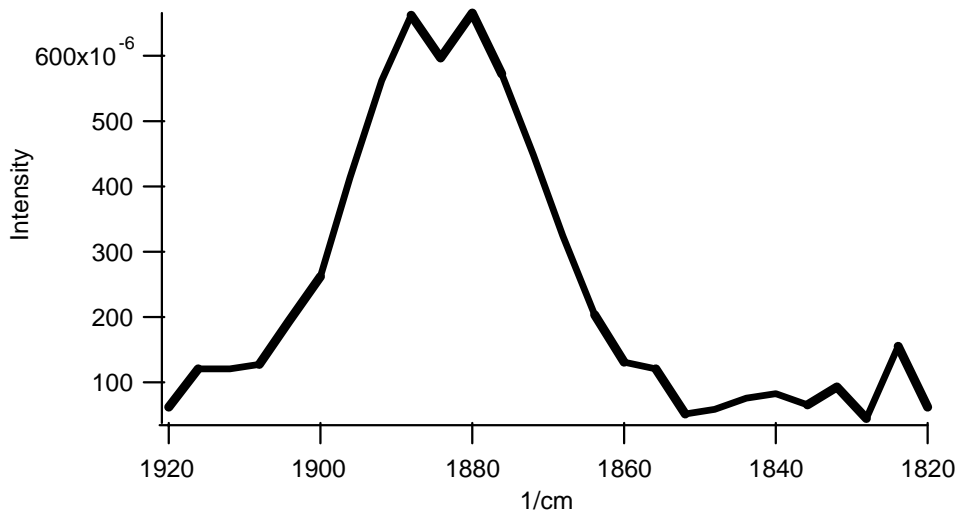


Figure 2.46 Transient IR spectra produced by flash photolysis of 4H in CH₃CN (266 nm excitation, 3.1 ms after the pulse, 3 mM azide concentration)

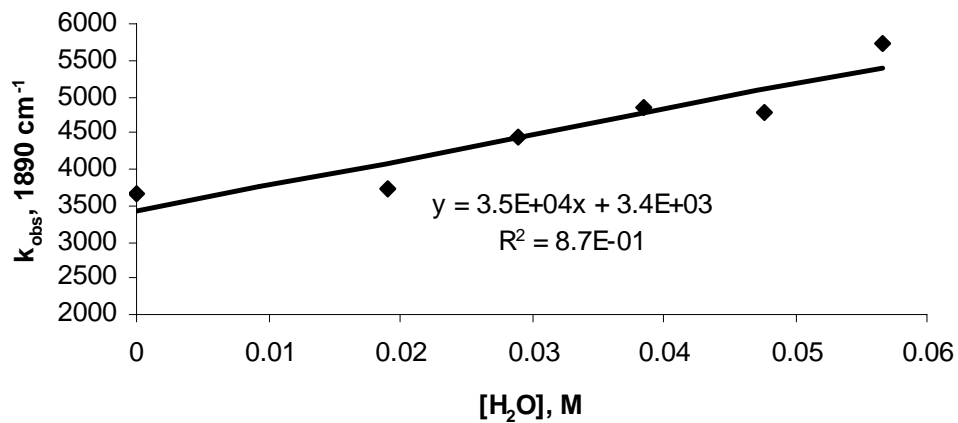


Figure 2.47 First order quenching of ketenimine **7H** with water in CH₃CN (266 nm excitation, 1890 cm⁻¹ detection, 3 mM concentration of 4H).

Stern Volmer Analysis

Please refer to Chapter 3, section 3.3.4. for an in depth explanation of Stern Volmer analysis.

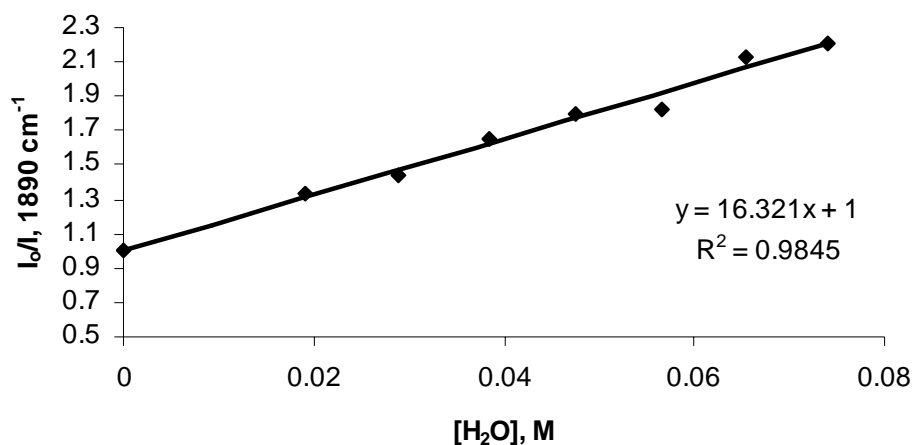


Figure 2.48 Stern Volmer treatment of the quenching of 4H ketenimine with water in CH₃CN (266 nm excitation, 1890 cm⁻¹ detection, 3 mM, 4H concentration).

Discussion of TRIR Studies of 4H Intermediates

The triplet nitrene **3a** and ketenimine **7a** have similar, nondescript UV spectra which lends doubt to the assignments of the carrier of the transient absorptions observed by LFP. However the IR spectra of these species are distinct. 1,2-Didehydroazepines have intense bands around 1900 cm⁻¹¹⁷ and triplet nitrenes¹⁸ do not. Li and Schuster¹³ demonstrated using TRIR spectroscopy that the rate of quenching of the ketenimine can be studied unambiguously. LFP of 4H in acetonitrile produces the transient IR spectrum of Figure 2.46, which is characteristic of a cyclic ketenimine^{17,18}.

It is interesting to note that water also quenches the yield of ketenimine of 4H. A Stern Volmer plot (Figure 2.55) is linear with slope $k_q\tau = 16$, where τ is the lifetime of singlet nitrene of 4H in acetonitrile, (1 ns as measured by Gritsan et. al^{14,19}). Thus, we deduce that water “reacts” with singlet nitrene **2a** with $k_q=1.6 \times 10^{10} \text{ M}^{-1}\text{s}^{-1}$. Based on the product studies by Li and Schuster and on TRIR studies, we conclude that water catalyzes the intersystem crossing of **2a** to triplet nitrene **3a** at a diffusion controlled rate (6a). If these results can be extrapolated to neat water than one predicts that the lifetime of singlet nitrene of 4H is 1.1 ps in water. Thus, photolysis of probes derived from Hixson and Hixson’s reagent in a hydrophilic environment will produce long-lived triplet nitrenes which will form anilines and nitro-aromatic compounds rather than cross-links. In hydrophobic environments derivatives of ketenimines from 4H will be formed which will react slowly with nucleophiles. In the absence of nucleophiles the ketenimines will equilibrate with the singlet and then ultimately relax irreversibly to the triplet nitrenes.

2.4 Conclusions

The study of the photochemistry of 4H (**1a**) has yielded new data on the reactivity of 4H intermediates in an aqueous environment and the discovery of a large solvent effect relating to which intermediate is formed.

Upon photolysis in water 4H (**1a**) was found to produce mostly triplet nitrene **3a** and eventually nitro **6a**, amine **5a**, and azo dimer **7a** compounds. The increased speed of intersystem crossing is thought to be due to hydrogen bonding between the water solvent and the zwitterionic state of the singlet nitrene. Quenching studies involving reducing

reagents such as glutathione and sodium ascorbate confirm that triplet nitrene is present in solution.

Upon photolysis in organic solvents 4H was found to produce mostly ketenimine and its derivatives, namely polymers. The fast isomerization of the singlet nitrene to ketenimine is the normal route in aryl azide mechanistic chemistry and without any interference from water the rearrangement readily takes place. The ketenimine was found to have low reactivity with several nucleophiles such as N-methylimidazole, phenol, dibutylsulfide, and indole. This indicates that the 4H ketenimine may form adducts and cross links in a hydrophobic environment, however, its slow rate is a major drawback to using this reagent.

Overall, 4H was found to be a poor PAL reagent. The fact that its major intermediates are triplet nitrene and ketenimine shows that there is little chance of a cross link being formed. The conversion to triplet nitrene and ketenimine proceeds at a rate that is much too fast to allow cross links and the singlet nitrene **2a** lifetime is too short to react with any useful residue in an enzyme.

The conclusion that 4H is a poor PAL reagent leads one to wonder what would be a better reagent and how would one go about making it.

CHAPTER 3: 2,3,5,6-TETRAFLUORO-4-AZIDOACETOPHENONE (4F)

3.1. Introduction

After studying the photochemistry of 4-azidoacetophenone in water and in benzene it was obvious that there is a need for a better PAL reagent, however, 4H had many useful characteristics that should be incorporated into a new design. The Platz laboratory had previously studied 2,6-difluorophenyl azide. Photolysis of this azide in pentane releases a singlet nitrene which has a lifetime of 250 ns. This is 250 times longer than that of singlet phenylnitrene²⁰.

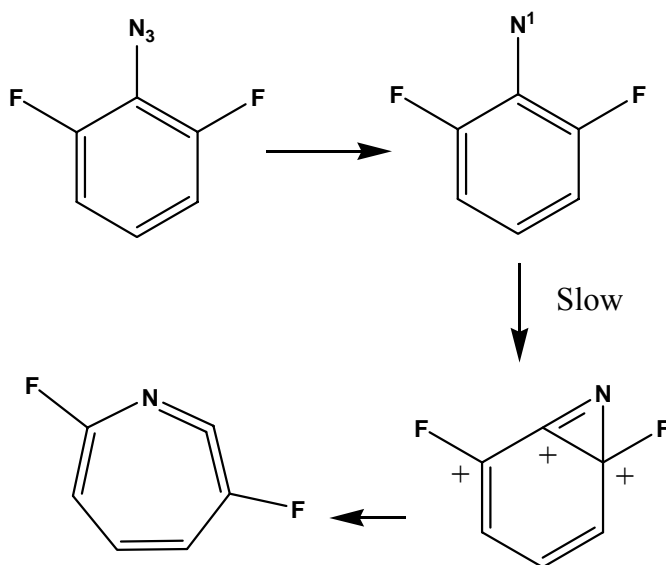


Figure 3.1 Photochemistry of 2,6-difluorophenyl azide.

Cyclization of 2,6-difluoro singlet phenylnitrene to the corresponding benzazirine is a slow reaction because forming C double bond N develops a positive charge on the carbon. This leads to a molecule with three contiguous positively charged carbons

as the C-F carbons are positive due to the electronegativity of fluorine. The unfavorable electrostatic interactions raise the energy of the benzazirine and depress the rate of its formation.

As the fluorinated aryl nitrenes have longer lifetimes they have an increased opportunity for reacting with CH bonds to form the kind of robust adducts desired in a PAL experiment. Singlet pentafluorophenyl nitrene illustrates this point nicely as it reacts with cyclohexane to form an adduct in 22 % yield²¹.

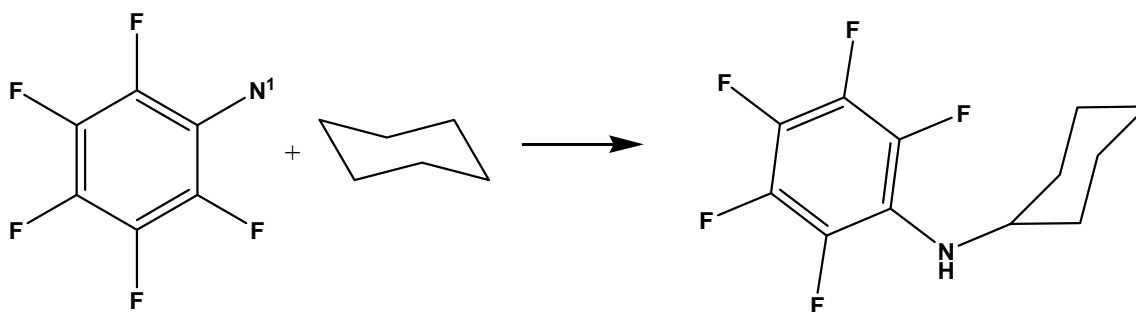


Figure 3.2 Formation of adduct using singlet pentafluorophenyl nitrene.

Thus, we hypothesized that 2,3,5,6-tetrafluoro-4-azidoacetophenone (4F) would absorb at long wavelengths because of the carbonyl group and release a long lived singlet nitrene capable of insertion into a CH bond.

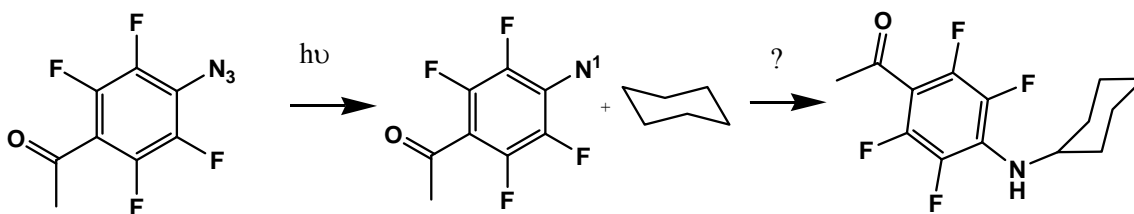


Figure 3.3 Proposed adduct formation with 4F.

3.2. Methods

3.2.1. Procedure for Synthesizing 2,3,5,6-tetrafluoro-4-azidoacetophenone (4F)²²

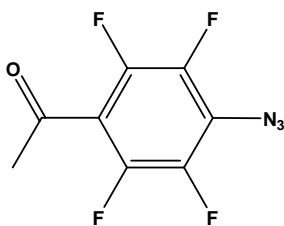


Figure 3.4 The reagent 4F.

To prepare this azide 2.1 g of 2,3,4,5,6-pentafluoro acetophenone and 0.71 sodium azide were placed in a 25 mL round bottom flask. Then, 6 mL of water and 16 mL of acetone were added and the solution was refluxed for eight hours. The refluxed solution was then allowed to cool to room temperature and then the reaction mixture along with 100 mL of diethyl ether was added to a 500 mL separatory funnel. The reaction mixture was then extracted once with 20 mL of distilled water, followed by extraction with 30 mL of a 5% sodium carbonate solution (5 g sodium carbonate and 95 g water). A spatula tip of charcoal was added to remove any unwanted impurities. A spatula tip of magnesium sulfate was then used to dry the solution; it was then filtered and concentrated on the rotovap. It was pale yellow in color. Column chromatography was then used to purify the product. The solvent used for the column was 10% ether and 90% hexanes. The first fraction off of the column was the desired product as shown by IR, H-NMR, F-NMR and GC-MS. It was then collected, concentrated by rotary evaporation, and stored in a dark cool place.

3.2.2. Purification and Analysis of Azides for Laser Flash Photolysis (LFP) and Time-Resolved Infrared (TRIR) Spectroscopy Work

4F was studied by LFP and TRIR techniques; however, before LFP work could be performed it was necessary to ensure stringent purity of the previously prepared azide. A plug column was prepared to filter out any unwanted impurities. The column used was packed with silica gel (approx. 75 mL) and approx. 150 mL of a 90% hexanes/10% ether solution. The oil, 4F, was then added to the top of the column. After the addition of the azide, approx. 1 inch of sea sand was added to the top of the column. The column was eluted with hexanes and fractions of approx. 15 mL were collected in test tubes. Air pressure was used to increase the flow through the column. Then, Thin Layer Chromatography (TLC) was used to analyze each fraction. The azide was the first compound to elute off of the column. Test tubes of the pale yellow azido solutions were alternately tested for the presence of the azide using TLC chromatography plates and hexanes. After all of the tubes found to contain the azide were combined the solution was concentrated by rotary evaporation. The resulting product was usually a pale yellow color. The azide was then stored in a clean vial.

Usually, the sample to be used for LFP work was prepared the day before the laser work. The main goal was to have the absorbance of the solution to be studied the next day equal to about 1 at laser wavelength used to study the solution. A test solution would be prepared in a 5 mL cuvette and a small amount of azide would be added. The solvent would then be poured into the cuvette and it would be analyzed by UV-Vis spectroscopy. The solution was modified depending on its absorbance, if its absorbance was more than 1 it was diluted accordingly, if it was less than 1, more azide was added. This procedure was then repeated if a larger volume (example 25 mL) was desired.

Samples used for the TRIR generally had a concentration of 3 or 5 mM and were prepared the day of the experiment.

3.2.3. Procedure for Preparation of Samples for Product Study

For photolysis experiments 0.01 M solutions were prepared in either 5 mL or 10 mL portions depending on the amount of compound available. After the stock solutions were prepared 1 mL would be extracted (via 10 mL syringe) and placed in small (1-2 mL) capped glass vials. The prepared solutions would then be photolyzed for 30 minutes using 365 nm light.

3.2.4. Synthesis of Product Study Standards

All solvents and starting materials were used as received from the vendor without further purification unless specifically stated otherwise. The nitro compound made when 4F was photolyzed was commercially available.

Synthesis of Amine 5b

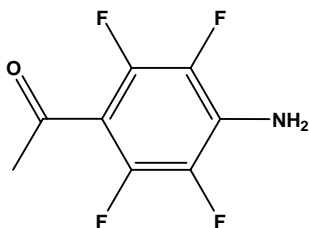


Figure 3.5 The amine produced upon photolysis of 4F.

Amine **5b** was synthesized by refluxing 0.5 g (0.0024 mol) of 2,3,4,5,6-pentafluoroacetophenone in 5 mL of THF with 10 mL of NH₄OH water solution for 48 hours. The reaction mixture was then extracted three times with ethyl acetate (50 mL). The organic layer was dried with MgSO₄, and the solvent was removed under reduced pressure to yield a white solid. ¹H NMR (500 MHz, CDCl₃): 2.6 (t, 3H, 1.5 Hz), 4.4 (s, 2H) ppm; ¹³C NMR (500 MHz, CDCl₃): 32.5 (s), 106.7 (s), 129.8 (s), 136.8 (d), 145.0 (d), 192.0 (s) ppm; IR (NaCl, CCl₄): 3337, 3210, 1658, 1539, 1495, 1308 cm⁻¹, mp (ethyl acetate/pentane): 104 – 106 °C MS:

Synthesis of Azo dimer 7b (4F Azo dimer)

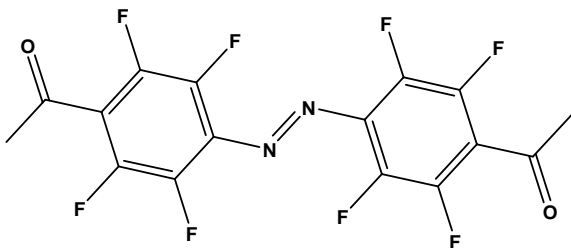


Figure 3.6 The azo dimer photo product produced upon photolysis of 4F.

Azo dimer **7b** was isolated from reaction mixture of a 0.01 M solution of azide 4F (**1b**) in acetonitrile, which was photolyzed for 5 hours with 365 nm light in a rayonet reaction chamber. The acetonitrile was then removed under reduced pressure, and the resulting orange oil was purified by column chromatography on a silica gel column with 5% ether in hexanes as the eluant. ¹H NMR (500 MHz, CDCl₃): 2.70 (t, 3H, J=1.5 Hz). IR (NaCl, CHCl₃): 2130, 1964, 1709, 1684 cm⁻¹; mp (tetrahydrofuran/hexanes): 88-90 °C.

Synthesis of Nitro **6b** (4F nitro compound)

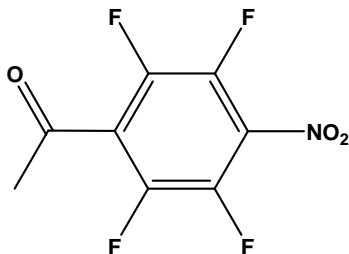


Figure 3.7 The nitro compound produced upon photolysis of 4F.

Nitro compound **6b** was synthesized by oxidation of amine **5b**. To a solution of 250 mg (0.0011 mol) of amine **5b** in 2 mL of dichloromethane was slowly added 0.45 mL of trifluoroacetic anhydride and 0.25 mL of 50% H₂O₂ in water. The reaction was allowed to reflux for an hour and another addition of 0.45 mL of trifluoroacetic anhydride and 0.25 mL of 50% H₂O₂ was added. The reaction was then refluxed for 24 hours until a green color was observed. The solution was extracted with dichloromethane (3 x 25 mL) and the organic layer was dried with MgSO₄. The solvent was removed under reduced pressure and the resulting pale green solid was purified by sublimation to yield pure **6b**. mp: 25 °C. IR (CCl₄): 1719, 1646, 1401, 1356 cm⁻¹.

Synthesis of Cyclohexane adduct **8b** (4F + cyclohexane)

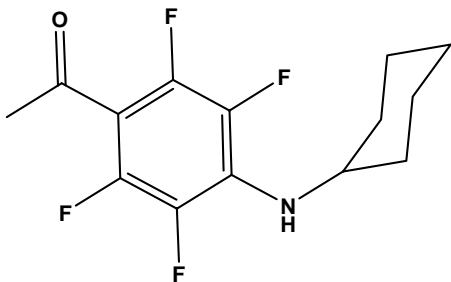


Figure 3.8 The adduct produced upon photolysis of 4F in cyclohexane.

Synthesis of adduct **8b** was accomplished by refluxing 0.5 g (0.0024 mol) of 2,3,4,5,6-pentafluoroacetophenone with 0.231 g (0.0024 mol) of cyclohexyl amine in 10 mL of THF. The solution was refluxed overnight, and then extracted with ethyl ether (3 x 50 mL). The organic layer was then dried with MgSO_4 and the solvent removed under reduced pressure. The crude reaction mixture was then purified by column chromatography to yield the product **8b** (0.34g, 50% yield). mp (ethyl acetate\ hexanes): 128-132 °C. IR (CHCl_3): 3505, 3411, 1668, 1654 cm^{-1} .

3.3. Results

3.3.1. Laser Flash Photolysis Study of 4F

For details about what an LFP study is and how it works please refer to Chapter 2, section 2.3.1. The following OMA's show the transient spectra produced by LFP of 4F azide in different solvents.

OMA's of Products Formed from Photolysis of 4F in Varying Solvents in Air

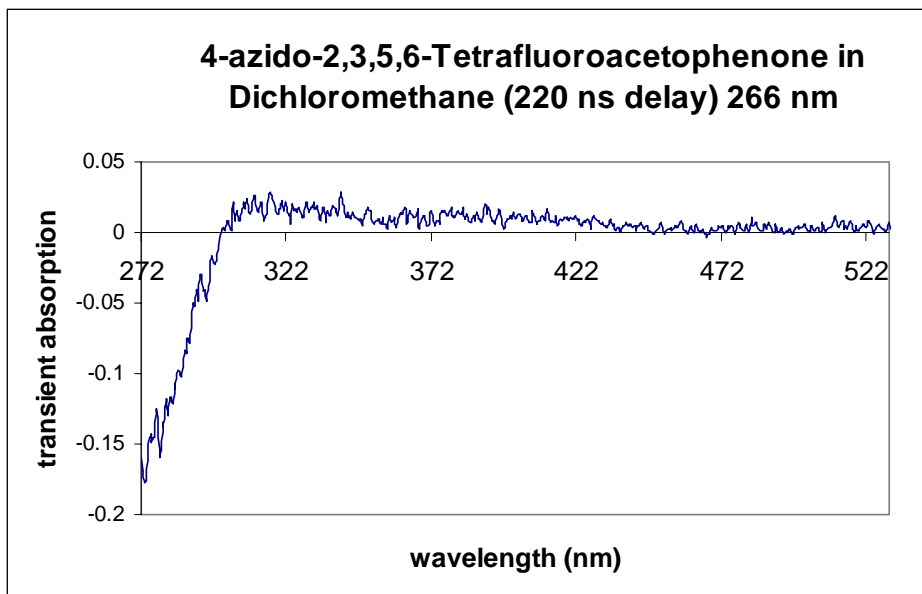


Figure 3.9 The transient spectrum produced by LFP of 4F in dichloroethane. The spectrum was recorded 220 ns after the pulse with 266 nm excitation.

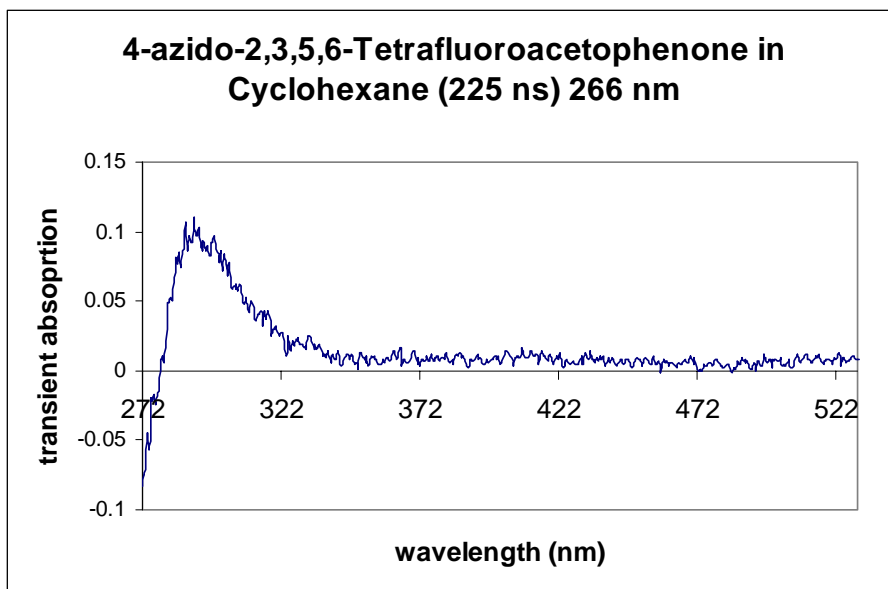


Figure 3.10 The transient spectrum produced by LFP of 4F in cyclohexane. The spectrum was recorded 225 ns after the pulse with 266 nm excitation.

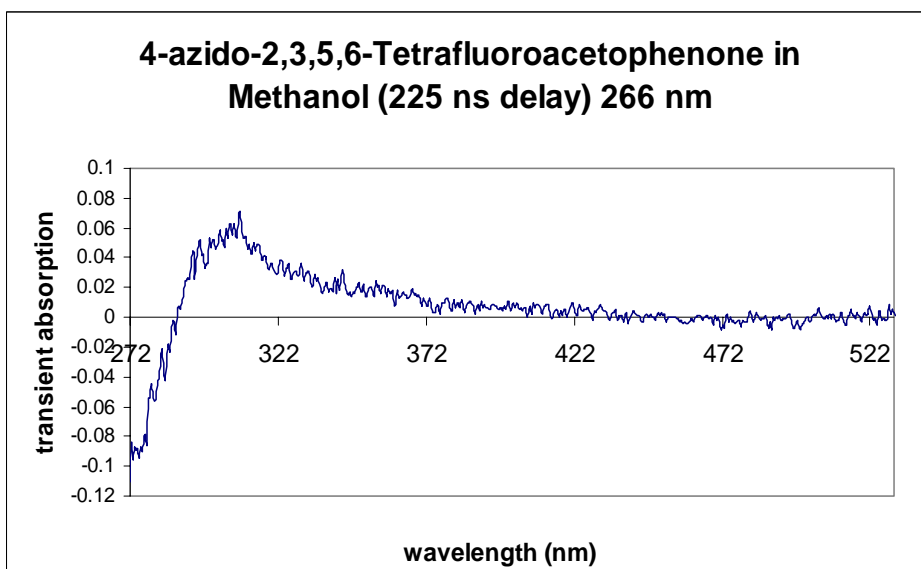


Figure 3.11 The transient spectrum produced by LFP of 4F in methanol. The spectrum was recorded 225 ns after the pulse with 266 nm excitation.

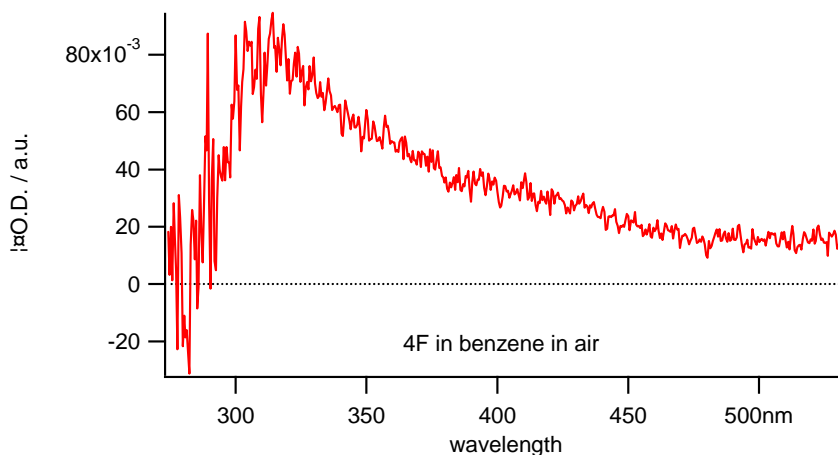


Figure 3.12 The transient spectrum produced by LFP of 4F in benzene. The spectrum was recorded 225 ns after the pulse and with 266 nm excitation.

Variation of the Time Delay on Transient Spectra

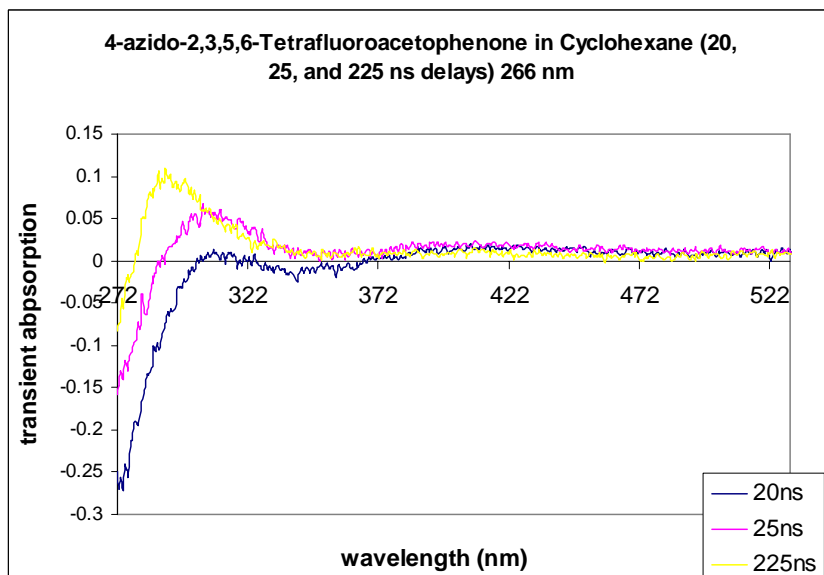


Figure 3.13 The transient spectrum produced by LFP of 4F in cyclohexane. The absorption seen in the figure is the result of growth of the 4F azo dimer. The spectrums were recorded 20, 25, and 225 ns after the pulse with 266 nm excitation.

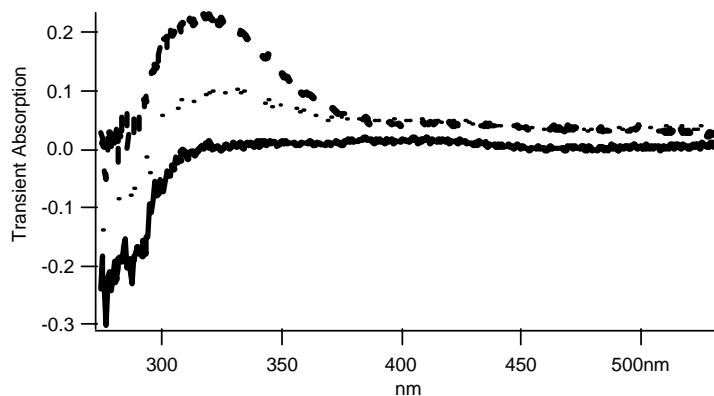


Figure 3.14 Transient UV spectra produced by LFP of 4F in water at 10 ns delay (solid line), 1 ms (dotted line), and 10 ms (dashed line), 308 nm excitation. With increasing delay the azo dimer grows in.

With increasing delay times, the photo product grows in. This behavior is characteristic of the formation of azo dimer, by reaction of the triplet nitrene with the azide precursor.

3.3.2. OMA's Produced by LFP of 4F in Varying Solvents with 1M pyridine: A Singlet Nitrene Trapping Study

The transient signals obtained by LFP of 4F are weak. They are also long lived which suggests we are detecting the triplet nitrene. The fact that transient absorption grows at 320 nm can be explained as reaction of the triplet with azide precursor to form azo dimer which absorbs at this wavelength.

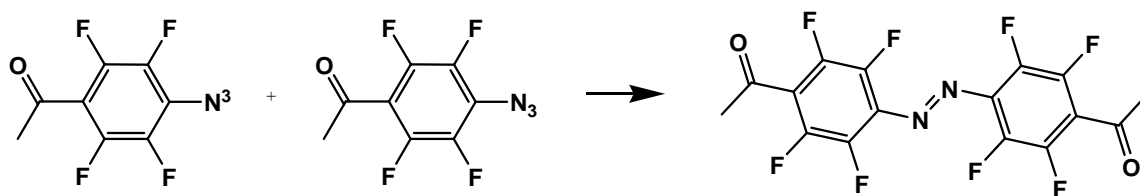


Figure 3.15 Production of azo dimer.

The singlet nitrene, the species capable of forming useful cross links, has not been observed. Singlet polyfluorinated aryl nitrenes react to form ylides which are stable and absorb intensely in the visible region of the spectrum. This has been shown to be an ideal method of probing the kinetics of singlet nitrenes. Hence, these studies were performed with 4F

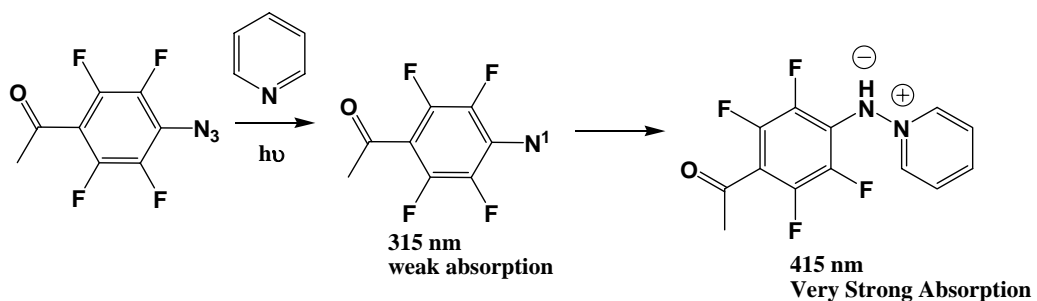


Figure 3.16 Production of the pyridine ylide.

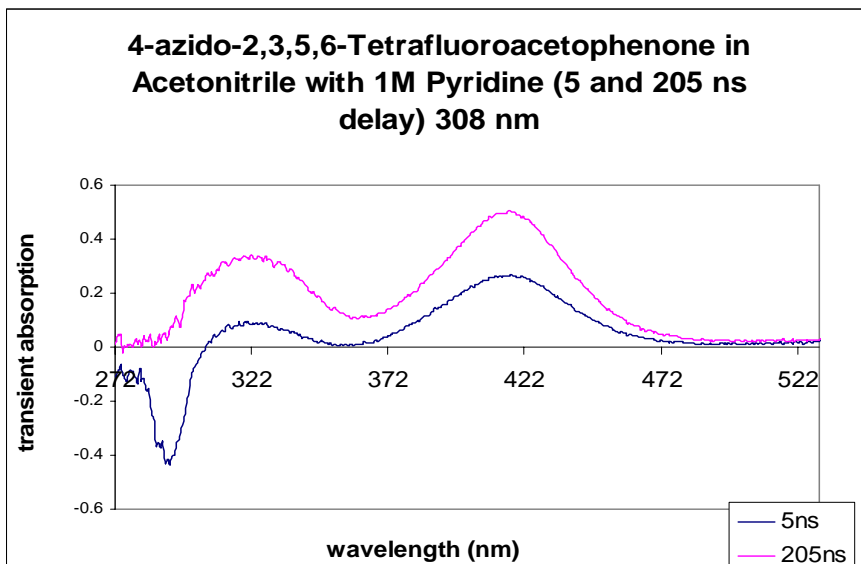


Figure 3.17 Transient spectrum produced by LFP (308 nm) of 4F in acetonitrile containing 1M pyridine. The spectrum was recorded 5ns (blue) and 25 ns (purple) after the laser pulse.

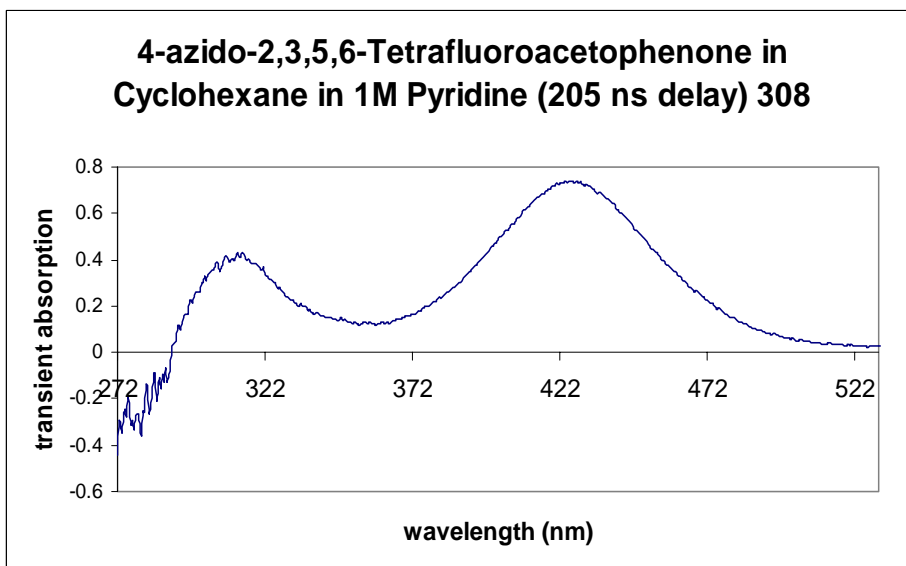


Figure 3.18 Transient spectrum produced by LFP (308 nm) of 4F in cyclohexane containing 1M pyridine.

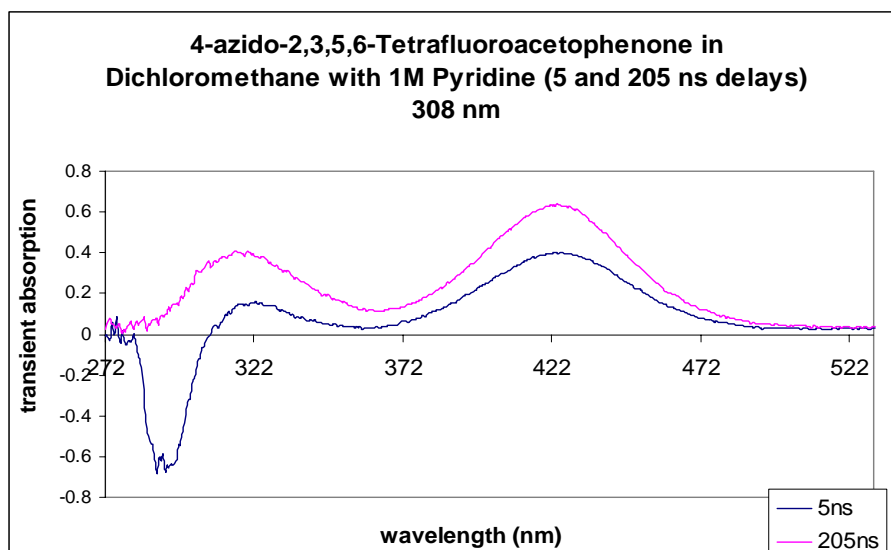


Figure 3.19 Transient spectrum produced by LFP (308 nm) of 4F in dichloromethane containing 1M pyridine. The spectrum was recorded 5ns (blue) and 205 ns (purple) after the laser pulse.

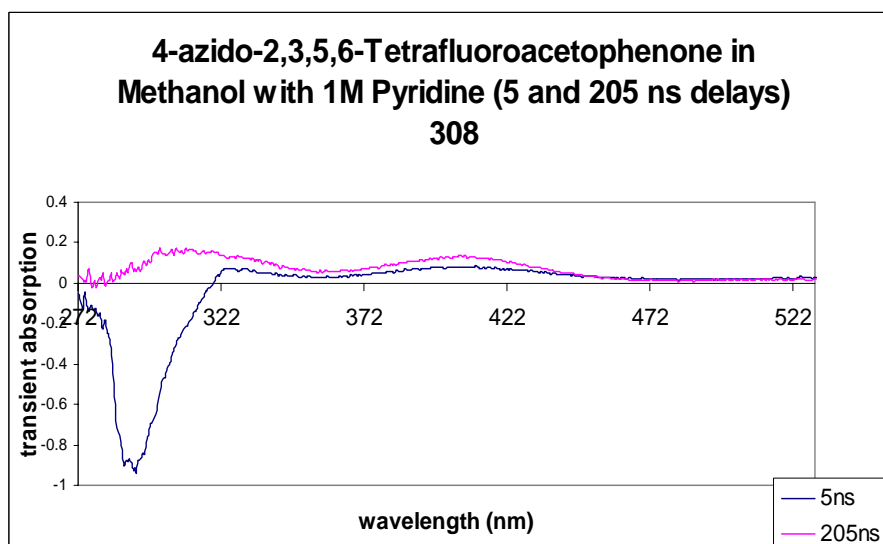


Figure 3.20 Transient spectrum produced by LFP (308 nm) of 4F in methanol containing 1M pyridine. The spectrum was recorded 5ns (blue) and 25 ns (purple) after the laser pulse.

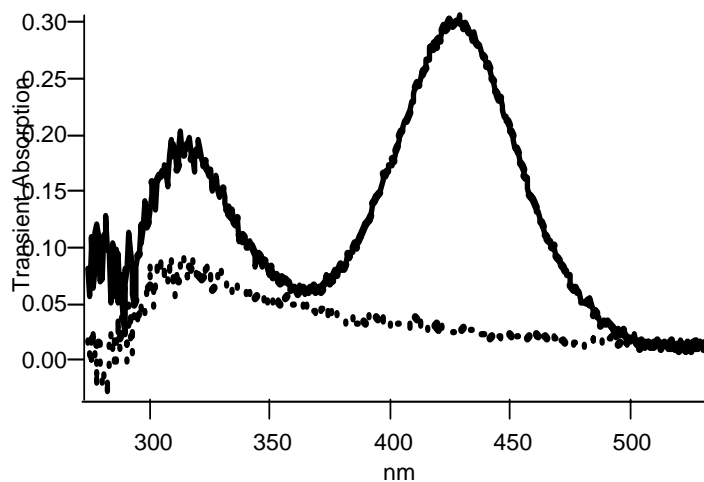


Figure 3.21 Transient spectrum produced by LFP of 4F in benzene containing 1M pyridine (dark line) and 0M pyridine (dotted line).

The addition of pyridine traps the singlet and causes the ylide to grow in at about 400-415 nm in aprotic solvents. The ylide spectrum is weak in methanol. We suspect that methanol catalyzes relaxation from the singlet to the triplet nitrene. This shortens the singlet lifetime and makes pyridine trapping of the singlet nitrene inefficient.

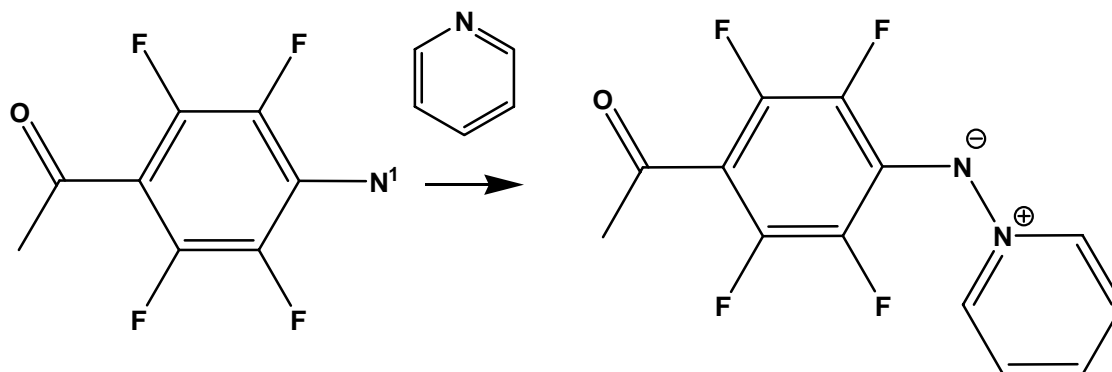


Figure 3.22 Singlet Nitrene reacts with Pyridine to form the Pyridine Ylide.

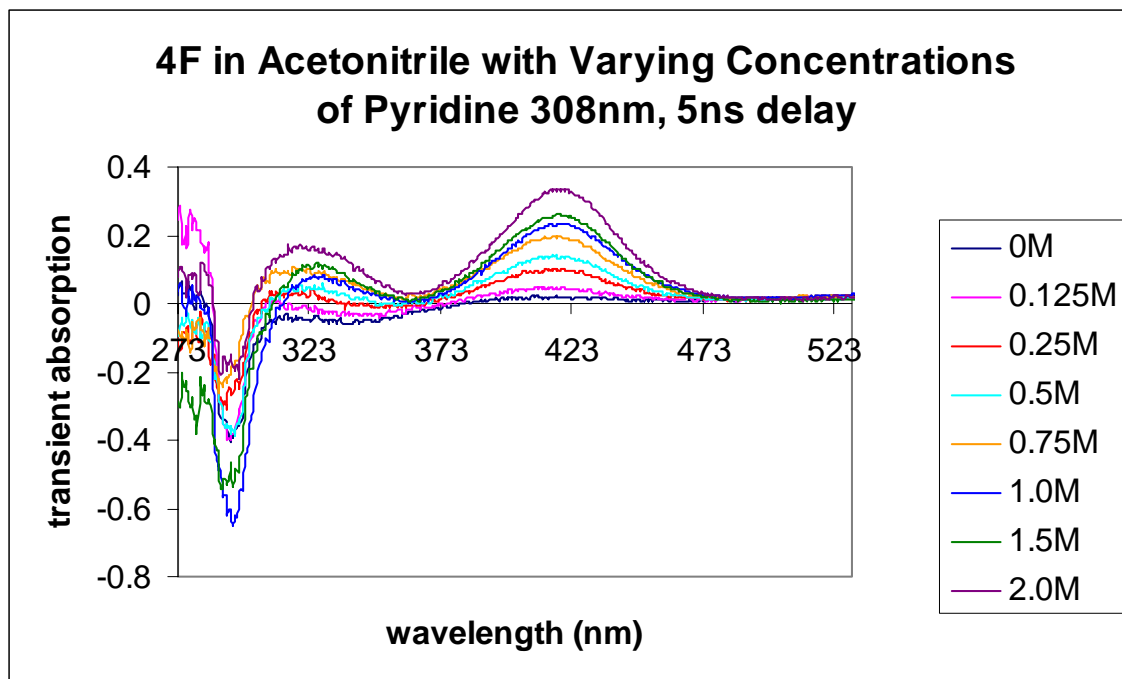


Figure 3.23 Transient spectrum produced by LFP of 4F in acetonitrile containing varying concentration of pyridine.

This experiment shows that the absorbance at 415 nm is dependent on the concentration of pyridine, making it even more likely that the carrier of the absorption is the desired ylide.

3.3.3. Kinetics with Pyridine: Determining the Reactivity of Singlet Nitrene in Varying Solvents

It was possible to resolve the growth of absorbance of the ylide at 415 nm. The growth kinetics could be fit to an exponential function and solved to yield time constant, k_{observed} , and the observed pseudo first order rate constant of ylide formation. Under the experimental conditions equation 3.1 is valid:

$$K_{\text{observed}} = k_0 + k_{\text{pyridine}}[\text{pyridine}] \quad 3.1$$

Where k_0 is the sum of all pseudo first order rate constants of all processes which consume singlet tetrafluoro para-acetylphenylnitrene in the absence of pyridine, and k_{pyridine} is the absolute second order rate constant of reaction of the nitrene with pyridine. Equation 3.1 predicts that plots of k_{observed} versus $[\text{pyridine}]$ will be linear with slope = k_{pyridine} . The intercept of the plot is k_0 and the lifetime, $\tau = 1/k_0$.

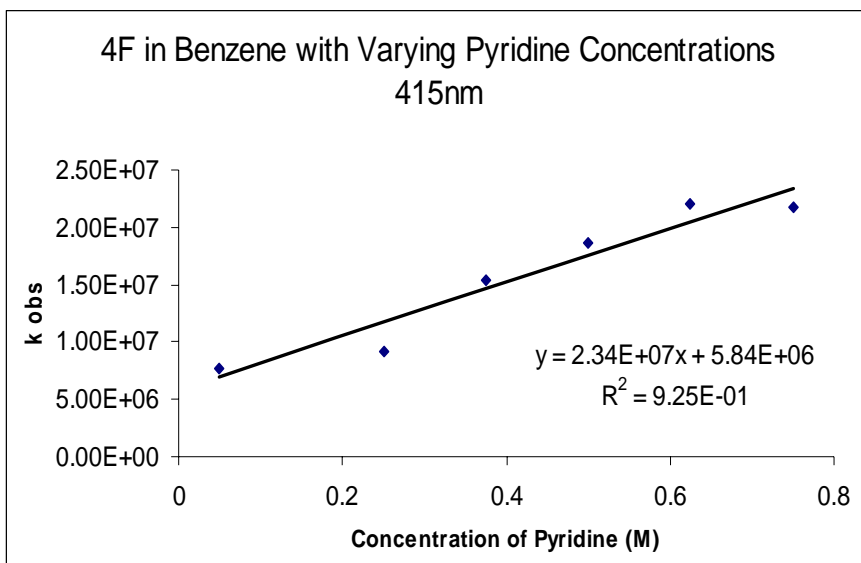


Figure 3.24 A plot of k_{obs} versus [Pyridine] concentration obtained by LFP of 4F in benzene.

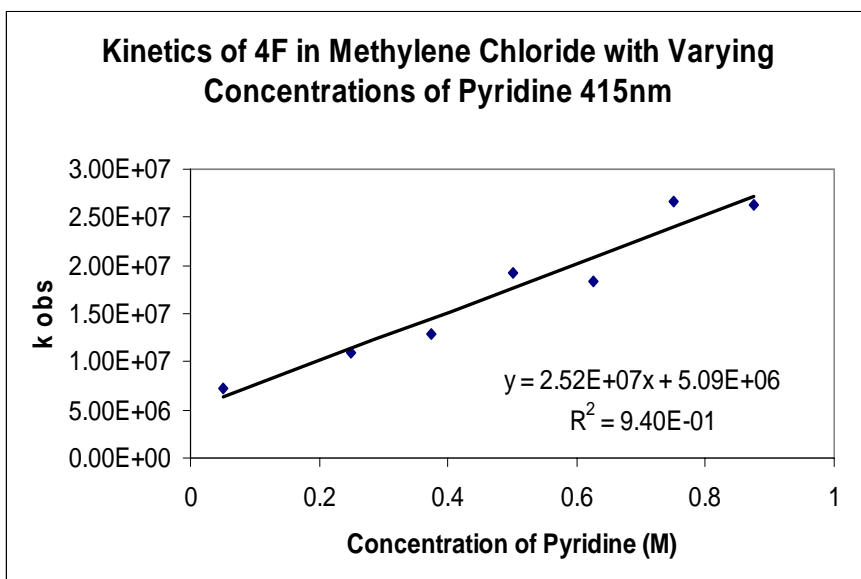


Figure 3.25 A plot of k_{obs} versus [Pyridine] concentration obtained by LFP of 4F in methylene chloride.

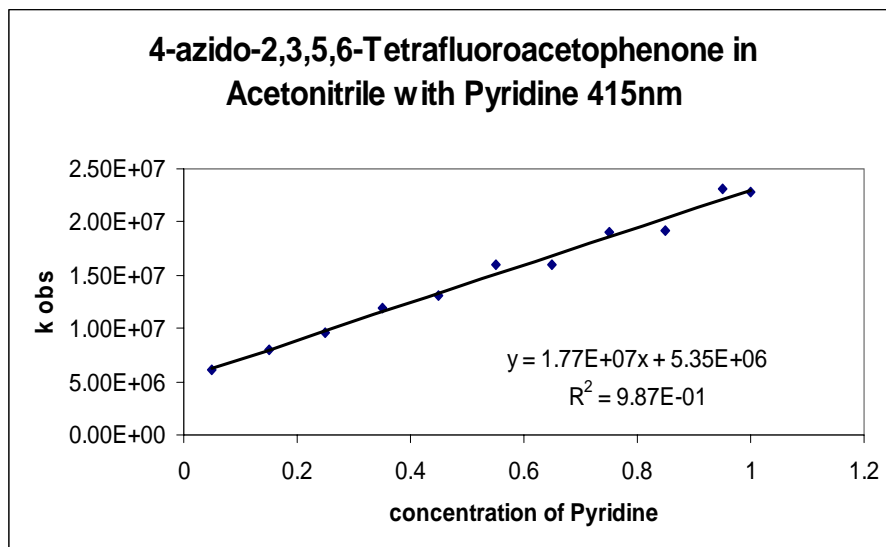


Figure 3.26 A plot of k_{obs} versus [Pyridine] concentration obtained by LFP of 4F in acetonitrile.

The above kinetics has shown that the expected linear fashion dependence on the concentration of pyridine is observed in benzene, methylene chloride, and acetonitrile.

Table 3.1 Summary of the Reactivity of Singlet Nitrene in Various Solvents

Solvent	$k_{\text{pyr}} (\text{M}^{-1}\text{s}^{-1})$	τ (ns)
C_6H_6	2.3×10^7	172
CH_2Cl_2	2.5×10^7	196
CH_3CN	1.8×10^7	185

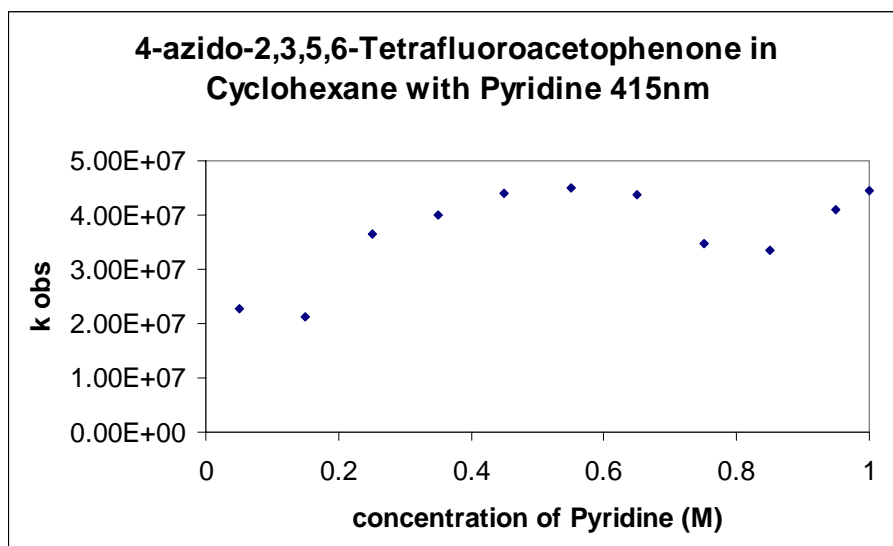


Figure 3.27 A plot of k_{obs} versus [Pyridine] concentration obtained by LFP of 4F in cyclohexane.

As shown in Figure 3.27 the expected linear relationship was not observed. We found that photolysis of 4F in cyclohexane produces the desired adduct:

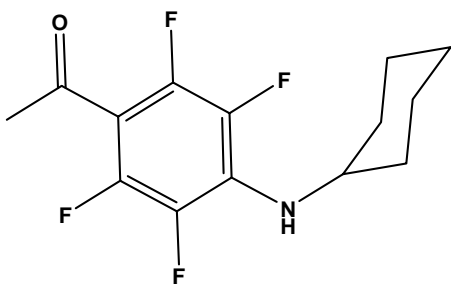


Figure 3.28 The adduct formed upon photolysis of 4F in cyclohexane.

LFP of the above adduct produces a transient which absorbs in the same region of the spectrum as the reactant, see below Figure 3.29. This complicates the transient spectrum leading to a non-linear plot (Figure 3.27).

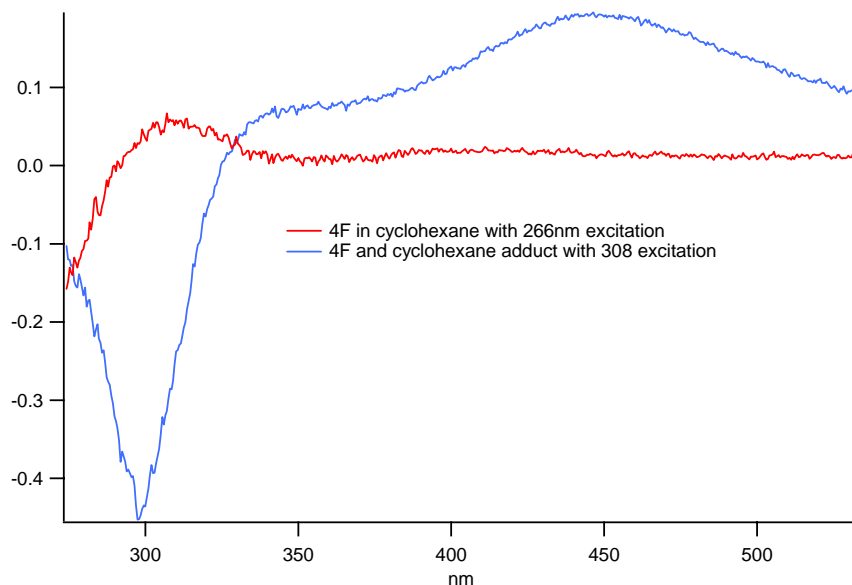


Figure 3.29 Transient spectrums produced by LFP of 4F in cyclohexane containing adduct (blue) and without adduct (red).

Photolysis of 4F in cyclohexane produces an adduct. LFP of the adduct formed in cyclohexane produces a transient which absorbs at about the same wavelengths as the ylide and so it is difficult to measure the effect of pyridine because there are competing absorptions.

3.3.4. Study of 4F Singlet Nitrene with Biological Quenchers in Organic Solvent

The presence of a second singlet nitrene quencher Q, will reduce the yield of pyridine ylide.

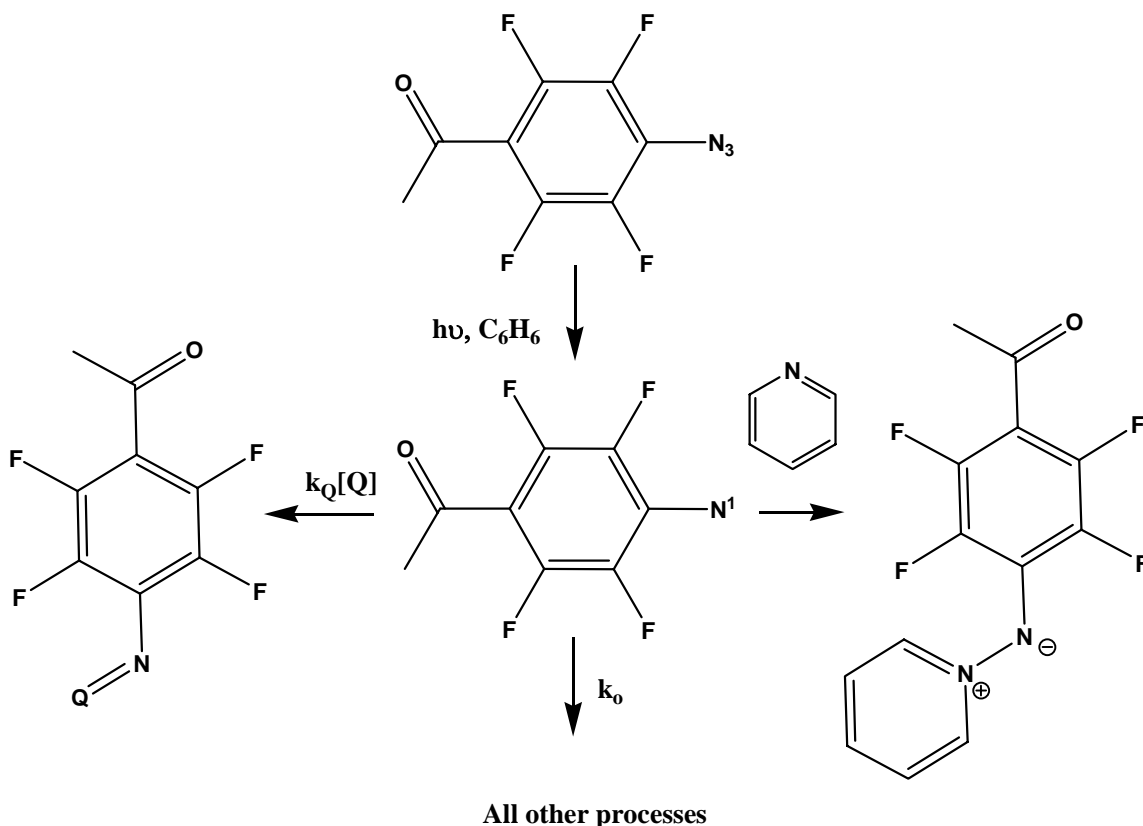


Figure 3.30 Mechanistic representation of how 4F singlet nitrene can be measured in the presence of biological quenchers.

As k_{pyr} is known, values of k_Q can be obtained by a Stern Volmer Analysis. In this experiment the optical yield of ylide when $Q = 0$ is I_0 and is I when Q does not equal 0. Under these conditions:

$$I_0 = \frac{k_{\text{pyr}}[\text{pyr}]}{k_0 + k_{\text{pyr}}[\text{pyr}]} \quad 3.2$$

$$I = \frac{k_{\text{pyr}}[\text{pyr}]}{k_o + k_{\text{pyr}}[\text{pyr}] + k_Q[\text{Q}]} \quad 3.3$$

$$\frac{I_o}{I} = \frac{k_Q[\text{Q}]}{k_o + k_{\text{pyr}}[\text{pyr}]} \quad 3.4$$

Thus, a plot of I_o/I versus $[\text{Q}]$ at constant $[\text{pyr}]$ should be linear with a slope of $k_Q/(k_o + k_{\text{pyr}}[\text{pyr}])$.

The solvent used in the experiments was benzene and 1M pyridine was used to form the ylide.

Quenching of 4F Pyridine Ylide

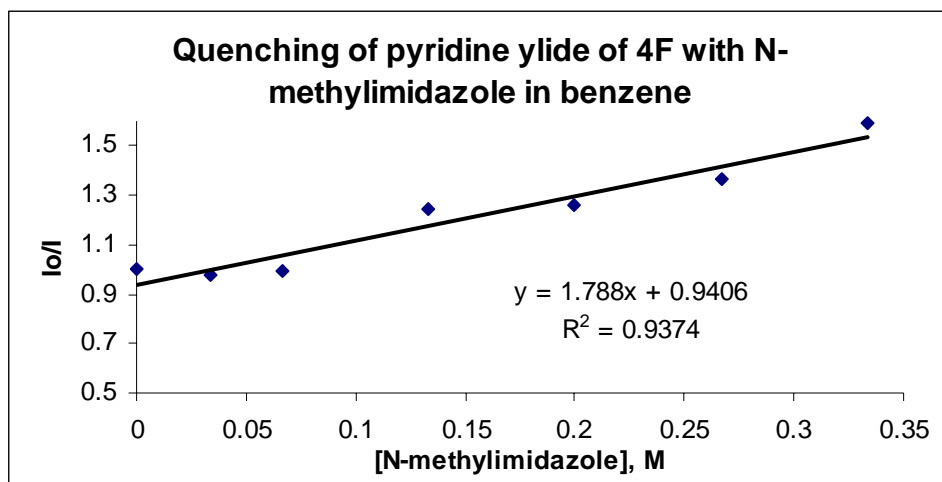


Figure 3.31 Stern Volmer analysis of the quenching of the yield of ylide by N-methylimidazole.

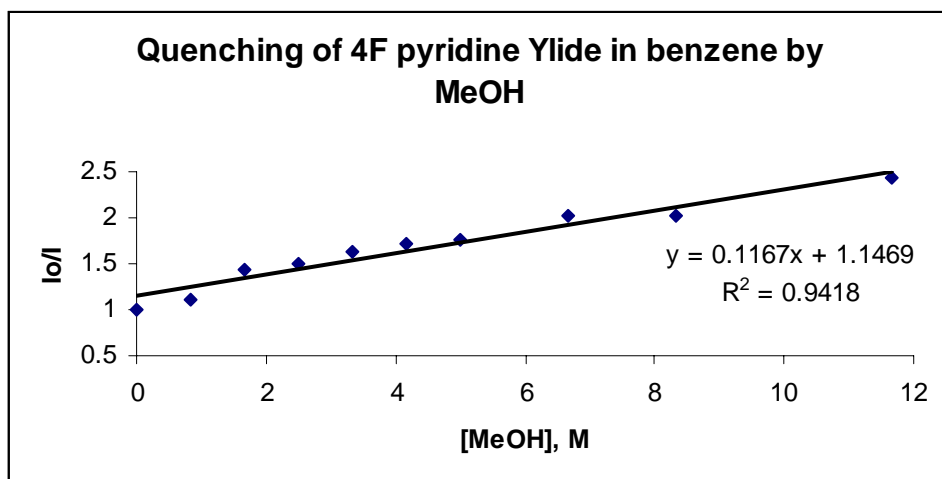


Figure 3.32 Stern Volmer analysis of the quenching of the yield of ylide by methanol.

The methanol experiment indicates the $k_{\text{methanol}} = (0.117) (k_o + k_{\text{pyr}}[\text{pyr}])$ (where $k_{\text{pyr}} = 2.3 \times 10^7 \text{ M}^{-1}\text{s}^{-1}$, $[\text{pyr}] = 1\text{M}$ and $k_o = 2.7 \times 10^6 \text{ M}^{-1}\text{s}^{-1}$ and $k_o = 5.8 \times 10^6 \text{ s}^{-1}$. As neat methanol is 23 M. the singlet nitrene lifetime is predicted to be 13 ns in neat methanol. This is an order of magnitude smaller than the singlet nitrene lifetime in benzene (171 ns) and explains why pyridine trapping of the singlet nitrene is not efficient in methanol solvent. Once again it appears that methanol catalyzes singlet to triplet nitrene intersystem crossing.

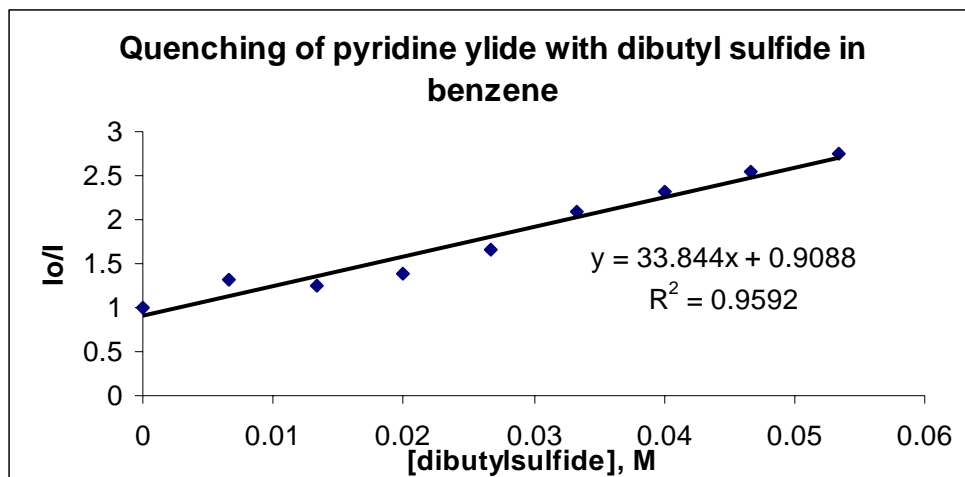


Figure 3.33 Stern Volmer analysis of the quenching of the yield of ylide by dibutyl sulfide.

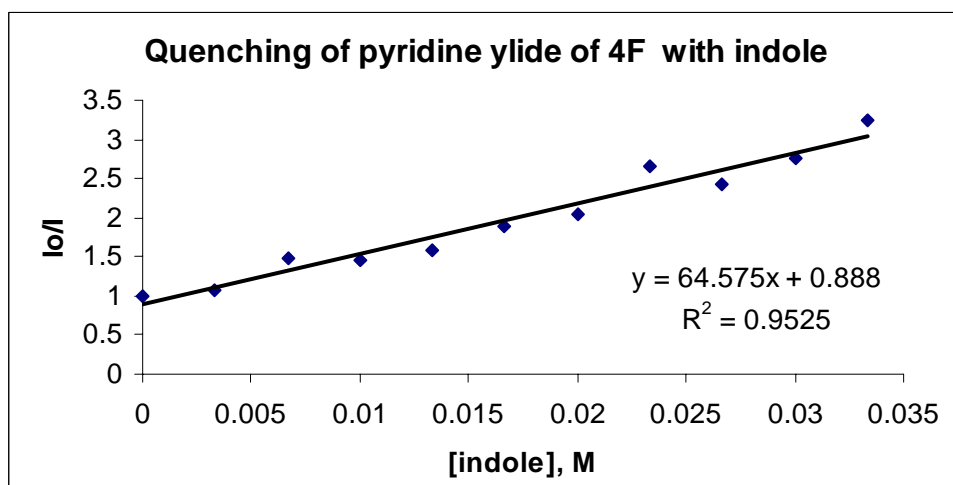


Figure 3.34 Stern Volmer analysis of the quenching of the yield of ylide by indole.

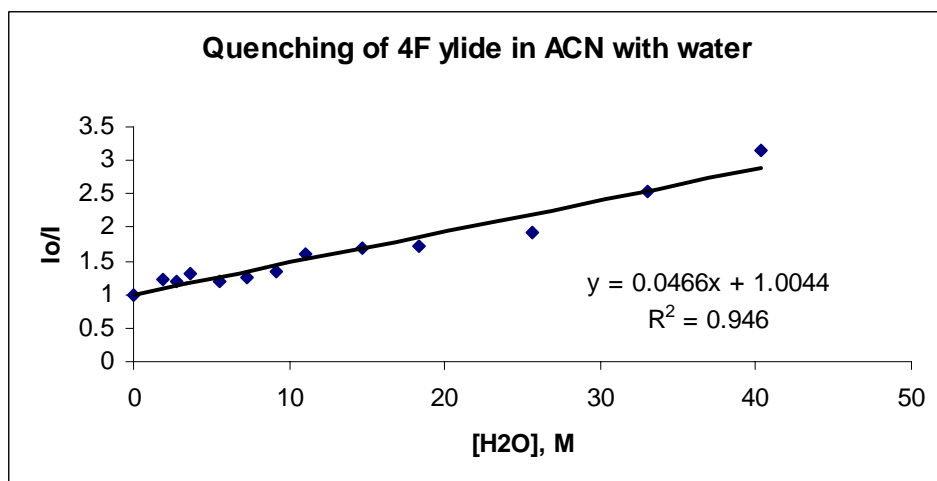


Figure 3.35 Stern Volmer analysis of the quenching of the yield of ylide by water.

Summary of Data from Biological Quenchers

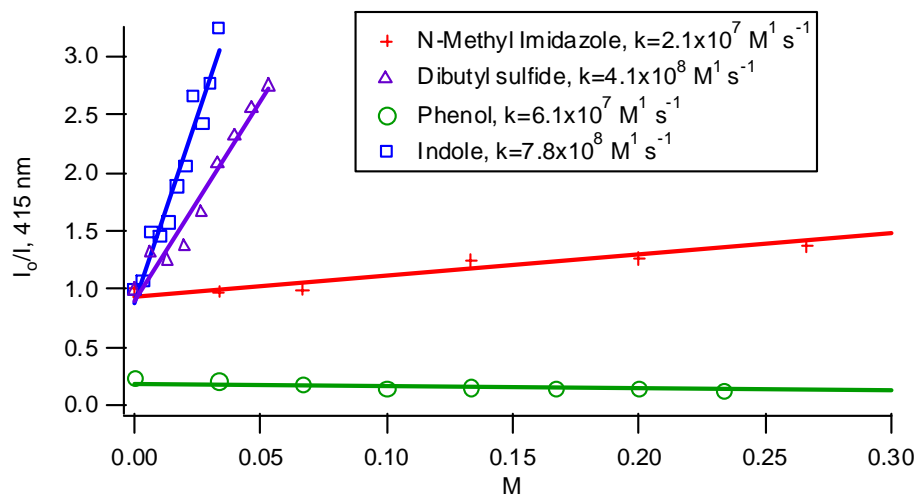


Figure 3.36 Stern Volmer analysis of the quenching of the yield of ylide by all biological quenchers.

The large reactivity observed with indole and dibutyl sulfide indicates that 4F may make an acceptable PAL reagent in hydrophobic areas of biological systems.

3.3.5. Study to Determine Presence or Absence of Ketenimine

4F with DEA and Imidazole

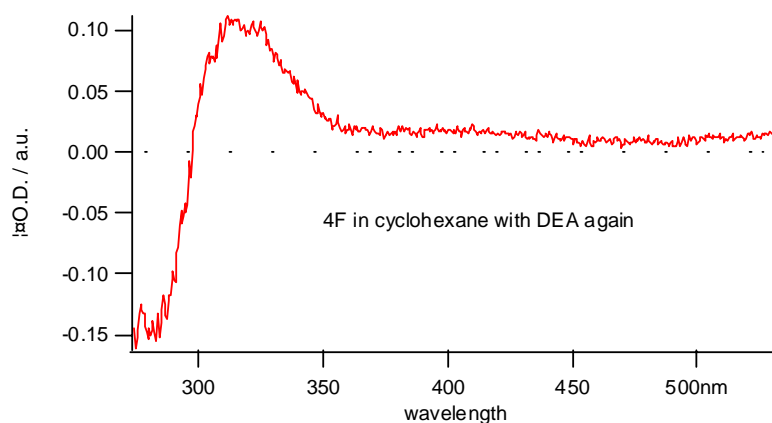


Figure 3.37 Transient spectrum produced by LFP of 4F in cyclohexane containing diethylamine (DEA), a ketenimine quencher.

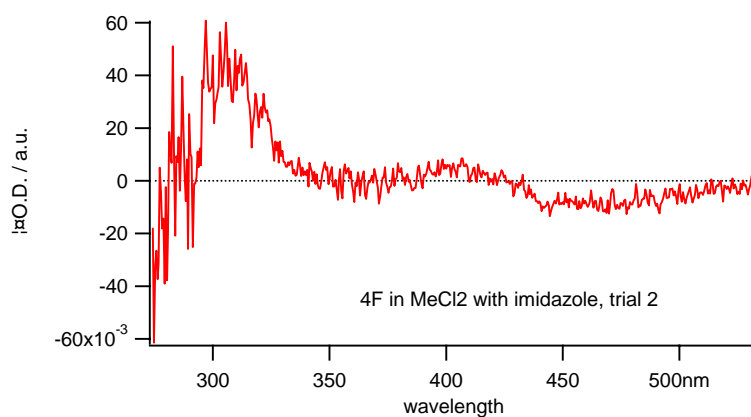


Figure 3.38 Transient spectrum produced by LFP of 4F in methylene chloride containing imidazole, a ketenimine quencher.

The above figures show that the presence of diethyl amines and imidazole, excellent quenchers of ketenimines, do not have an affect on the transient produced by LFP of 4F. This indicates that no ketenimine is forming because DEA and imidazole will trap the ketenimine.

3.3.6. Triplet Quencher Study

The transient spectra indicate that triplet nitrene is formed upon LFP of 4F in water. To confirm the assignment we studied the reactivity of the transient observed in water with the known triplet quenchers glutathione (GSH) and sodium ascorbate.

As mentioned previously the OMA spectrum obtained by LFP of 4F in water shows the growth of azo dimer. The azo dimer is formed by reaction of the triplet nitrene with the azide precursor.

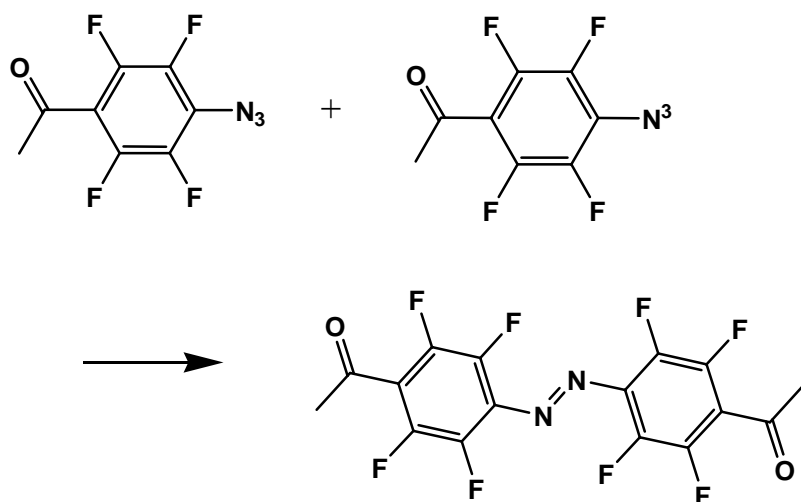


Figure 3.39 Production of Azo Dimer

The kinetics of azo growth is the same as the triplet nitrene decay and follows pseudo first order kinetics because the azide is in excess. Thus,

$$\frac{d[\text{Azo}]}{dt} = \frac{-d[\text{triplet nitrene}]}{dt} = k_o + k_{\text{azo}}[\text{Azide}][\text{triplet nitrene}] + k_Q[\text{triplet nitrene}][\text{Q}] \quad 3.5$$

where k_o is the sum of all possible first order processes which consume the triplet nitrene (other than azo dimer formation), and k_{azo} is the second order rate constant of reaction of triplet nitrene with quencher Q. Thus, a plot of k_{obs} ($= k_o + k_{\text{azide}}[\text{azide}] + k_Q[\text{Q}]$) versus Q will be linear with slope k_Q .

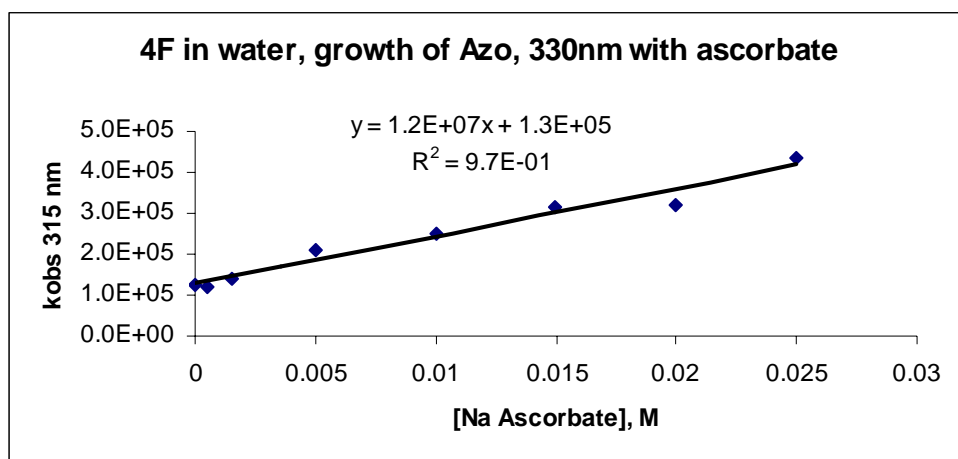


Figure 3.40 A plot of k_{obs} versus [Sodium Ascorbate] concentration obtained by LFP of 4F in water.

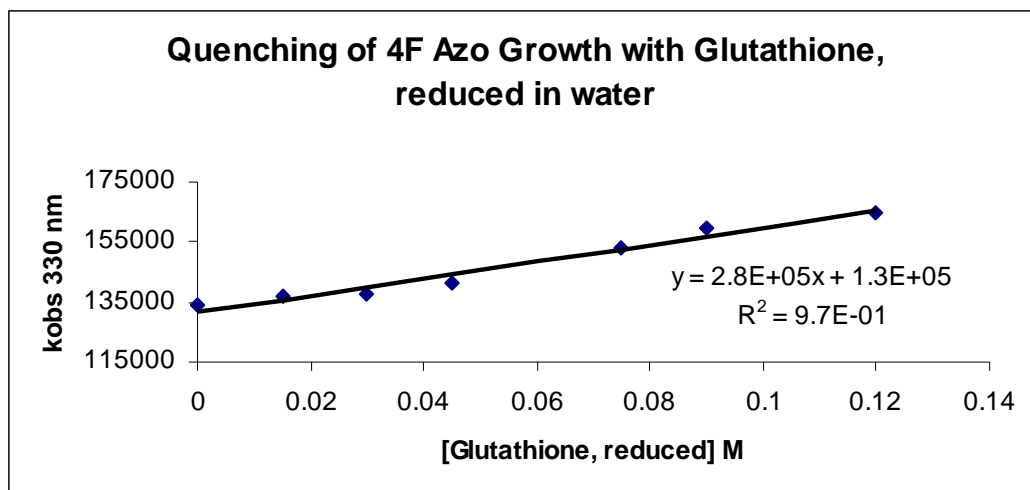


Figure 3.41 A plot of k_{obs} versus [glutathione] obtained by LFP of 4F in water.

3.3.7. 5F Photochemistry – Control Experiments

The photochemistry of pentafluoroacetophenone (5F) was studied. The purpose of this control experiment was to eliminate the possibility that the transient signals obtained with 4F are produced from an impurity. As shown in figures 3.38 to 3.41, the transient spectrum produced by LFP of 5F in acetonitrile solvent is not similar to that produced by LFP of 4F. We can conclude that the 5F photochemistry does not interfere with the study of 4F.

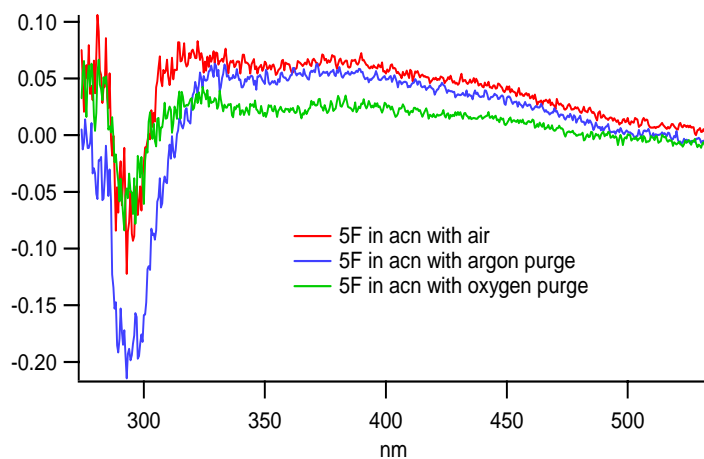


Figure 3.42 Transient spectrum produced by LFP of 5F in acetonitrile.

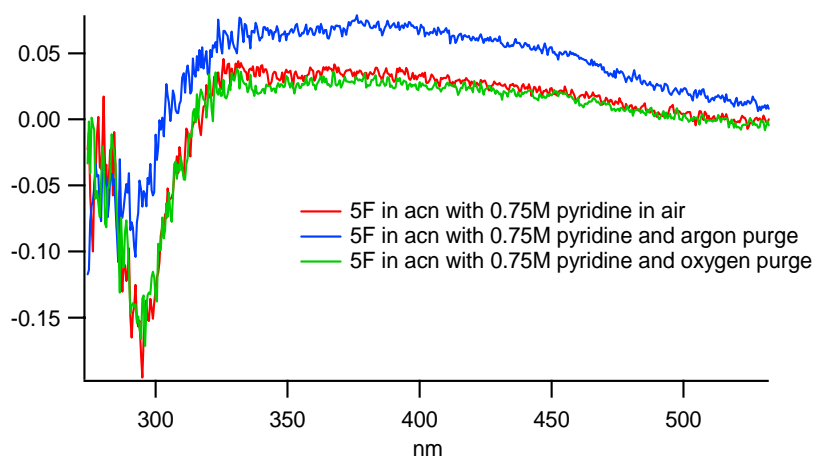


Figure 3. 43 Transient spectrum produced by LFP of 5F in acetonitrile with 0.75 M pyridine.

Comparisons of 4F and 5F

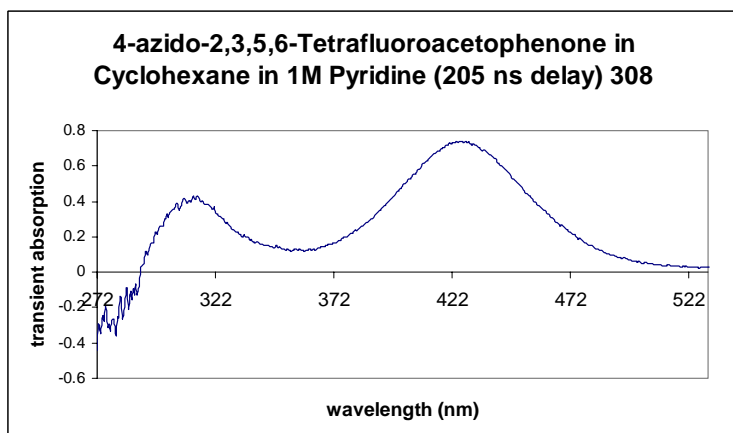


Figure 3.44 Transient spectrum produced by LFP of 4F in cyclohexane with 1 M pyridine.

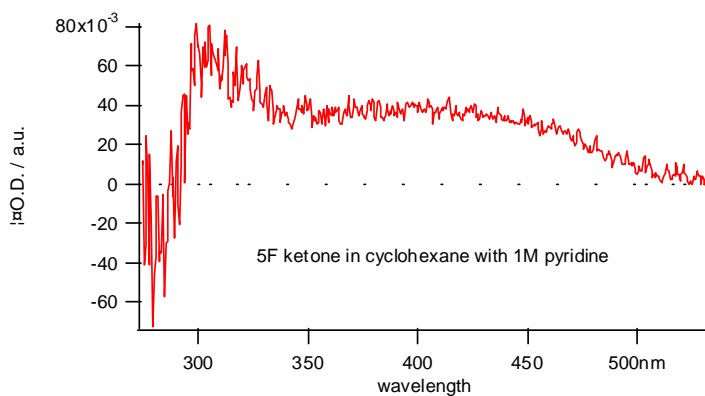


Figure 3.45 Transient spectrum produced by LFP of 5F in cyclohexane with 1 M pyridine.

Figures 3.41 and 3.43 are produced by LFP of 4F and 5F in cyclohexane with 1 M pyridine. The transient spectra are very different which provides further evidence that LFP of 4F and pyridine produces ylide and that LFP of 5F as an impurity does not produce the transient spectra observed upon LFP of 4F.

3.3.8. DFT Calculations of the Vibrational Spectra of Reactive Intermediates

Calculations at the B3LYP 6-31G* level of theory and basis using the PCM model of acetonitrile were performed to predict the spectra of intermediates created from the irradiation of 4F.

4F Computational IR Spectra in Acetonitrile

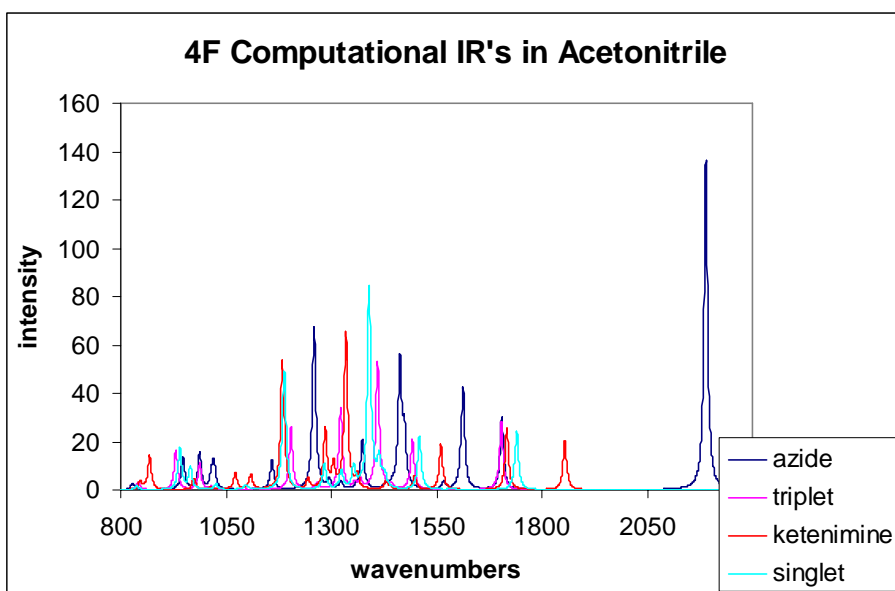


Figure 3.46 Complete theoretical IR of reactive intermediates produced upon irradiation of 4F.

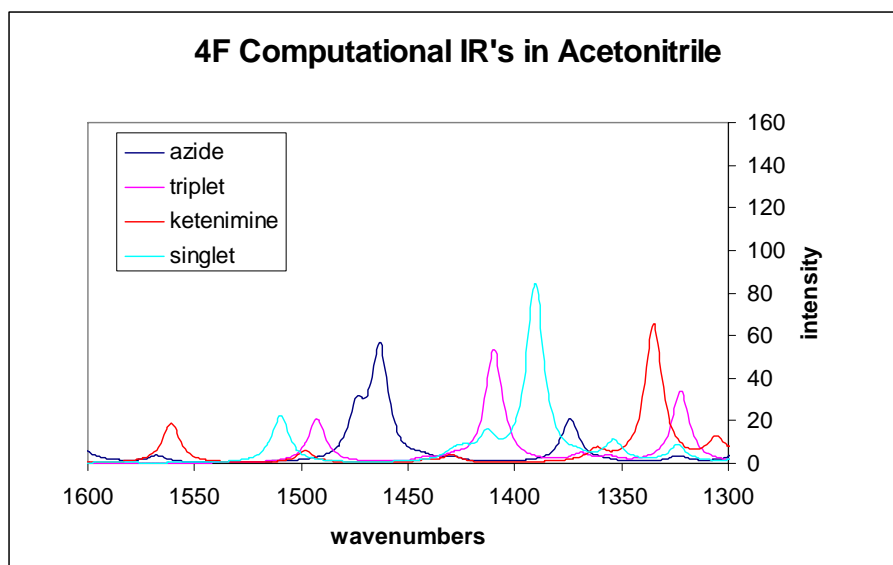


Figure 3.47 Theoretical calculations for the vibrational bands in the region of interest of reactive intermediates produced upon irradiation of 4F.

The computational work is performed in order to learn where to expect and then observe vibrational bands of reactive intermediates. Frequencies where the azide absorbs will show up in the TRIR spectrum as bleaching regions while the intermediates will have absorptions.

3.3.9. TRIR Studies

For information regarding TRIR studies, please refer to Chapter 2, section 2.3.6.

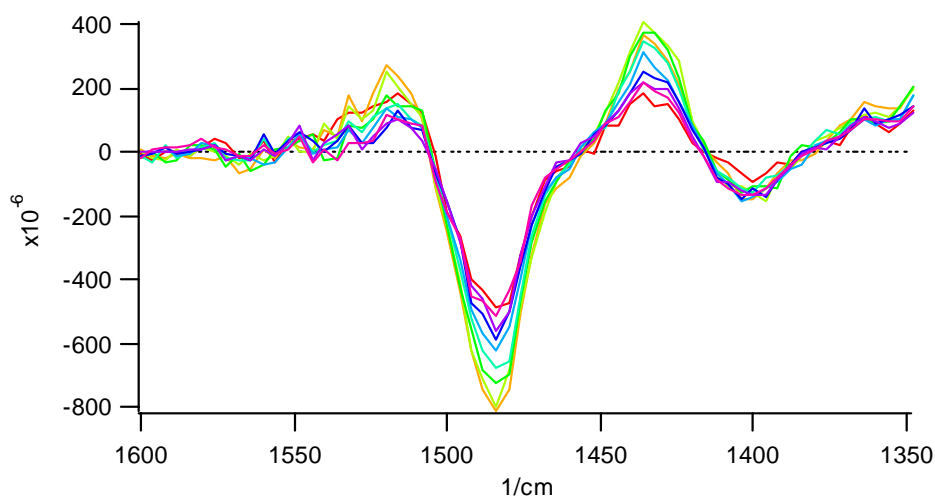


Figure 3.48 TRIR spectrum of 4F reactive intermediates produced upon photolysis of 4F from 1600 cm^{-1} to 1350 cm^{-1} .

The 1520 peak is theorized to be the singlet nitrene, the 1438 peak theorized to be the triplet nitrene based on DFT calculations, and the bleaching at 1490 is due to azide ground state depletion.

The following is a complete TRIR scan with 4F precursor in deuterated acetonitrile.



Figure 3.49 Complete TRIR spectrum produced by flash photolysis of 4F. Maximum range of 1950 cm⁻¹ to 1250 cm⁻¹.

The gap between 1600 to 1650 wavenumbers is due to the fact that data was not collected in this region because the data was collected in segments at different times and diagnostic bands were not expected in the missing segment.

Kinetics in Deuterated Acetonitrile

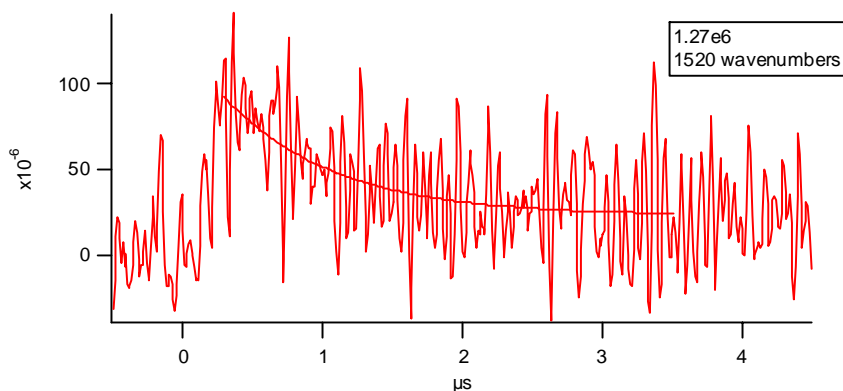


Figure 3.50 The transient decay kinetics produced upon flash photolysis of 4F. The kinetics were recorded at 1520 cm^{-1} . The decay kinetics were assigned to the singlet nitrene with a rate constant of 1.27e6 s^{-1} and a lifetime of $800\text{ }\mu\text{s}$. There is much error in this number because of the poor signal to noise ratio.

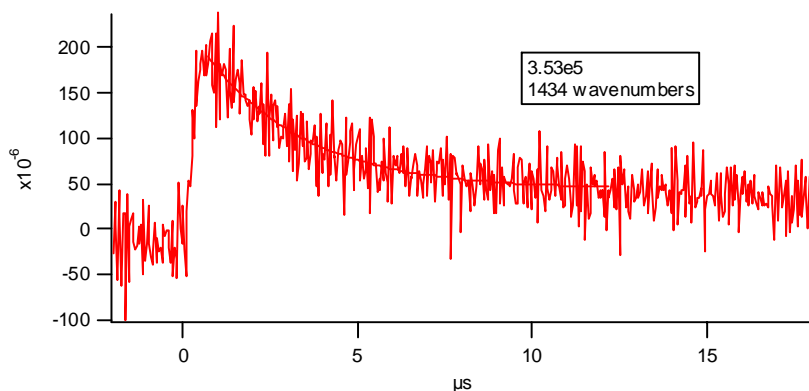


Figure 3.51 The transient decay kinetics produced upon flash photolysis of 4F. The kinetics were recorded at 1434 cm^{-1} . The decay kinetics were assigned to the triplet nitrene with a rate constant of 3.53e5 s^{-1} .

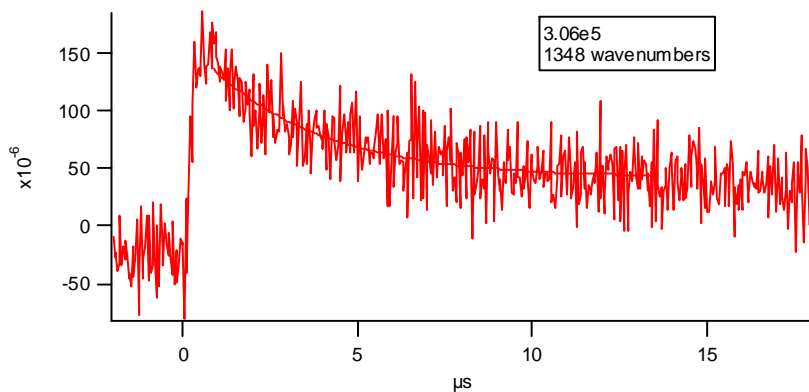


Figure 3.52 The transient decay kinetics produced upon flash photolysis of 4F. The kinetics were recorded at 1348 cm^{-1} . The decay kinetics were assigned to the triplet nitrene with a rate constant of $3.06\text{e}5\text{ s}^{-1}$.

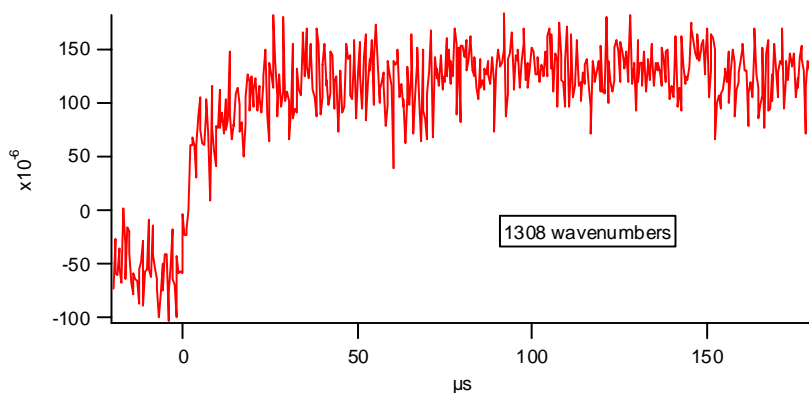


Figure 3.53 The growth of transient absorption produced upon flash photolysis of 4F. The kinetics were recorded at 1308 cm^{-1} . The growth kinetics were assigned to azo dimer formation. The concentration of azo dimer grows in with time and does not decay.

Comparison of Kinetics in Air and with Argon Purge in Deuterated Acetonitrile

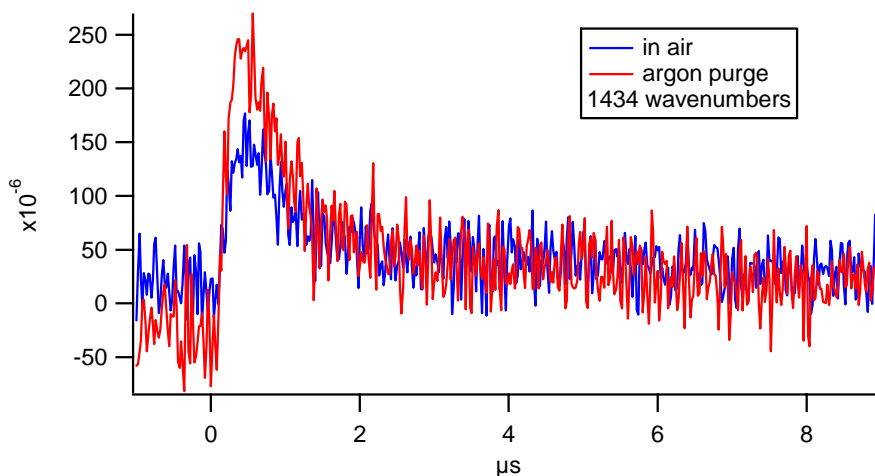


Figure 3.54 The transient decay kinetics produced upon flash photolysis of 4F measured at 1434 cm^{-1} in deuterated acetonitrile. The decay kinetics has been assigned to the triplet nitrene with a rate constant of 1.50e s^{-1} in air and 1.32e6 s^{-1} under argon purge.

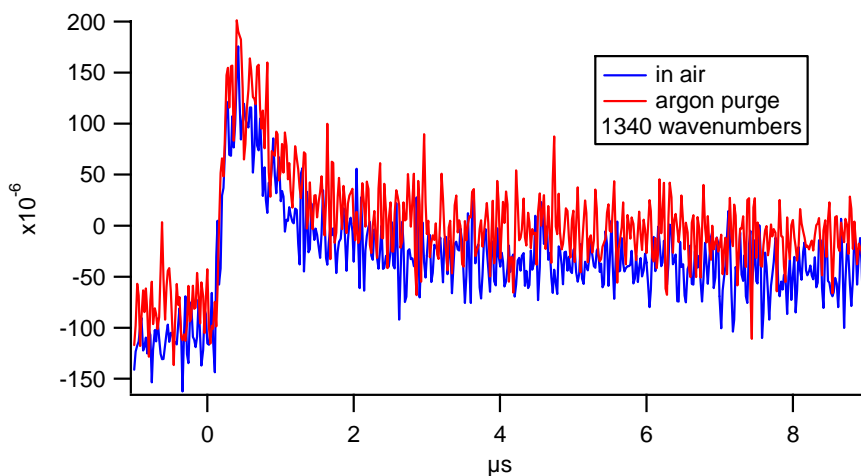


Figure 3.55 The transient decay produced upon flash photolysis of 4F measured at 1340 cm^{-1} in deuterated acetonitrile. The decay spectrum has been assigned to the triplet nitrene with a rate constant of 1.35e s^{-1} in air and 1.46e6 s^{-1} under argon purge.

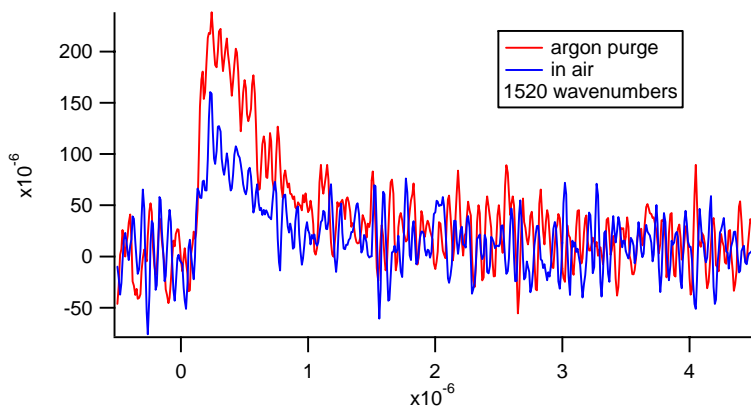


Figure 3.56 The transient decay produced upon flash photolysis of 4F measured at 1520 cm^{-1} in deuterated acetonitrile. The decay kinetics has been assigned to the singlet nitrene with a rate constant of $2.30 \times 10^6 \text{ s}^{-1}$ in air and $2.60 \times 10^6 \text{ s}^{-1}$ under argon purge.

Low Temp ($\sim 30^\circ\text{C}$) in Deuterated Acetonitrile

Experiments were conducted at low temperature in an attempt to extend the singlet nitrene lifetime.

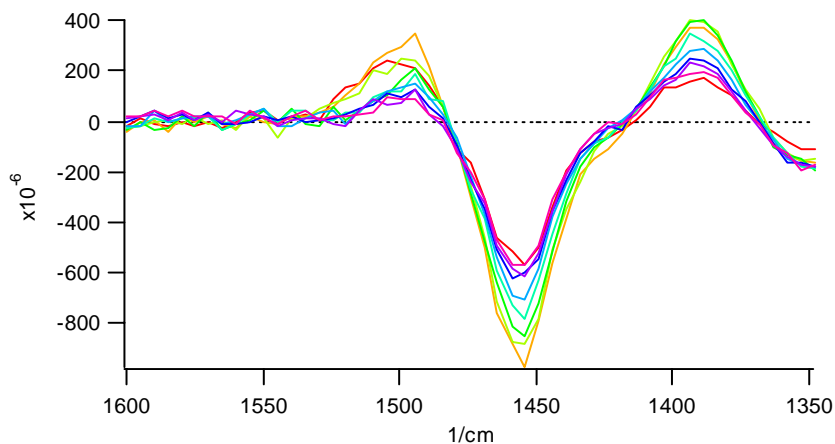


Figure 3.57 TRIR spectrum of 4F reactive intermediates produced upon photolysis of 4F at low temperature in deuterated acetonitrile

Kinetics at Low Temp in Deuterated Acetonitrile

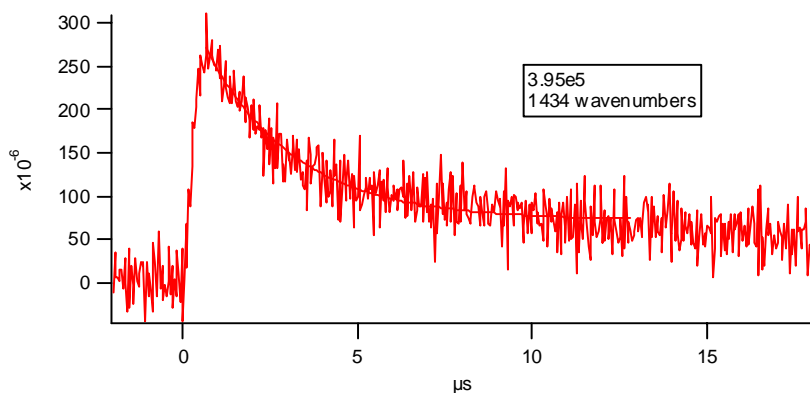


Figure 3.58 The transient decay kinetics produced upon flash photolysis of 4F at 1434 cm^{-1} in deuterated acetonitrile. The decay kinetics were assigned to the triplet nitrene with a rate constant of $3.95 \times 10^5 \text{ s}^{-1}$ in air.

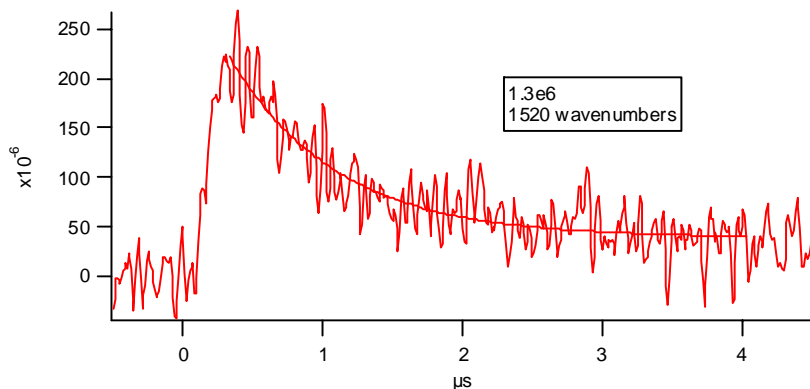


Figure 3.59 The transient decay kinetics produced upon flash photolysis of 4F measured at 1520 cm^{-1} in deuterated acetonitrile. The decay kinetics were assigned to the singlet nitrene with a rate constant of $1.3 \times 10^6 \text{ s}^{-1}$ in air.

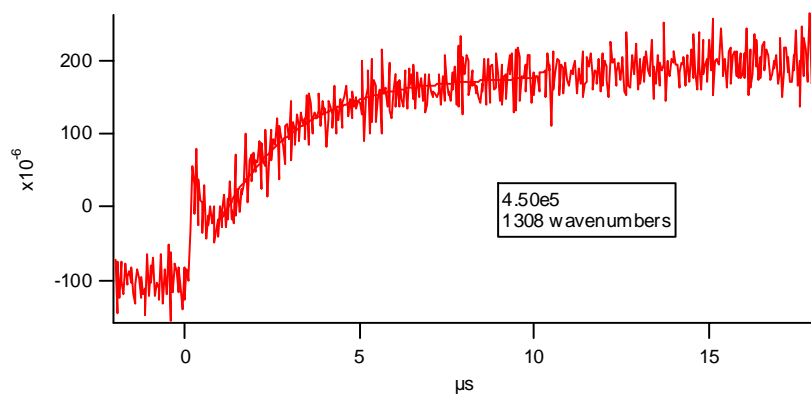


Figure 3.60 The transient absorption kinetics produced upon flash photolysis of 4F. The kinetics were recorded at 1308 cm^{-1} . The growth kinetics are assigned as azo dimer formation.

Due to the kinetics being close to the time resolution of the laser and the unfavorable signal to noise ratio, the triplet growth does not equal the singlet decay in this study.

TRIR in Deuterated Cyclohexane

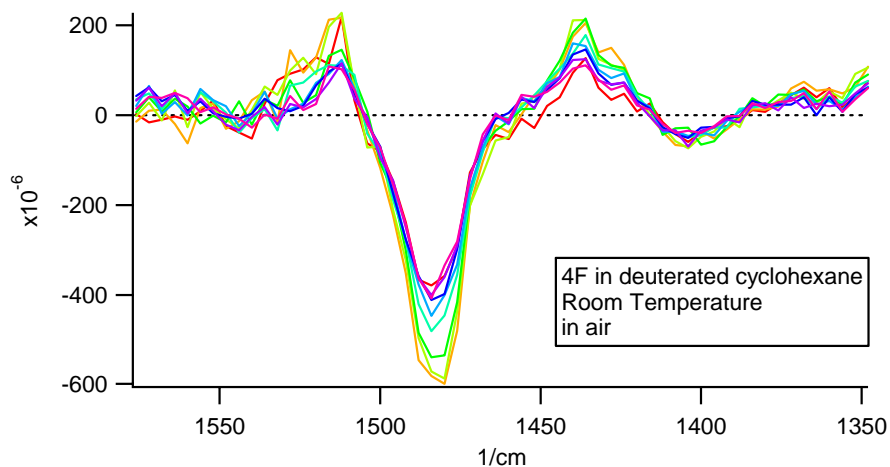


Figure 3.61 TRIR spectrum of 4F reactive intermediates produced upon photolysis of 4F at room temperature ($\sim 23^\circ\text{C}$) in deuterated cyclohexane.

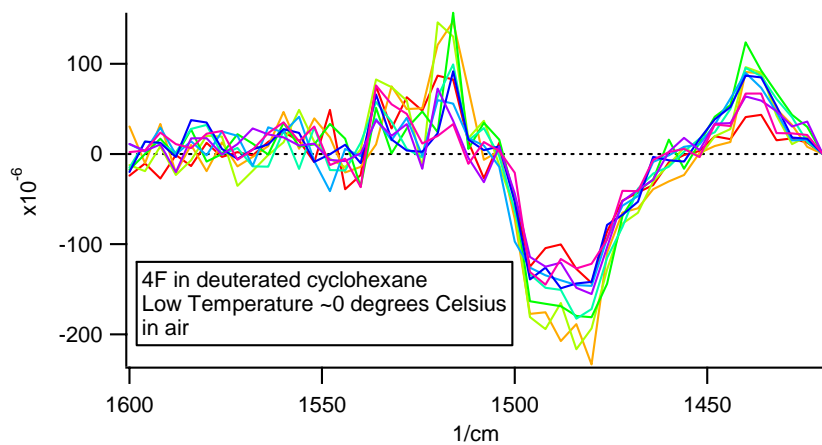


Figure 3.62 TRIR spectrum of 4F reactive intermediates produced upon photolysis of 4F at low temperature ($\sim 0^\circ\text{C}$) in deuterated cyclohexane.

3.3.10. Product Study of 4F Reaction Products

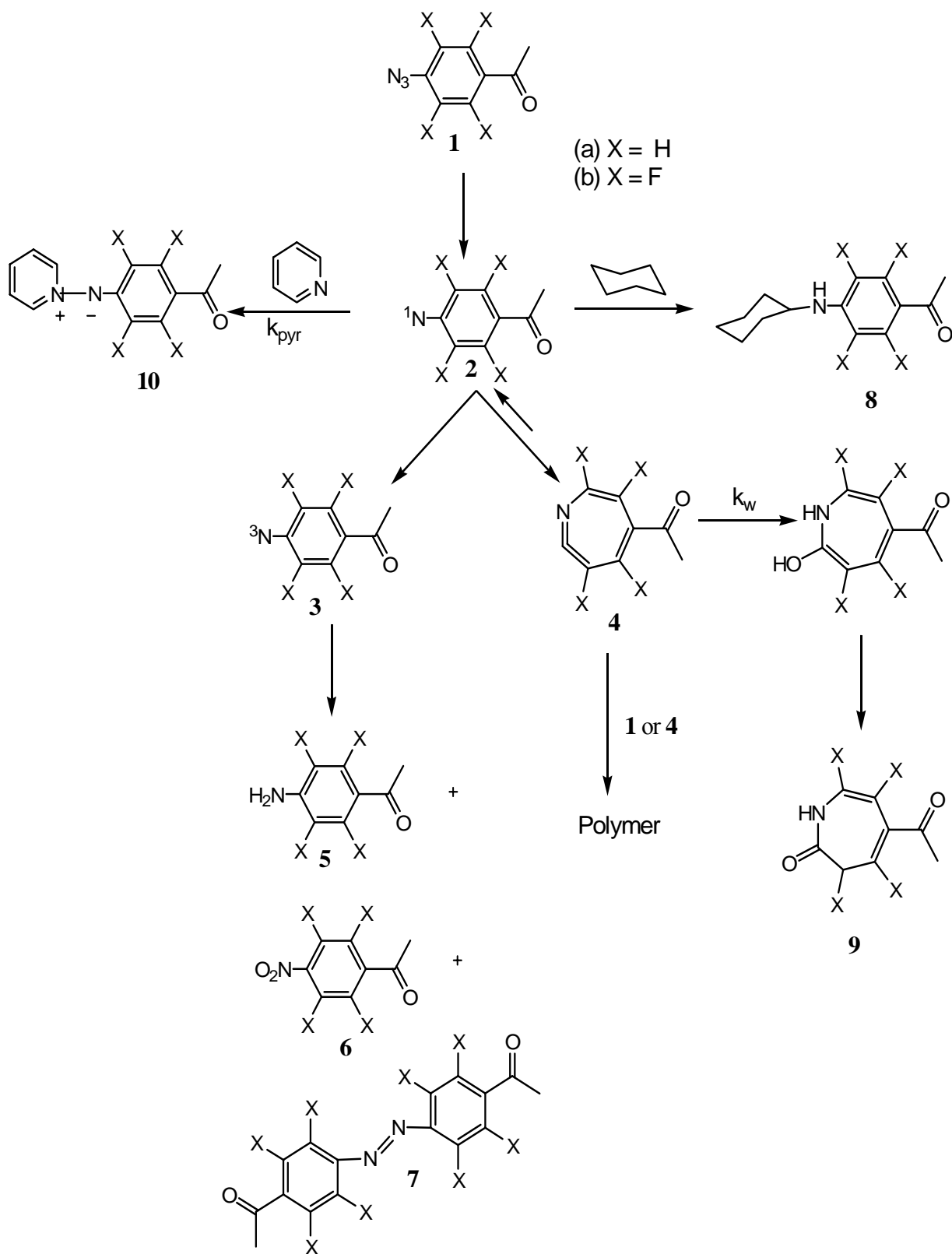
The stable products formed on photolysis of 4F (**1b** from Scheme 1 in Chapter 1) were investigated in acetonitrile and cyclohexane. The results are given in Table 3.1.

Table 3.2 Stable products formed in various solvents upon photolysis of 0.01M 4F (**1b**).

Azide	Solvent	5	6	7	8	9
1b	CH ₃ CN	0.2	84	a	a	a
1b	c-C ₆ H ₁₂	7.5	a	a	45.5	a

a = not observed by HPLC

Scheme 1



The major product of photolysis in acetonitrile was the nitro compound **6b**. The product is associated the oxidation of triplet nitrene **3b**. In cyclohexane, a 45.5 % yield of adduct **8b** was observed. This is an encouraging result because this is exactly the type of cross-linking chemistry one hope for in a PAL experiment.

There was no evidence for the formation of **9b** upon photolysis of 4F (**1b**) in water/methanol solutions. This type of product is known to form upon photolysis of parent phenyl azide in water, due to trapping of 1,2-didehydroazepine¹⁵. Large molecular weight products were observed in these systems which are attributed to reaction of the anilines with formaldehyde (created from methanol oxidation by the triplet nitrene). When the azide is diluted by a factor of ten to 0.001M the yield of products increases because the rate of polymerization of the azide, initiated by a reactive intermediate such as a ketenimine, is reduced.

In summary, the trapping data argues against the formation of ketenimines **4b** in protic solvents and for the rapid relaxation of singlet nitrenes **2b** to the lower energy triplet nitrene **3b**.

Photolysis of tetrafluorinated azide (4F also **1b**) in water and methanol indicates the intermediacy of triplet nitrene **3b**. No product was formed that could not be attributed to the addition of water or methanol to ketenimine **4b**.

Photolysis of 4F (**1b**) in cyclohexane leads to the formation of a CH insertion adduct, **9b**. This indicates that photolysis of 4F (**1b**) (or its close analogs) in a hydrophobic environment can lead to the desired cross-linking chemistry. Nitrene **2b** does not form adducts with benzene, however, in appreciable yields.

3.4. Conclusions

LFP of 2,3,5,6-tetrafluoro-4-azidoacetophenone (4F) produces weak signals (300-350 ns) with microsecond lifetimes. The carrier(s) of the transient spectrum can not be singlet nitrene, which has a sub-microsecond lifetime. Thus, the UV-vis transient spectra must be due to ketenimine or triplet nitrene, or to a mixture of these species.

Several pieces of evidence indicate that the species detected is the triplet nitrene. First, there is the slow formation of persistent species with a spectrum typical of an azo compound. Azo compounds are formed by the reaction of triplet nitrenes with azide precursors.

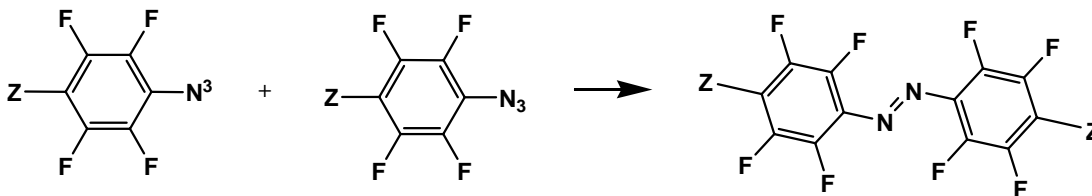


Figure 3.63 Example of the formation of an azo compound.

Secondly, photolysis of 4F in acetonitrile gives products that can be reasonably attributed to reaction of the triplet nitrene.

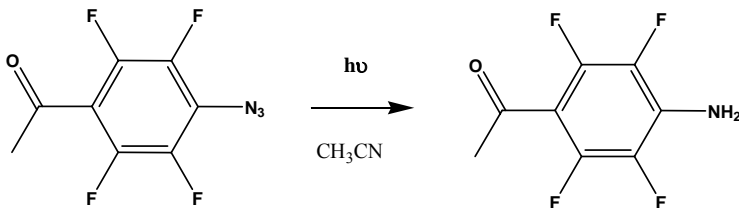


Figure 3.64 Triplet nitrene reaction.

Finally, DFT calculations predicted that the vibrational spectra of the singlet and triplet nitrenes and the ketenimine. TRIR spectroscopy positively identified the singlet and triplet nitrene and the IR spectrum of the ketenimine was conspicuously absent. Thus, we confidently assign the weak transient observed by LFP to the triplet nitrene.

Although we did not directly detect the singlet nitrene produced from photolysis of 4F, we could trap it with pyridine to form an intensely absorbing persistent ylide in aprotic solvents. In aprotic solvents we could resolve the formation of ylide and by plotting the pseudo first order rate constant of ylide formation versus [pyridine] we obtained absolute rate constants of nitrene reaction with pyridine and the singlet nitrene lifetimes in various solvents. The absolute rate constants of bimolecular reaction with pyridine are in acetonitrile and benzene, respectively. From our results, we can conclude that our original hypothesis that tetrafluorination would extend the lifetime of the singlet nitrene is confirmed.

Using Stern Volmer analyses we demonstrated that the singlet nitrene formed upon photolysis of 4F reacts with indole, N-methylimidazole, phenol, and dibutyl sulfide in benzene. Chemical analysis (HPLC) of a reaction mixture demonstrated that the fluorinated singlet nitrene will react with the unactivated CH bonds of cyclohexane to form a robust adduct.

Thus, photolysis of 4F in a hydrophobic environment forms a reactive singlet nitrene which can rapidly form cross links. This is exactly the result desired in a photoaffinity labeling reagent.

The effective catalysis of singlet to triplet nitrene intersystem crossing in protic solvents has precedent²³ with 4F but the extreme enhancement observed in the

photochemistry of 4H is extraordinary. Protic catalyses of spin relaxation destroy the ability of 4H and 4F to serve as cross-linking reagents in water.

Intersystem crossing (ISC) usually proceeds by the coupling of spin and orbital angular momentum. This process is rapid when the singlet species has a closed shell zwitterionic structure as in a carbene.

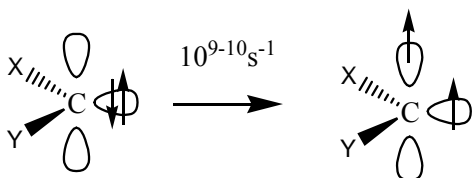


Figure 3.65 Closed shell nature of a singlet carbene.

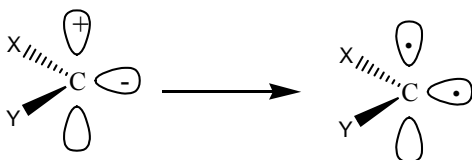


Figure 3.66 Zwitterionic singlet carbene relaxing to a biradical triplet state.

Singlet aryl nitrenes have open shell electronic structures. Thus, ISC is forbidden by a spin orbit coupling mechanism^{ref}.

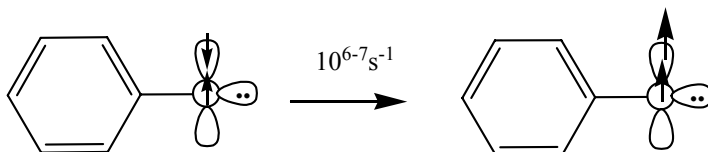


Figure 3.67 Singlet aryl nitrene open shell electronic structure.

Singlet phenylnitrene has a quinoidal biradical structure.

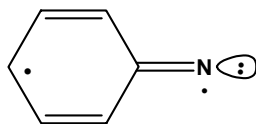


Figure 3.68 Quinoidal structure of singlet phenylnitrene.

We speculate that the acetyl substituted singlet nitrene has an extended, dipolar, quinoidal structure stabilized by hydrogen bonding in water.

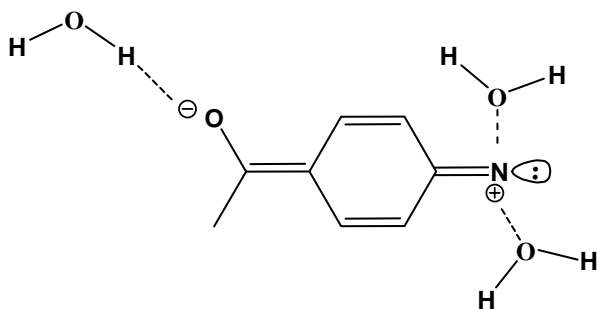


Figure 3.69 Hydrogen bonding with quinoidal structure.

This structure is closed shell and zwitterionic. This is the perfect electronic configuration for spin-orbit assisted intersystem crossing. Thus, we propose that protic catalysis of ISC by water and methanol, in acetyl substituted singlet nitrenes are based on this principal.

CHAPTER 4: CREATION OF AN AZIDE LIBRARY

4.1 Introduction

The goal of this research was to synthesize a series of substituted aryl azides from substituted anilines for study by laser flash photolysis and product studies in water and PBS buffer. The specific compounds prepared include: phenyl azide, para-methylphenyl azide, para-azido ethyl benzoate, para-azidoacetophenone (4H), para-chlorophenyl azide, para-nitrophenyl azide, para-cyanophenyl azide, 2,3,5,6, tetrafluorophenyl azide, para-fluorophenyl azide, 4-azido salicylic acid ethyl ester, 4-bromo phenyl azide, 2-fluoro phenyl azide, 4-azido cinnamic acid, 5-azido salicylic acid, 2-trifluoro methyl phenyl azide, 4-trifluoro methyl phenyl azide, 4-azido-2,3,5,6-tetrafluoro ethyl benzoate, 2-azido-3,4,5,6,7,8-heptafluoro naphthalene, 1-azido naphthalene, 2-azido naphthalene, and 4-azido-2,3,5,6-tetrafluoro acetophenone (4F)²⁴.

4.2 Standard Procedures

Stock Solutions Prepared

At the beginning of the project three stock solutions were prepared for use throughout the project. Stock Solution A was composed of 100 ml of concentrated HCl diluted with 900 mL of distilled water. Stock Solution B was composed of 56 g of NaNO₂ diluted in 800 mL of distilled water. Stock Solution C was composed of 72 g of NaN₃ and diluted into 800 mL of distilled water.

A stock solution of HEPES buffer was also prepared by mixing 50 mM HEPES salt (MW 238) with 50 mM concentrations of KCl and MgCl_2 . To prepare 1 liter of HEPES buffer 11.9 g of HEPES salt was added to 10.165 g MgCl_2 , 3.73 g KCl, and 1 liter of water.

General Procedure for Preparation of an Aryl Azide

A solution of 0.02 mol of the selected substituted aniline was dissolved in 10 mL of THF (Tetrahydrofuran) and placed in a three necked round bottom flask containing a magnetic stir bar. To the flask 90 mL of Stock Solution A ($\text{HCl}/\text{H}_2\text{O}$) was added. The flask was then placed in an ice bath on top of a magnetic stirrer and clamped to a ring stand. Ethyl alcohol was added to the ice bath to help keep the temperature of the reaction below 5-10 °C. The reaction mixture was then stirred for 15 minutes. Next, 40 mL of Stock Solution B ($\text{NaNO}_2/\text{H}_2\text{O}$) was added to the reaction mixture dropwise at 0 °C. The reaction mixture was kept below 5 °C and stirred for 15 minutes. Excess nitrous acid was removed by the addition of a spatula tip of urea. To the cooled reaction mixture 40 mL of Stock Solution C ($\text{NaN}_3/\text{H}_2\text{O}$) was added dropwise to the reaction mixture at a temperature between 0 °C and 5 °C. In most cases the solution bubbled as Stock Solution C was added indicating the formation of nitrogen gas. After the addition was complete the reaction mixture was then stirred for 1.5 hours at room temperature. The reaction mixture was then stored in the laboratory refrigerator.

In a few cases (para-chloro, acetyl, nitro, and cyano) the product precipitated. In these cases we followed work-up procedure (B). In the absence of crystals procedure (A) was followed.

(A) Standard Procedure for the Extraction of Oily Azides

The reaction mixture was taken from the refrigerator and extracted using 2 volumes of 100 mL of ethyl ether. The first extract was of the entire reaction mixture and the second extraction was of the water layer recovered from the first wash to ensure that the entire product had been recovered. The ether solution was then washed with 100 mL of dilute (0.1M) HCl. This removes any unreacted aniline. This mixture was prepared using 5 mL of 2M HCl and 95 mL of distilled water. The solution was then washed with 100 mL of 0.35 NaOH. This mixture was prepared using 10 mL of 3.55M NaOH and 90 mL of distilled water. The purpose of the base wash is to get rid of any phenol byproduct formed in the reaction mixture. The reaction mixture is then dried using anhydrous magnesium sulfate (MgSO_4). After filtering the MgSO_4 the ether is then removed by rotary evaporation at reduced pressure.

Purification of Azides Using Column Chromatography

The resulting oil obtained from the rotary evaporation was stored in the dark while a column was prepared. The column was packed with silica gel (approx. 150 mL) and approx. 300 mL of hexanes. The oily azide was carefully added dropwise to the top of the column. After the addition of the oily azide, approx. 1 inch of sea sand was added

to the top of the column. The column was eluted with hexanes and fractions of approx. 15 mL were collected in test tubes. Air pressure was used to increase the flow through the column. Then, Thin Layer Chromatography (TLC) was used to analyze each fraction. The azide was the first compound to elute off of the column. Test tubes of the pale yellow azido solutions were alternately tested for the azide using TLC chromatography plates and hexanes. After all of the tubes found to contain the azide were combined the solution was put on the rotary evaporation machine to evaporate off the hexanes. The resulting product was usually a pale yellow color.

(B) Purification of Crystalline Azides

Crystallization

The reaction mixture was taken from the refrigerator and crystals collected using a vacuum filtration process. A funnel was set up in an Erlenmeyer filter flask and the vacuum hose was attached to the flask. An appropriately sized piece of filter paper was placed in the funnel to avoid losing crystals. The solution containing the crystals was poured quickly into the funnel and any crystals that remained in the previous flask were scraped out and placed into the funnel. The crystals were left to dry in the funnel for an hour. After the crystals were dried they were added to heated solvent (ether or hexanes depending on the particular azide) in the hood. After the crystals were added the solution was placed on a hot plate, warmed, and stirred so that the crystals would go into solution. After the crystals had dissolved the remaining solution was placed in the fume hood to evaporate off excess solvent. After some solvent had evaporated away, the remaining

mixture was placed in the refrigerator to crystallize in an ice bath. If no crystals were formed in the refrigerator then liquid nitrogen was used to cool the solution and induce crystallization. The crystals were then suction filtered again and left to dry. Once these crystals were dried they were placed in a vial and stored in the refrigerator. If the mother liquid still contained crystals the same procedure would be followed again to yield as many crystals as possible. These crystals would, upon drying, be added to the initial product of crystals.

(C) Procedure for Synthesizing 4-azido cinnamic acid ethyl ester

This ester was prepared by adding 4.08 g (0.02M) of 4-amino cinnamic acid hydrochloride to 200 ml of absolute ethanol and a spatula tip of toluene sulfonic acid (as a catalyst) together in a round bottom flask. The solution was then refluxed for 1 hour at a variac setting of 50. The solution was then allowed to cool to room temperature and then it was rotoevaporated to dryness. The residue recovered was transformed into an azide by using Procedure (A). Upon addition of Stock Solution C the azide crystallized and was then filtered and washed with water. The crystals were dried in a desiccator under vacuum for three days.

(D) Procedure for Synthesizing 5-azido salicylic acid ethyl ester

The first step in preparing this azide was to purify the starting material, 5-amino salicylic acid. 10.01 g of starting material was added to 100 mL of 0.1M NaOH and 100 mL of water. The mixture was stirred with a magnetic stir bar for 5 minutes. Three spatula tips of charcoal were then added to the solution and it was stirred for 10 minutes.

The solution was then filtered and submerged in ice and water. After vacuum filtration for approximately 2 hours the resulting solution was set aside. Two pipettes full of concentrated HCl were added to the solution. Upon addition a white precipitate was formed. It was then filtered and the precipitate was then put in a desiccator under vacuum to dry.

To the recovered material a spatula tip of toluene sulfonic acid was added as a catalyst along with 100 mL of dry ethanol and it was then stirred for three hours. The solution was refluxed for two hours. The recovered solution and precipitate were put on the rotovap and the obtained materials were then treated by Procedure (A). After addition of Stock Solution C, 100 mL of ether was added to avoid ester hydrolysis. The resulting solution and precipitate was then filtered, the precipitate was set aside for later inspection. The solution was extracted twice with 100 mL of ether. The ether layer was washed twice with 100 mL of 10% sodium bicarbonate and once with 60 mL of 10% sodium bicarbonate. The ether layer was then dried with magnesium sulfate and concentrated on the rotovap. The sodium bicarbonate layer was treated with concentrated HCl until it was neutralized. Water was also added to wash down the sides. This beaker was placed in an ice bath. Both products were later stored.

(E) Procedure for Synthesizing 4-azido-2,3,5,6-tetrafluoro ethyl benzoate

This azide was prepared by taking 0.9 g of the starting material, 4-azido-2,3,5,6-tetrafluoro benzoic acid and dissolving it in 20 mL of absolute ethanol. Two drops of concentrated sulfuric acid was then added to the solution as a catalyst. The solution was then placed in the dark in a safe place for two days. Upon returning the solution was then

dissolved in 200 mL of ethyl ether. It was extracted using three 50 mL washes of 0.1M NaOH. It was then dried using magnesium sulfate and then concentrated by rotoevaporation.

(F) Procedure for Synthesizing 2-azido-1,3,4,5,6,7,8-heptafluoro naphthalene

To prepare this azide 0.91 g starting material, octafluoronaphthalene, was added to 0.26 g sodium azide, 2 mL of water, and 5 mL of acetone. The solution was allowed to reflux for four hours on a variac setting of 45. The solution was allowed to cool to room temperature. It was then washed with 50 mL of ether and poured into a separation funnel for extraction. Then 100 mL of saturated brine was poured into the separation funnel. The ether layer was extracted and the brine layer was washed twice with 50 mL of ether. The three ether solutions were then combined, dried with magnesium sulfate, and rotovaped.

Several other methods were tried in the production of this azide; however, they were not successful and will not be described here.

(G) Procedure for Synthesizing 4-azido-2,3,5,6-tetrafluoro acetophenone

To prepare this azide 2.1 g of 2,3,4,5,6-heptafluoro acetophenone and 0.71 sodium azide were placed in a 25 mL round bottom flask. Then, 6 ml of water and 16 mL of acetone were added and the solution was refluxed for eight hours. The refluxed solution was then washed with 50 ml saturated brine and extracted using three 50 ml washes of dichloromethane. A spatula tip of charcoal was added to remove any unwanted impurities. A spatula tip of magnesium sulfate was then used to dry the

solution; it was then filtered and concentrated on the rotovap. The recovered oil was stored in the refrigerator.

4.3. Results

The following azides were obtained and cataloged. They were analyzed by Infra Red (IR) spectroscopy and Nuclear Magnetic Resonance (NMR) spectroscopy. Their yields in grams and percentages and whether or not they were tested using proton NMR or IR

Phenyl Azide

1.565 g. of phenyl azide was prepared in 84% yield. A proton NMR was taken of this product on April 28th, 2004. It was found that the azide was present but also that there were some hexanes still present. An IR was also obtained with this product on May 5th 2004. Both tests showed that the product was the desired azide.

Para-Methylphenyl Azide

2.04 g. of para-methylphenyl azide were recovered in a percent yield of 77%. A proton NMR was taken of this product on April 28th 2004. An IR was also taken of this product on May 5th 2004. Both tests showed that the product was the desired azide.

Para-Azido Ethyl Benzoate

2.701 g. of para azido ethyl benzoate were recovered producing a percent yield of 70.7%. A proton NMR was taken of this product on April 28th 2004, and an IR was taken on May 5, 2004. Both tests showed that the product was the desired azide. While taking the IR of this product the vial containing the sample broke and some of the product was lost. The recovered product was tested and found to be still pure so it was added back into the saved product.

Para-Azidoacetophenone

2.39 g. of para azido acetophenone were recovered producing a percent yield of 88%. An IR was taken of product and it was found to be the desired azide.

Para-Chlorophenyl Azide

0.583g. of para chloro phenyl azide were recovered producing a percent yield of 22.8%. No tests have yet been performed on this product. The azide precipitated as a crystal in the preparation process; however, problems occurred because the crystals melted near room temperature and continuously went through the filter during the suction filtration. This might be a reason as to why the yield was low.

Para-Nitrophenyl Azide

No results have been recorded for this compound yet; however, there are para nitro phenyl azide crystals currently present in the lab refrigerator. No tests have been performed on this azide yet.

Para-Cyanophenyl Azide

No results have been recorded for this compound. The compound was used as soon as it was made by Dr. Sarah Mandel and Dr. Chris Martin.

4-bromo phenyl azide

2.96 g of azide was recovered giving a yield of 86 %. No tests have been taken on this product.

2-fluoro phenyl azide

2.02 g of azide was recovered giving a yield of 91 %. No tests have been taken on this product.

4-azido cinnamic acid ethyl ester

3.35 g of azide were recovered. No tests have been taken on this product.

5-azido salicylic acid ethyl ester

0.6 g of product was recovered from the ether layer and 0.3 g of crystals was recovered from the sodium bicarbonate layer. Neither of these products has yet to be

tested, but judging from the yields is unlikely that very much of the desired azide was recovered.

2-trifluoro methyl phenyl azide

3.29 g of azide was recovered. No testing has been done on this product.

4-trifluoro methyl phenyl azide

2.81 g of azide was recovered giving a yield of 71.1 %. No testing has been done on this product.

4-azido-2,3,5,6-tetrafluoro ethyl benzoate

It is unclear how much azide was recovered from this procedure. The yield was very low and the product was eventually discarded.

2-azido-1,3,4,5,6,7,8-heptafluoro naphthalene

Several methods were tried in an attempt to prepare this azide, however, the most successful method recovered 0.92 g. An IR was done on the product and it showed the presence of azide. It was later found, however, that although the IR revealed the presence of azide a GC-MS analysis demonstrated that the residue was almost completely starting material

1-azidonaphthalene

5.71 g of azide was recovered giving a yield of 99%. This yield is questionable as there may possibly be some hexanes that did not get completely removed during rotary evaporation. This product was tested by IR and showed a large azide band.

2-azidonaphthalene

5.35 g of azide was recovered. This product was also tested by IR spectroscopy and showed a large azide band.

4-azido-2,3,5,6-tetrafluoro acetophenone

A dark yellow liquid weighing 2.2 g was recovered and stored in the refrigerator. An IR has been taken of this material, which reveals a large azide band.

REFERENCES

- 1) Meisenheimer, K. M.; Koch, T. H. "Photocross-linking of Nucleic Acids to Associated Proteins." *Critical Reviews in Biochemistry and Molecular Biology*, **1997**, 32, 101-140.
- 2) Hanna, M. M.; Meares, C. F. "Synthesis of a Cleavable Dinucleotide Photoaffinity Probe of Ribonucleic Acid Polymerase: Application to Trinucleotide Labeling of an *Escherichia coli* Transcription Complex." *Biochemistry*, **1983**, 22, 3546-3551.
- 3a) Renfron, M. B.; Naryshikin, N.; Lewis, L. M.; Chen, H.-T.; Ebright, R. H.; Scott, R. A. "Transcription Factor B Contacts Promoter DNA Near the Transcription Start Site of the Archaeal Transcription Initiation Complex." *J. Biol. Chem.* **2004**, 279, 2825-2831.
- 3b) Dissinger, S.; Hanna, M. M. "Active Site Labeling of *Escherichia coli* Transcription Elongation Complexes with (5-(14-Azidophenacyl)thio) Uridine 5'-Triphosphate." *J. Biol. Chem.* **1990**, 265, 7662-7668.
- 4) Buchmueller, K. L.; Weeks, K. M. "Near Native Structure in an RNA Collapsed State." *Biochemistry*, **2003**, 42, 13869-13878.
- 5a) Hixson, S.H.; Hixson, S.S.; "p-Azidophenacyl bromide, a versatile photolabile bifunctional reagent. Reaction with glyceraldehydes-3-phosphate dehydrogenase." *Biochemistry* **1975**, 14, 4251-4254.
- 5b) Burgin, A. B.; Pace, N. R. "Mapping the active site of ribonuclease P RNA using a substrate containing a photoaffinity agent." *EMBO J.* **1990**, 9, 4111-4118.
- 5c) Wang, J.-F.; Downs, W. D.; Cech, T. R. "Movement of the guide sequence during RNA catalysis by a group I ribozyme." *Science*, **1993**, 260, 504-508.
- 6a) Costas, C.; Yuriev, E.; Meyer, K. L.; Guion, T. S.; Hanna, M. M. "RNA Protein Crosslinking to AMP Reside at Internal Positions in RNA with A New Photocross-Linking ATP Analog." *Nucleic Acids Research*, **2000**, 28, 1849-1856.
- 6b) Niranjanakumari, S.; Stams, T.; Crary, S. M.; Christianson, D. W.; Fierke, C. A. "Protein Component of the Ribozyme Ribonucleases P Alters Substrate Recognition by Directly Contacting Precursor tRNA." *Proc. Natl. Acad. Sci.* **1998**, 95, 15212-15217
- 7) Lannotti, B.J.; Persinger, J.; Bartholomew, B. "Probing the Protein-DNA Contacts of a Yeast RNA Polymerase III Transcription Complex in a Crude

Extract: Solid Phase Synthesis of DNA Photoaffinity Probes Containing a Nova Photoreactive Deoxycytidine Analog.” *Biochemistry*, **1996**, 35, 9821-9831.

- 8) Alley, S. C.; Ishmael, F. T.; Jones, A. D.; Benkovic, S. J. “Mapping Protein Interactions in the Bacteriophage T4 DNA Polymerase Haloenzyme Using a Novel Trifunctional Photo-Cross-Linking and Affinity Reagent.” *J. Am. Chem. Soc.* **2000**, 122, 6126-6127.
- 9a) Moore, B. M.; II; Jalluri, R. K.; Doughty, M. B. “DNA Polymerase Photoprobe 2-[(4-Azidophenacyl)thio]-2-deoxyadenosine 5'-Triphosphate Labels an *Escherichia coli* DNA Polymerase I Klenow Fragment Substrate Binding Site.” *Biochemistry*, **1996**, 35, 11642-11651.
- 9b) Kang, M. E.; Dahmus, M. E. “The Photoactivated Cross-linking of Recombinant C-Terminal Domain to Proteins in a HeLa Cell Transcription Extract that Comigrate with Transcription Factors IIE and IIF.” *J. Biol. Chem.* **1995**, 270, 23390-23397.
- 9c) Spinelli, D.; Zanirato, P. “On the Chemical, NMR and Kinetic Properties of 2-Azido- and 3-Azido-Thiophene: Recent Development.” *J. Chem. Soc. Perkin Trans.* **1993**, 2, 1129-1133.
- 10a) A search of the topic “Photoaffinity Labeling with Azides” of SciFinder Scholar leads to 3,783 citations.
- 10b) These numbers were generated by a search of the Scifinder Scholar and Pubmed databases. See also Hixson, S. H.; Hixson, S. S. “*p*-Azidophenacyl Bromide, A Versatile Photolabile Bifunctional Reagent.” *Biochemistry*, **1975**, 14, 4251-4254.
- 11a) Hanna, M. M.; Bentsen, L.; Lucido, M.; Sapre, A. “RNA-Protein Cross-linking with Photoreactive Nucleotide Analog.” *Meth. Mol. Biol.* **1989**, 118, 21-33.
- 11b) Hanna, M. M. “Photoaffinity Cross-linking Methods for Studying RNA-Protein Interaction.” *Methods in Enzymol.* **1989**, 180, 383-408.
- 12) Sylvers, L. A.; Wower, J. “Nucleic Acid-Incorporated Azidonucleotides: Probes for Studying the Interaction of RNA or DNA with Proteins and Other Nucleic Acids.” *Bioconjugate Chem.* **1993**, 4, 411-418.
- 13) Li, Y.Z.; Kirby, J.P.; George, M.W.; Poliakoff, M.; Schuster, G.B.; “1,2-Didehydroazepines from the photolysis of substituted aryl azides: Analysis of their chemical and physical properties by time resolved spectroscopic methods.” *J. Am. Chem. Soc.*, **1988**, 110, 8092-8098.

- 14) Gritsan, N. P.; Tigelaar, D.; and Platz, M. S. "A Laser Flash Photolysis Study of Some Simple Para-Substituted Derivatives of Singlet Phenyl Nitrene." *J. Phys. Chem. A*. **1999**, *103*, 4465-4469.
- 15) Doering, W.V.E.; Odum, W., *Tetrahedron*, **1966**, *22*, 81
- 16) Rizk, M.; Shi, X.; and Platz, M.S. "Lifetimes and Reactivities of Some 1,2-Didehydroazepines Commonly Used in Photoaffinity Labeling Experiments in Aqueous Solutions." *Biochemistry*. **2006**, *45*, 543-551.
- 17) Chapman, O.L.; LeRoux, J.P. *J. Am. Chem. Soc.*, **1978**, *100*, 282
- 18) Hayes, J.C.; Sheridan, R.S.; *J. Am. Chem. Soc.*, **1990**, *112*, 5879
- 19) Gritsan, N. P.; Platz, M. S. "Kinetics and spectroscopy of substituted phenylnitrenes. *Adv. Phys. Org. Chem.*, **2001**, *36*, 255-304.
- 20) Mandel, S.M.; Liu, J.; Hadad, C.M.; and Platz, M.S. "Study of Singlet and Triplet 2,6-Difluorophenylnitrene by Time-Resolved Infrared Spectroscopy." *J. Phys. Chem. A*. **2005**, *109*, 2816-2821.
- 21) Poe, R.; Schnapp, K.; Young, M.J.T.; Grayzar, J.; Platz, M.S.; "Chemistry and Kinetics of Singlet (Pentafluorophenyl) Nitrene" *J. Am. Chem. Soc.*, **1992**, *114*, 5054-5067.
- 22) Keana, J.F.W.; Cai, S.X. "Functionalized perfluorophenyl Azides: New Reagents for Photoaffinity Labeling." *J. Fluor. Chem.*, **1989**, *43*, 151-154.
- 23) Poe, R.; Grayzar, J.; Young, M.J.T.; Leyva, E.; Schnapp, K.A.; Platz, M.S. "Remarkable Catalysis of Intersystem Crossing of Singlet (Pentafluorophenyl) Nitrene." *J. Am. Chem. Soc.*, **1991**, *113*, 3209.
- 24) These azides have been synthesized previously, see references 13, 14, and 19.